

NASA TECHNICAL NOTE



NASA TN D-6089

C.1

NASA TN D-6089

**LOAN COPY: RETURN TO
AFWL (DOGL)
KIRTLAND AFB, N. M.**



**AN EXPERIMENTAL AND ANALYTICAL
VIBRATION STUDY OF ELLIPTICAL
CYLINDRICAL SHELLS**

*by John L. Sewall, William M. Thompson, Jr.,
and Christine G. Pusey*

*Langley Research Center
Hampton, Va. 23365*



0132963

1. Report No. NASA TN D-6089		2. Government Accession No.		3. Recipient's Catalog No.	
4. Title and Subtitle AN EXPERIMENTAL AND ANALYTICAL VIBRATION STUDY OF ELLIPTICAL CYLINDRICAL SHELLS				5. Report Date February 1971	
7. Author(s) John L. Sewall; William M. Thompson, Jr., Naval Ship and Development Center; and Christine G. Pusey				6. Performing Organization Code	
9. Performing Organization Name and Address NASA Langley Research Center Hampton, Va. 23365				8. Performing Organization Report No. L-6632	
12. Sponsoring Agency Name and Address National Aeronautics and Space Administration Washington, D.C. 20546				10. Work Unit No. 124-08-13-04	
15. Supplementary Notes				11. Contract or Grant No.	
16. Abstract This paper reports an experimental and analytical vibration study of free-free isotropic elliptical cylindrical shells of constant mass ranging in cross-sectional eccentricity from zero (circular shell) to 0.916. Experimental resonant frequencies, nodal patterns, and mode shapes were obtained by use of an air-jet shaker or an electrodynamic shaker with a noncontact inductance probe that could be moved over most of the shell surface. Experimental frequencies were in generally good agreement with analytical frequencies calculated by means of a Rayleigh-Ritz type of analysis featuring multiterm longitudinal and circumferential modal expansions. Frequencies for shells with eccentricity of 0.916 were as much as 40 percent below the corresponding circular-shell frequencies. As eccentricity increased, analytical and experimental mode shapes indicated considerable longitudinal and circumferential modal coupling.				13. Type of Report and Period Covered Technical Note	
17. Key Words (Suggested by Author(s)) Structural analysis Structural vibration Shells (structural forms) Vibration				14. Sponsoring Agency Code	
18. Distribution Statement Unclassified - Unlimited					
19. Security Classif. (of this report) Unclassified		20. Security Classif. (of this page) Unclassified		21. No. of Pages 81	22. Price* \$3.00

AN EXPERIMENTAL AND ANALYTICAL VIBRATION STUDY OF
ELLIPTICAL CYLINDRICAL SHELLS

By John L. Sewall, William M. Thompson, Jr.,*
and Christine G. Pusey
Langley Research Center

SUMMARY

This paper reports an experimental and analytical vibration study of free-free isotropic elliptical cylindrical shells of constant mass ranging in cross-sectional eccentricity from zero (circular shell) to 0.916 (corresponding to a major-to-minor axis ratio of 2.5). Experimental resonant frequencies, nodal patterns, and mode shapes were obtained by use of an air-jet shaker or an electrodynamic shaker with a noncontact inductance probe that could be moved over most of the shell surface. Experimental frequencies are in generally good agreement with analytical frequencies calculated by means of a Rayleigh-Ritz type of analysis featuring multiterm longitudinal and circumferential modal expansions. As many as four longitudinal terms, including beam-vibration functions, were required along with an increasing number of circumferential trigonometric terms in each shell displacement series to obtain converged results with increasing eccentricity. As many as 32 circumferential terms were required for the highest eccentricity shell.

Frequencies for shells with eccentricity of 0.916 were as much as 40 percent below the corresponding circular-shell frequencies. As eccentricity increased, fewer higher order experimental shell vibration modes could be identified, and there were more higher order analytical modes with two frequencies for each pair of longitudinal and circumferential mode numbers. Analytical and experimental mode shapes for eccentricities of 0.760 and 0.916 indicate considerable longitudinal and circumferential modal coupling that tends to preclude positive identification according to longitudinal and circumferential components.

Frequencies calculated by methods involving various approximations to the noncircular curvature are in good agreement with both experimental and analytical frequencies of the present study for the inextensional modes, at least up to an eccentricity of 0.760 (corresponding to a major-to-minor axis ratio of 1.538).

*Underwater Explosions Research Division, Naval Ship Research and Development Center, Portsmouth, Virginia.

INTRODUCTION

In the study of the response of shell structures to static and dynamic loading, considerably more attention has been given to shells of revolution than to shells of noncircular cross section. However, although many structural components of aerospace and submarine vehicles can be adequately treated as actual or equivalent shells of revolution, this approach may well be unacceptable for shells with significantly noncircular curvature. It is therefore profitable to examine the behavior of noncircular shells, not only to obtain basic data, but also to define the limitations of certain near-circular shell analyses.

Some noncircular-shell investigations are reported in references 1 to 14. References 1 to 5 are concerned with particular aspects of the static structural characteristics of slightly noncircular shells, and references 6 to 14 deal with dynamic characteristics. Specifically, references 1 to 3 are concerned with unstiffened and ring-stiffened oval cylinders subjected to hydrostatic pressure and show large effects of noncircularity on static stresses and displacements. Reference 4 presents a finite-difference analysis of stresses and displacements in an orthotropic noncircular shell of arbitrary curvature and varying circumferential thickness. Reference 5 presents series solutions to Donnell's equations for the displacements due to pressure loads for open noncircular shells with arbitrary end conditions. References 6 to 11 are vibration studies, of which references 7 to 9 indicate relatively small effects of noncircularity on the frequencies of free vibration of infinitely long oval cylinders. Reference 12 contains a considerable amount of experimental frequency and mode-shape data for clamped-free elliptical cylinders; however, all these cylinders had the same cross-sectional eccentricity. In reference 14, the method of reference 5 is applied to the vibration of noncircular curved panels. Most of references 1 to 14 are entirely theoretical with no experimental data included for comparison with analytical results. Experimental and analytical static stresses are compared in reference 4. Reference 11 contains experimental frequencies for a variety of noncircular shells and includes comparisons of these frequencies with approximate analytical frequencies based on frequency equations of circular shells with equivalent radii.

The purposes of the present paper are to compare measured and calculated vibration data of short, free-free elliptical cylinders of constant mass and to determine the effects of cross-sectional eccentricity on shell frequencies and mode shapes. Attention is given to the effects of eccentricity (or noncircularity) both on the two sets of inextensional modes, as in references 9 and 10, and on two sets of higher order longitudinal modes. Vibration tests were conducted on four thin-shell isotropic cylinders of equal length, perimeter, and thickness, and with eccentricities ranging from zero (circular cylinder) to 0.916, corresponding to major-to-minor axis ratios from 1 to 2.5, respectively.

Analytical frequencies were obtained by application of an energy approach utilizing the Rayleigh-Ritz procedure in multiterm circumferential and longitudinal modal expansions. Trigonometric terms were used for the circumferential series and beam functions for the longitudinal series. Measured frequencies are compared with frequencies computed both by this analysis and, where possible, by the analyses of references 9 to 11. In references 9 and 10, the frequency is approximated by expressions involving the frequency of the circular cylinder plus power-series terms containing eccentricity parameters for ovals. The approximate frequency expressions of reference 11 are essentially circular-shell equations with equivalent or average values of the radius of curvature chosen to represent the noncircular cross section.

Analytical mode shapes obtained in the present analysis are included to illustrate the nature of circumferential and longitudinal modal coupling due to noncircularity, and many of these mode shapes are compared with experimentally determined mode shapes for the radial (or normal) displacement. Pertinent details of the analysis are given in appendix A. In addition, analytical frequencies of the elliptical shell models with assumed freely supported ends are included in appendix B, and comparisons are made with the analytical frequencies of reference 10.

SYMBOLS

$$\left. \begin{array}{l} A_{ijmp}, B_{ijmp}, C_{ijmp} \\ F_{ijmp}, G_{ijmp}, H_{ijmp} \end{array} \right\} \text{ elements of stiffness matrix (see appendix A)}$$

a,b length of semimajor and semiminor axis, respectively, of elliptical shell

a_{mp}, b_{mp}, c_{mp} generalized coordinate for antisymmetric-mode displacement u, v, and w, respectively

$\bar{a}_{mp}, \bar{b}_{mp}, \bar{c}_{mp}$ generalized coordinate for symmetric-mode displacement u, v, and w, respectively

E Young's modulus

e eccentricity of elliptical shell, $e^2 = 1 - \left(\frac{b}{a}\right)^2$

f circular frequency, hertz

h shell thickness

I_1 to I_9	circumferential integrals (see appendix A)
i	longitudinal mode number; $\sqrt{-1}$ in equations (5)
J_1 to J_{16}	longitudinal integrals (see appendix A)
j, p	half the number of longitudinal node lines for elliptical shells
K	stiffness submatrix (see eq. (9))
L	length of shell
M	mass submatrix (see eq. (9))
m	longitudinal mode number
N	beam eigenvalue (see appendix A)
n	circumferential mode number for circular shell
P, Q	integers identifying upper limits on number of modes used in the analysis (see eqs. (5))
$q_{mp}(t)$	generalized coordinate
R	radius of curvature of shell
R_0	arbitrary reference radius
s	arc length around shell
s_0	total circumference of shell
T	kinetic energy
t	time
U	strain energy

u, v, w longitudinal, circumferential, and radial shell displacement, respectively
(see fig. 6)

X_{mu}, X_{mv}, X_{mw} mth longitudinal mode shape for u-, v-, and w-displacement, respectively

x, y, z longitudinal and cross-sectional coordinates (see fig. 6)

$\alpha_{ijmp}, \beta_{ijmp}, \gamma_{ijmp}$ elements of mass matrix (see appendix A)

γ beam eigenvalue property (see appendix A)

$\epsilon_x, \epsilon_\theta, \epsilon_{x\theta}$ membrane strains (see eqs. (1))

θ angle between the minor axis and the radius vector R (see fig. 6)

$\kappa_x, \kappa_\theta, \bar{\kappa}_{x\theta}$ changes of curvature (see eqs. (1))

μ Poisson's ratio

ρ shell mass density

$$\Phi = 1 - e^{2\cos^2\theta}$$

ϕ central angle (see fig. 6)

ω angular frequency, radians/second

Subscripts:

a antisymmetric

i, m identifies ith and mth longitudinal modal components

j, p identifies jth and pth circumferential modal components

s symmetric

Superscript T denotes transpose of a matrix.

Matrix elements and integrals with bars are associated with symmetric mode.

Dots over quantities denote differentiation with respect to time.

Primes denote differentiation with respect to x , for example, $X'_m = \frac{dX_m(x)}{dx}$ and

$$X''_{mw} = \frac{d^2 X_{mw}(x)}{dx^2}.$$

EXPERIMENTAL INVESTIGATION

Models

Four cylindrical shell models of equal perimeter, length, and thickness were used in the investigation. One model was circular in cross section, and three were elliptical. Each model was 24 inches (61.0 cm) long and was made from two shaped sections butt-welded together with smoothed seams at the ends of the major axis. Each section was 6061 aluminum alloy and was 0.032 inch (0.813 mm) thick. Keeping the perimeter, length, and thickness the same for all models maintained a constant total mass. The model dimensions and eccentricities, along with the material properties E , μ , and ρ , are indicated in table I.

Test Apparatus and Procedure

Vibration tests were conducted with each model suspended by 12 soft elastic supports attached at equidistant points around the perimeter at one end of the cylinder, as shown in figure 1. The basic parts of the test apparatus are the same as those reported in reference 15 and are shown schematically in figure 2 as arranged for some of the tests in this investigation. Each model was excited by an oscillatory force directed normal to the shell surface. Two types of vibration exciters were used, an air-jet shaker of the type described in reference 16 and a small electrodynamic shaker capable of a $1\frac{1}{2}$ -pound (6.67-N) vector force output. At low frequencies (less than 50 Hz), the air shaker provided a noncontact excitation force which permitted unrestricted, large-amplitude motion of the cylinder wall. For relatively low-amplitude responses at higher frequencies, the electrodynamic shaker was used and was attached to the cylinder wall by means of a lightweight vacuum cup. Of the two shakers, the air shaker was believed to give more reliable lower frequencies because of the appreciable stiffness and mass effects of the electrodynamic shaker on these frequencies. (See also ref. 17.) Stationary and movable noncontact inductance probes of the type described in reference 15 were used to determine resonant peaks, phase shifts, and mode shapes in normal displacement. Resonant frequencies were obtained by tuning the shaker for maximum amplitude response normal to the shell wall at an antinode.

With the test setup of figure 2, nodes of the normal displacement were located by monitoring the outputs of the fixed and movable probes in the forms of Lissajous figures on an oscilloscope and by observing the phase shifts for different positions of the movable probe. No mode-shape measurements were made. This apparatus was used for all the tests on model 2 and for some of the tests on model 4.

For the rest of the test program, normal mode shapes were measured with the aid of the motorized movable probe apparatus shown in figures 1 and 3. The movable inductance probe was driven by an electric motor along a track mounted on a concentric, 3/8-inch (0.952-cm) steel elliptical strap surrounding the model, as shown in figure 1, in order to obtain circumferential mode-shape components. This strap was supported on four vertical threaded rods and could be rotated by another electric motor through a chain drive in order to obtain longitudinal mode-shape components. The supporting instrumentation was more involved than that represented in figure 2 and is detailed in reference 15. Figure 3 is a closeup view of the motorized probe assembly between the elliptical track support and the model. The thin white wire leading upward from the back of the probe itself goes to the electronic instrumentation which controls the distance of the probe from the model and the operation of an x-y plotter that traces out normal shell displacements as the probe travels over the shell surface.

Experimental Results

Resonant frequencies of the four cylindrical shells are listed in tables II to IV. The mode identification integers m , n , and p used in tables II and III are defined in figure 4. Mode shapes corresponding to frequencies in tables III(b) and IV for model 3 ($\frac{a}{b} = 1.538$, $e = 0.760$) are shown in figure 5. The air shaker was used for frequencies up to about 170 Hz for the circular shell and up to about 50 Hz for the elliptical shells, and the electrodynamic shaker (designated as "electric shaker" in the tables and figures) was used for all other modes (except as noted in tables II and III(c)). Erratic random deviations of some of the mode shapes in figure 5 were due to occasional drifts from resonance during mode-shape measurement. This drift was more apt to occur with the air shaker than with the electrodynamic shaker. The closely spaced ripples superimposed on the responses at the lowest frequencies are attributed to the closeness of these frequencies to the natural frequency of the probe servo system.

The modal identifications in figure 4 apply to normal (or radial) shell displacements. The longitudinal mode number m denotes the number of circumferential nodes. The circumferential mode numbers n and p denote, respectively, the number of circumferential waves for the circular shell and one-half the number of longitudinal nodes for the elliptical shells. The modes for $m = 0$ and 1 are designated as "inextensional" because of their straight-line variations in the longitudinal direction and because of the

monotonically increasing frequencies with increasing n or p , consistent with purely bending vibrations of the shell. Modes for $m \geq 2$ are characterized by curved (indicating elastic) longitudinal mode-shape components and by the existence of relative minimums in the variation of frequency with n or p consistent with the well-known shell behavior associated with combined bending and stretching (or membrane) deformations.

Nearly all resonances excited for the circular shell (table II) and most of the lower frequency inextensional modes of the elliptical shells (table III) could be clearly classified according to figure 4. In addition, the identifiable elliptical-shell modes were either symmetric or antisymmetric with respect to the minor axis, and this distinction is clearly evident in figure 5 for the lower frequency modes. The symmetric modes were excited by aligning the shaking force along the minor axis, and the antisymmetric modes were obtained with the shaker located part way between the ends of the major and minor axes at a point of relatively large displacement. Most symmetric and antisymmetric frequencies differed by less than 1 Hz.

The number of identifiable resonances decreased with increasing frequency and increasing eccentricity e until few elliptical-shell modes could be exclusively identified as $m = 2$ or 3 . Many of these modes were highly coupled with $m = 0$ or 1 and/or more than one p mode, as is evident in figure 5 by the different values of m and/or p in different parts of the model. Moreover, both symmetric and antisymmetric characteristics were present in the circumferential mode shapes of most of these modes. Localized effects due to the electrodynamic shaker also contributed to the uncertainty and ambiguity of modal identification, mainly by causing local longitudinal mode-shape distortions that tended to become more severe with increasing frequency, as is shown in figure 5. Consequently, the frequencies in table IV are simply listed in order of increasing value.

METHOD OF ANALYSIS

The analytical method derived and applied in this paper is an application of the well-known Rayleigh-Ritz procedure. The assumed forms for the inplane and radial (or normal) displacements were finite series representing circumferential and longitudinal (or axial) components of these displacements. Elementary trigonometric functions represented the circumferential components for both symmetric- and antisymmetric-mode frequencies. Longitudinal displacement components were chosen to satisfy geometric end conditions (displacement and slope). For the free-free end conditions, longitudinal mode-shape components for the two lowest sets of modes ($m = 0$ and 1) were approximated by simple constant and linear algebraic expressions, and as in reference 18, the longitudinal mode-shape components for the higher modes ($m \geq 2$) were approximated by

free-free beam-vibration functions. Longitudinal mode-shape components are also included for the freely supported end conditions and are given by trigonometric functions.

Strain-Displacement Relations

The elliptical geometry embodied in the analysis is detailed in figure 6, and the analysis is formulated on the basis of thin-shell theory in terms of circumferential and axial coordinates θ and x . The deformation of the shell middle surface is expressed in terms of the displacements u , v , and w in the axial, circumferential, and normal directions, respectively, with the positive normal direction considered to be outward. By use of Sanders' theory (ref. 19), the strains ϵ_x , ϵ_θ , and $\epsilon_{x\theta}$ and changes of curvature κ_x , κ_θ , and $\bar{\kappa}_{x\theta}$ are given in terms of the displacements by the relations

$$\left. \begin{aligned} \epsilon_x &= \frac{\partial u}{\partial x} & \epsilon_\theta &= \frac{1}{R} \left(\frac{\partial v}{\partial \theta} + w \right) & \epsilon_{x\theta} &= \frac{1}{2} \left(\frac{\partial v}{\partial x} + \frac{1}{R} \frac{\partial u}{\partial \theta} \right) \\ \kappa_x &= -\frac{\partial^2 w}{\partial x^2} & \kappa_\theta &= -\frac{1}{R^2} \left[\frac{\partial^2 w}{\partial \theta^2} - \frac{\partial v}{\partial \theta} - \frac{1}{R} \frac{dR}{d\theta} \left(\frac{\partial w}{\partial \theta} - v \right) \right] \\ \bar{\kappa}_{x\theta} &= \frac{3}{4R} \frac{\partial v}{\partial x} - \frac{1}{R} \frac{\partial^2 w}{\partial x \partial \theta} - \frac{1}{4R^2} \frac{\partial u}{\partial \theta} \end{aligned} \right\} \quad (1)$$

where R is the radius of curvature which, for the elliptical cross section, is given by

$$R = \frac{b^2}{a\Phi^{3/2}} \quad (2)$$

with $\Phi = 1 - e^2 \cos^2 \theta$ and $e^2 = 1 - \left(\frac{b}{a}\right)^2$. The $\frac{dR}{d\theta}$ term of κ_θ is due to the noncircularity of the cross section.

Strain and Kinetic Energies

The strain energy of an isotropic shell of uniform thickness h may be written as follows in terms of the strains and changes of curvature:

$$\begin{aligned} U &= \frac{Eh}{2(1-\mu^2)} \int_0^L \int_0^{2\pi} \left[\epsilon_x^2 + 2\mu\epsilon_x\epsilon_\theta + \epsilon_\theta^2 + 2(1-\mu)\epsilon_{x\theta}^2 \right] R \, d\theta \, dx \\ &+ \frac{Eh^3}{24(1-\mu^2)} \int_0^L \int_0^{2\pi} \left[\kappa_x^2 + 2\mu\kappa_x\kappa_\theta + \kappa_\theta^2 + 2(1-\mu^2)\bar{\kappa}_{x\theta}^2 \right] R \, d\theta \, dx \end{aligned} \quad (3)$$

where E is Young's modulus and μ is Poisson's ratio.

The shell kinetic energy is

$$T = \frac{\rho h}{2} \int_0^L \int_0^{2\pi} (\dot{u}^2 + \dot{v}^2 + \dot{w}^2) R \, d\theta \, dx \quad (4)$$

where ρ is the mass density of the shell.

Modal Functions

Each displacement u , v , or w is assumed to be a finite series, each term of which is the product of circumferential and axial modal functions weighted by an appropriate amplitude coefficient (or generalized coordinate) $q_{mp}(t)$. With the assumption of simple harmonic motion of frequency ω , the assumed displacements may be written as

$$\left. \begin{aligned} u(x, \theta, t) &= \sum_{m=0}^P \sum_{p=0}^Q (\bar{a}_{mp} \cos p\theta + a_{mp} \sin p\theta) X_{mu}(x) e^{i\omega t} \\ v(x, \theta, t) &= \sum_{m=0}^P \sum_{p=0}^Q (\bar{b}_{mp} \sin p\theta - b_{mp} \cos p\theta) X_{mv}(x) e^{i\omega t} \\ w(x, \theta, t) &= \sum_{m=0}^P \sum_{p=0}^Q (\bar{c}_{mp} \cos p\theta + c_{mp} \sin p\theta) X_{mw}(x) e^{i\omega t} \end{aligned} \right\} \quad (5)$$

where \bar{a}_{mp} , \bar{b}_{mp} , and \bar{c}_{mp} are amplitude coefficients for the symmetric modes and a_{mp} , b_{mp} , and c_{mp} are amplitude coefficients for the antisymmetric modes. Upper limits for the series of axial and circumferential modal functions are denoted by P and Q , respectively.

The X_m functions in equations (5) approximate the longitudinal modal components which are chosen to satisfy displacement and slope conditions at the ends of the shell. For example, the conditions of zero displacement for v and w at the ends of a simply (or freely) supported shell without axial constraint are satisfied by the familiar trigonometric functions

$$\left. \begin{aligned} X_{mu} &= \cos \frac{m\pi x}{L} \\ X_{mv} &= X_{mw} = \sin \frac{m\pi x}{L} \end{aligned} \right\} \quad (6)$$

The arbitrary end displacements and slopes of a free-free shell can be satisfied by choosing the following modal functions:

$$\left. \begin{aligned} X_{0u} &= 0 \\ X_{0v} &= X_{0w} = 1 \end{aligned} \right\} \quad (m = 0) \quad (7a)$$

$$\left. \begin{aligned} X_{1u} &= \frac{1}{L} \\ X_{1v} &= X_{1w} = \frac{x}{L} - \frac{1}{2} \end{aligned} \right\} \quad (m = 1) \quad (7b)$$

$$\left. \begin{aligned} X_{mu} &= X'_m \\ X_{mv} &= X_{mw} = X_m = \cosh N_m x + \cos N_m x \\ &\quad - \gamma_m (\sinh N_m x + \sin N_m x) \end{aligned} \right\} \quad (m \geq 2) \quad (7c)$$

where $X'_m = \frac{dX_m(x)}{dx}$ and N_m and γ_m are the eigenvalue properties of a free-free vibrating beam, as tabulated in reference 20, for example. The functions in equations (7c) are essentially the same as those used in reference 18. The existence of the inextensional mode shapes approximated by equations (7a) and (7b) is demonstrated experimentally in this paper and, for free-free circular cylinders, in reference 21.

Derivation of Frequency Equation

With the substitution of equations (1), (5), and (7) into equations (3) and (4), the equations of motion are obtained from the following relations consistent with the Rayleigh-Ritz procedure:

$$\left. \begin{aligned} \frac{\partial}{\partial a_{ij}} [U(x, \theta) - \omega^2 T(x, \theta)] &= \frac{\partial}{\partial b_{ij}} [U(x, \theta) - \omega^2 T(x, \theta)] = \frac{\partial}{\partial c_{ij}} [U(x, \theta) - \omega^2 T(x, \theta)] = 0 \\ \frac{\partial}{\partial a_{ij}} [U(x, \theta) - \omega^2 T(x, \theta)] &= \frac{\partial}{\partial b_{ij}} [U(x, \theta) - \omega^2 T(x, \theta)] = \frac{\partial}{\partial c_{ij}} [U(x, \theta) - \omega^2 T(x, \theta)] = 0 \end{aligned} \right\} \quad (8)$$

The operations represented by equations (8) lead to the familiar eigenvalue-eigenvector formulation which may be expressed in the following general matrix form:

$$\begin{bmatrix} \overline{K}_s & 0 \\ 0 & \overline{K}_a \end{bmatrix} - \Delta \begin{bmatrix} \overline{M}_s & 0 \\ 0 & \overline{M}_a \end{bmatrix} \begin{Bmatrix} q_s \\ q_a \end{Bmatrix} = 0 \quad (9)$$

where \overline{K} and \overline{M} represent square stiffness and mass matrices of size $3(P + 1)$ by $Q + 1$, q denotes an eigenvector, and the subscripts s and a identify symmetric and antisymmetric matrix elements, respectively. The eigenvalue is given by

$$\Delta = \frac{\omega^2 R_0^2 \rho (1 - \mu^2)}{E}$$

The off-diagonal blocks vanish, and equation (9) uncouples into two simpler equations, one for the symmetric and the other for the antisymmetric modes. The equation for the symmetric mode may be put in the form

$$\begin{bmatrix} \overline{A} & \overline{B} & \overline{C} \\ \overline{B}^T & \overline{F} & \overline{G} \\ \overline{C}^T & \overline{G}^T & \overline{H} \end{bmatrix} - \Delta \begin{bmatrix} \overline{\alpha} & 0 & 0 \\ 0 & \overline{\beta} & 0 \\ 0 & 0 & \overline{\gamma} \end{bmatrix} \begin{Bmatrix} \overline{a} \\ \overline{b} \\ \overline{c} \end{Bmatrix} = 0 \quad (10)$$

The equation for the antisymmetric mode is identical except the matrix elements do not have bars. The superscript T denotes the transpose of a matrix. Each letter in the square matrices of equation (10) represents a submatrix, the elements of which are given in detail in appendix A. Longitudinal modal components of the matrix elements for the freely supported shell, based on equations (6), are given in appendix B.

For the circular cylindrical shell ($e = 0$), R is constant and can be considered to be equal to R_0 , and each series of circumferential terms in equations (5) reduces to a single trigonometric function. Equation (10) then gives the same frequencies for symmetric and antisymmetric modes.

ANALYTICAL RESULTS AND COMPARISON WITH EXPERIMENT

The analysis described was applied to the circular and elliptical cylindrical shells of table I. Analytical frequencies of the free-free shells are included along with experimental frequencies in tables II to IV. Analytical mode shapes are presented in figures 7 to 12, and experimental mode shapes are included for comparison in figures 7 and 9 to 11.

Circumferential mode-shape components are presented in figures 7 to 10 and 12, and experimental components included in figure 9 are the topmost mode shapes shown for each frequency in figure 5. Longitudinal mode-shape components are presented in figure 11 for model 4. Experimental nodes obtained with the simplified test apparatus of figure 2 are included in figure 10(a) for model 4. Other frequency comparisons are made in figures 13 and 14.

Elliptical-shell frequencies calculated by the method of the present paper are also compared in table III with frequencies calculated by the method of references 9 to 11. Analytical frequencies of the freely supported shells calculated by the present analysis are given in appendix B and are compared with analytical frequencies of reference 10 in figures 15 and 16.

Convergence of Analytical Results

Shell modes. - In the following table are listed the numbers of the longitudinal and circumferential functions used in each of the displacement series of equations (5) to obtain converged analytical frequencies and mode shapes:

Model	Tables	e	Number of terms in each series of equations (5)	
			Longitudinal	Circumferential
1	II	0	4	a ₁
2	III(a), IV	.526	4	13
3	III(b), IV	.760	4	16
4	III(c), IV	.916	2	32

^a p = n.

The numbers in this table apply to all even-numbered or all odd-numbered modal functions, since, as noted in appendix A, even-numbered and odd-numbered functions do not couple when included together in equation (10). Results were considered to be converged when the analytical frequencies of tables II to IV were negligibly changed with the inclusion of more terms in the series than those in the foregoing table. Beginning with the circular shell (model 1), which required only a single circumferential term in each series, converged solutions for this model were obtained with four terms, including beam-vibration functions, in each longitudinal displacement series, that is, $m = 0, 2, 4, 6$ and $m = 1, 3, 5, 7$ in separate calculations for each circumferential wave number n . (The circular-shell results in table II and in fig. 13 are actually based on five longitudinal modal functions, the fifth term being the beam functions for $m = 8$ and 9 in the foregoing

m sequences.) Analytical circular-shell frequencies of the inextensional modes ($m = 0$ and 1) were negligibly different from those in table II when just a single longitudinal modal function ($m = 0$ or 1) was included in each displacement series.

Next, for the elliptical shells in order of increasing eccentricity, the number of longitudinal terms was held to four, and the number of circumferential terms was increased to achieve convergence. As the foregoing table shows, more circumferential terms were required with increasing eccentricity, and at $e = 0.916$ the number of required terms exceeded the capacity of the computing facility utilized in this study (Control Data 6600 computer system at the Langley Research Center). Hence, the number of longitudinal terms had to be reduced to allow for more circumferential terms, and the combination of two longitudinal and 32 circumferential functions listed in the table gave results that are as close to convergence as could be obtained for this model. This observation is further borne out in comparisons of the analytical frequencies in tables III(c) and IV with those in table V for model 4. Comparison of tables III(c) with V shows frequencies for $m = 0$ and 1 to be satisfactorily converged with a single longitudinal term and 30 circumferential terms. However, it appears from tables IV and V that additional longitudinal terms were needed more than additional circumferential terms to obtain converged results for $m = 2$ and 3 ; and 32 circumferential terms appear to be enough.

Analytical circumferential mode shapes are shown for various modal approximations in figure 12. These mode shapes, together with their corresponding frequencies in table V, show the sensitivity of certain modes to variations in the number of circumferential terms included in each displacement series of equations (5). The existence of dual frequencies at some values of p and none at others also occurred for models 2 and 3, as may be seen in figures 8 and 9(e) to 9(h), and there appears to be no consistency to this behavior other than the increasing number of such modes with increasing eccentricity.

Rigid-body modes. - The lowest frequencies of free-free shells are zero frequencies for six rigid-body modes. These zero frequencies occur at p (or n) = 0 and 1 for the inextensional modal families $m = 0$ and 1 , and in table VI are listed the displacements with zero frequencies for both circular and elliptical shells. Six zeros were obtained for the circular shell regardless of the number of terms in the displacement series, and six zeros were obtained for two of the elliptical shells ($e = 0.526$ and 0.760) with the same number of terms as needed for convergence of the shell modes. As shown in the last column of the table, five zero frequencies were obtained for the remaining high-eccentricity elliptical shell ($e = 0.916$), but the sixth frequency was very low, 1.01 Hz. With only a single modal product in each displacement series, only three rigid-body modes could be obtained for any of the elliptical shells.

Effects of Eccentricity

The close agreement between analytical and experimental frequencies and mode shapes of the circular cylindrical shell (model 1) in table II and figure 7 afforded a satisfactory basis for evaluating eccentricity effects of the elliptical shells. Both analytical and experimental frequencies and the corresponding circumferential mode shapes of the elliptical shells showed greater distortions from sinusoidal-type responses as eccentricity increased. Tables III and IV show generally good frequency agreement over the eccentricity range of the models, and corresponding analytical and experimental mode shapes in figures 9 and 10 are fairly well correlated. This correlation is clearly better for the low-frequency inextensional modes than it is for the higher frequency modes, particularly those involving $m = 2$ and 3 . Experimental mode shapes are compared, somewhat arbitrarily, with analytical symmetric or antisymmetric mode shapes according to shaker position as indicated in figure 9, although, as previously noted, most modes involving $m = 2$ and 3 had both symmetric and antisymmetric characteristics regardless of shaker position. For the experimental mode shapes included in figure 10(b), the shaker was located at the end of the minor axis.

Variations of frequency with mode numbers are shown in figure 13 for eccentricities of zero (model 1) and 0.526 (model 2). Similar plots for the higher eccentricity shells were found to be impracticable because of the dual frequency behavior noted earlier. This property for model 2 is identified in the right-hand plot of figure 13 by the missing analytical frequency for $m = 3, p = 10$ and the second analytical frequency at $m = 3, p = 12$ (denoted by ■).

Eccentricity effects on both experimental and analytical frequencies are summarized in figure 14. Except for the experimental inextensional frequencies for $e = 0.526$ (table III(a)), a general decrease in frequency occurred with increasing eccentricity, and this decrease was largest for $e \geq 0.760$ (or $a/b \geq 1.538$). This effect was much smaller for the inextensional modes than for the minimum frequencies of $m = 2$ and 3 which, at $e = 0.916$, were approximately 40 percent lower than the minimum circular-shell frequencies. For $e = 0.526$, there was a slight, though consistent, rise in most experimental inextensional frequencies of about 2 or 3 percent, which was not predicted by the analysis.

Comparisons With Other Methods

Inextensional frequencies calculated by the methods of references 9 to 11 are included in table III and appear to be in almost as good agreement with experimental frequencies as are the frequencies calculated by the present analysis, at least for $e \leq 0.760$. The methods of references 9 and 10 are based on approximations to the noncircular radius of curvature that are contained in the terms of power series which include the

circular-shell frequency as the first term. The method of reference 9 is valid for $a/b < 2.06$ and is thus not applicable to $e = 0.916$ ($a/b = 2.5$) in the present study. The noncircular terms of reference 10 are based on a Fourier series representation of the radius of curvature in which the coefficients of the series may be obtained by approximating the noncircular cross section by two pairs of circular arcs, each having a different radius. By following the recommendations of both of these references, the frequencies in the two right columns of table III were obtained by retaining only a single noncircular power-series term, other than the circular-shell frequency, in the frequency equation. Most of the frequencies calculated in reference 9 are seen to be somewhat higher than those calculated in reference 10, the differences for $e = 0.760$ being greater than those for $e = 0.526$. (Compare tables III(a) and (b).)

The applicable frequency equation of reference 11 is essentially the circular-shell equation for $m = 1$ with the radius of curvature approximated by an average value based on the semimajor and semiminor axes of the elliptical shell. The frequencies given by this method are in about as good agreement with experiment as those of references 9 and 10 for $e = 0.526$ and 0.760 and tend to be slightly higher than those of the present analysis and reference 10 at higher values of p . However, the agreement at $e = 0.916$ is clearly poorest of all the methods considered, the discrepancy being as much as 14 percent (at $p = 5$).

CONCLUDING REMARKS

This paper reports a vibration study of free-free aluminum elliptical cylindrical shells of constant mass over a range of cross-sectional eccentricities from zero (circular shell) to 0.916 (corresponding to a major-to-minor axis ratio of 2.5). With increased eccentricity over this range, shell frequencies were reduced by as much as 40 percent. Experimental resonant frequencies, normal-displacement node locations, and mode shapes were obtained by use of an air-jet shaker or an electrodynamic shaker with a noncontact inductance proximity sensor that could be moved over most of the shell surface. Experimental frequencies are in generally good agreement with analytical frequencies calculated by means of a Rayleigh-Ritz type of analysis featuring multiterm longitudinal and circumferential modal expansions. Single longitudinal functions in each of the shell displacement series were sufficient to obtain converged results for the two families of inextensional free-free modes (longitudinal mode numbers of 0 and 1). Four longitudinal terms, including beam-vibration functions, were required in the series to obtain converged results for the next two higher order longitudinal modes (longitudinal mode numbers of 2 and 3). Along with these longitudinal approximations, an increasing number of circumferential trigonometric terms were required for convergence with

increasing eccentricity, and as many as 32 circumferential terms were required for the highest eccentricity shell.

As eccentricity increased, fewer higher order experimental shell vibration modes could be identified exclusively according to longitudinal and circumferential mode numbers, and there were more higher order analytical modes having two frequencies for each pair of longitudinal and circumferential mode numbers. Analytical circumferential mode shapes shed further light on this modal coupling and dual frequency behavior by indicating the presence of more than one longitudinal and/or circumferential mode in each mode shape.

Frequencies calculated by methods involving various approximations to the non-circular curvature are in good agreement with both experimental and analytical inextensional frequencies of the present study for eccentricities up to 0.760 (corresponding to a major-to-minor axis ratio of 1.538).

Langley Research Center,
National Aeronautics and Space Administration,
Hampton, Va., September 30, 1970.

APPENDIX A

MATRIX ELEMENTS AND INTEGRALS IN RAYLEIGH-RITZ VIBRATION ANALYSIS

This appendix contains detailed expressions of the matrix elements in equation (10). Also included are the circumferential and longitudinal integrals involved in these elements. The circumferential integrals were evaluated numerically by use of a 10-point Gaussian quadrature method with 20 subintervals for a total of 200 integrating stations.

The matrix elements in equation (10) may be written as follows for the symmetric modes of an elliptical cylindrical shell:

$$\bar{A}_{ijmp} = \frac{b^2}{a} \bar{I}_1 J_1 + \frac{a}{b^2} jp \frac{1-\mu}{2} \bar{I}_2 J_2 + \left(\frac{a}{b^2}\right)^3 jp \frac{h^2(1-\mu)}{96} \bar{I}_3 J_2 \quad (\text{A1a})$$

$$\bar{B}_{ijmp} = \pi \delta_{jp} \left(p\mu J_3 - j \frac{1-\mu}{2} J_4 \right) + \left(\frac{a}{b^2}\right)^2 \frac{jh^2(1-\mu)}{32} \bar{I}_4 J_4 \quad (\text{A1b})$$

$$\bar{C}_{ijmp} = \pi \mu \delta_{jp} (1 + \delta_{0j} \delta_{0p}) J_5 + \left(\frac{a}{b^2}\right)^2 jp \frac{h^2(1-\mu)}{24} \bar{I}_4 J_6 \quad (\text{A1c})$$

$$\bar{F}_{ijmp} = \frac{a}{b^2} jp \bar{I}_5 J_7 + \frac{b^2}{a} \frac{1-\mu}{2} \bar{I}_6 J_8 + \left(\frac{a}{b^2}\right)^3 \frac{h^2}{12} \bar{I}_7 J_7 + \frac{a}{b^2} \frac{3h^2(1-\mu)}{32} \bar{I}_2 J_8 \quad (\text{A1d})$$

$$\bar{G}_{ijmp} = \frac{a}{b^2} j \bar{I}_5 J_9 - \frac{a}{b^2} \frac{h^2}{12} \mu \bar{I}_8 J_{10} + \left(\frac{a}{b^2}\right)^3 \frac{h^2}{12} p \bar{I}_7 J_9 + \frac{a}{b^2} \frac{ph^2(1-\mu)}{8} \bar{I}_2 J_{11} \quad (\text{A1e})$$

$$\begin{aligned} \bar{H}_{ijmp} = & \frac{a}{b^2} \bar{I}_5 J_{12} + \frac{b^2}{a} \frac{h^2}{12} \bar{I}_1 J_{13} - \frac{a}{b^2} \frac{h^2}{12} \mu \left(j \bar{I}_8 J_{14} + p \bar{I}_9 J_{15} \right) + \left(\frac{a}{b^2}\right)^3 \frac{h^2}{12} jp \bar{I}_7 J_{12} \\ & + \frac{a}{b^2} jp \frac{h^2(1-\mu)}{6} \bar{I}_2 J_{16} \end{aligned} \quad (\text{A1f})$$

APPENDIX A – Continued

$$\bar{\alpha}_{ijmp} = \frac{b^2}{aR_0^2} \bar{I}_1 J_2 \quad (\text{A2a})$$

$$\bar{\beta}_{ijmp} = \frac{b^2}{aR_0^2} \bar{I}_6 J_7 \quad (\text{A2b})$$

$$\bar{\gamma}_{ijmp} = \frac{b^2}{aR_0^2} \bar{I}_1 J_{12} \quad (\text{A2c})$$

where \bar{I} is a circumferential integral and J is a longitudinal integral and where δ_{jp} , δ_{0j} , and δ_{0p} denote Kronecker delta functions of the form

$$\delta_{kl} = \begin{cases} 1 & (k = l) \\ 0 & (k \neq l) \end{cases}$$

for $k, l = 0, 1, 2, \dots, j, p$.

The circumferential integrals are defined as follows:

$$\bar{I}_1 = \int_0^{2\pi} \Phi^{-3/2} \cos j\theta \cos p\theta \, d\theta \quad (\text{A3a})$$

$$\bar{I}_2 = \int_0^{2\pi} \Phi^{3/2} \sin j\theta \sin p\theta \, d\theta \quad (\text{A3b})$$

$$\bar{I}_3 = \int_0^{2\pi} \Phi^{9/2} \sin j\theta \sin p\theta \, d\theta \quad (\text{A3c})$$

$$\bar{I}_4 = \int_0^{2\pi} \Phi^3 \sin j\theta \sin p\theta \, d\theta \quad (\text{A3d})$$

$$\bar{I}_5 = \int_0^{2\pi} \Phi^{3/2} \cos j\theta \cos p\theta \, d\theta \quad (\text{A3e})$$

$$\bar{I}_6 = \int_0^{2\pi} \Phi^{-3/2} \sin j\theta \sin p\theta \, d\theta \quad (\text{A3f})$$

APPENDIX A – Continued

$$\bar{I}_7 = \int_0^{2\pi} \Phi^{9/2} \left(j \cos j\theta + \frac{3}{2} e^{2\Phi-1} \sin 2\theta \sin j\theta \right) \left(p \cos p\theta + \frac{3}{2} e^{2\Phi-1} \sin 2\theta \sin p\theta \right) d\theta \quad (\text{A3g})$$

$$\bar{I}_8 = \int_0^{2\pi} \Phi^{3/2} \left(j \cos j\theta + \frac{3}{2} e^{2\Phi-1} \sin 2\theta \sin j\theta \right) \cos p\theta d\theta \quad (\text{A3h})$$

$$\bar{I}_9 = \int_0^{2\pi} \Phi^{3/2} \cos j\theta \left(p \cos p\theta + \frac{3}{2} e^{2\Phi-1} \sin 2\theta \sin p\theta \right) d\theta \quad (\text{A3i})$$

The antisymmetric matrix elements are identical in form to equations (A1) and (A2) and are obtained by simply interchanging $\sin j\theta$, $\sin p\theta$ for $\cos j\theta$, $\cos p\theta$ in equations (A3). In addition,

$$C_{ijmp} = \pi\mu \delta_{jp} \left(1 - \delta_{0j}\delta_{0p} \right) J_5 + \left(\frac{a}{b^2} \right)^2 j^p \frac{h^2(1-\mu)}{24} I_4 J_6 \quad (\text{A4})$$

For both symmetric and antisymmetric matrix elements, it can be shown that the integrals in equations (A3) vanish if $j \pm p$ is odd and have values if $j \pm p$ is even (i.e., $j, p = 0, 2, 4, \dots$ or $1, 3, 5, \dots$). Thus, two calculations must be made in every application of the analysis for symmetric or antisymmetric modes, one for all even circumferential modal functions and another for all odd functions.

Longitudinal Integrals for Arbitrary End Conditions

The longitudinal integrals are defined by the following general expressions, which can be evaluated in closed form for particular choices of modal functions and end conditions:

$$\left. \begin{aligned} J_1 &= \int_0^L X'_{iu} X'_{mu} dx & J_5 &= \int_0^L X'_{iu} X_{mw} dx \\ J_2 &= \int_0^L X_{iu} X_{mu} dx & J_6 &= \int_0^L X_{iu} X'_{mw} dx \\ J_3 &= \int_0^L X'_{iu} X_{mv} dx & J_7 &= \int_0^L X_{iv} X_{mv} dx \\ J_4 &= \int_0^L X_{iu} X'_{mv} dx & J_8 &= \int_0^L X'_{iv} X'_{mv} dx \end{aligned} \right\} \quad (\text{A5})$$

(Equations continued on next page)

APPENDIX A - Continued

$$\left. \begin{aligned}
 J_9 &= \int_0^L X_{iv} X_{mw} dx & J_{13} &= \int_0^L X_{iw}'' X_{mw}'' dx \\
 J_{10} &= \int_0^L X_{iv} X_{mw}'' dx & J_{14} &= \int_0^L X_{iw} X_{mw}'' dx \\
 J_{11} &= \int_0^L X_{iv}' X_{mw}' dx & J_{15} &= \int_0^L X_{iw}'' X_{mw} dx \\
 J_{12} &= \int_0^L X_{iw} X_{mw} dx & J_{16} &= \int_0^L X_{iw}' X_{mw}' dx
 \end{aligned} \right\} \quad (A5)$$

Longitudinal Integrals for Free-Free Shell

With the ends of the cylindrical shell free and the longitudinal modal functions given by equations (7), the integrals in equations (A5) reduce to the following forms on the basis of reference 22:

$i = 0$ (eq. (7a)):

$$\left. \begin{aligned}
 J_1 = J_2 = J_3 = J_4 = J_5 = J_6 = J_8 = J_{11} = J_{13} = J_{15} = J_{16} &= 0 && \text{(All values of } m) \\
 J_7 = J_9 = J_{12} &= \begin{cases} 0 & (i \neq m) \\ L & (i = m) \end{cases} \\
 J_{10} = J_{14} &= \begin{cases} 2N_m \gamma_m [1 - (-1)^{m+1}] & (m \geq 2) \\ 0 & (m = 0, 1) \end{cases}
 \end{aligned} \right\} \quad (A6a)$$

$i = 1$ (eq. (7b)):

$$\left. \begin{aligned}
 J_1 = J_3 = J_5 = J_{13} = J_{15} &= 0 && \text{(All values of } m) \\
 J_2 = J_4 = J_6 = J_8 = J_{11} = J_{16} &= \begin{cases} 0 & (m = 0) \\ \frac{1}{L} & (i = m) \\ -\frac{2}{L} [1 + (-1)^{m+1}] & (m \geq 2) \end{cases}
 \end{aligned} \right\} \quad (A6b)$$

(Equations continued on next page)

APPENDIX A – Concluded

$$\begin{aligned}
 J_7 = J_9 = J_{12} &= \begin{cases} 0 & (i \neq m) \\ \frac{L}{12} & (i = m) \end{cases} \\
 J_{10} = J_{14} &= \begin{cases} 2N_m\gamma_m [1 - (-1)^{m+1}] & (m \geq 2) \\ 0 & (i = m) \\ 0 & (m = 0) \end{cases}
 \end{aligned} \tag{A6b}$$

$i, m \geq 2$ (eq. (7c)):

$$\begin{aligned}
 J_1 = J_{13} &= \begin{cases} 0 & (i \neq m) \\ N_m^4 L & (i = m) \end{cases} \\
 J_2 = J_4 = J_6 = J_8 = J_{11} = J_{16} &= \begin{cases} \frac{4N_i N_m (\gamma_i N_m^3 - \gamma_m N_i^3)}{N_m^4 - N_i^4} [(-1)^{i+m} + 1] & (i \neq m) \\ N_m \gamma_m (\gamma_m N_m L + 6) & (i = m) \end{cases} \\
 J_3 = J_5 = J_{15} &= \begin{cases} \frac{4N_i^4 (\gamma_m N_m - \gamma_i N_i)}{N_m^4 - N_i^4} [(-1)^{i+m} + 1] & (i \neq m) \\ N_m \gamma_m (2 - \gamma_m N_m L) & (i = m) \end{cases} \\
 J_7 = J_9 = J_{12} &= \begin{cases} 0 & (i \neq m) \\ L & (i = m) \end{cases} \\
 J_{10} = J_{14} &= \begin{cases} \frac{4N_m^4 (\gamma_i N_i - \gamma_m N_m)}{N_i^4 - N_m^4} [(-1)^{i+m} + 1] & (i \neq m) \\ N_m \gamma_m (2 - \gamma_m N_m L) & (i = m) \end{cases}
 \end{aligned} \tag{A6c}$$

The coupling characteristics noted in the body of the paper are implicit in equations (A6), namely, the integrals vanish if $i \pm m$ is odd and have values if $i \pm m$ is even (i.e., $i, m = 0, 2, 4, \dots$ or $1, 3, 5, \dots$).

APPENDIX B

APPLICATION OF ANALYSIS TO FREELY SUPPORTED ELLIPTICAL SHELLS

This appendix demonstrates the application of the elliptical-shell vibration analysis developed in the body of the paper to the models of table I with assumed freely supported end conditions. With the use of equations (6), each series of longitudinal terms in equations (5) reduces to a single trigonometric function. The integrals in equations (A5) used in equations (A1) and (A2) thus reduce to the following for this end condition:

$$J_1 = J_8 = J_{11} = J_{16} = \frac{(m\pi)^2}{2L} \quad (\text{B1a})$$

$$J_2 = J_7 = J_9 = J_{12} = \frac{L}{2} \quad (\text{B1b})$$

$$J_3 = J_5 = -\frac{m\pi}{2} \quad (\text{B1c})$$

$$J_4 = J_6 = \frac{m\pi}{2} \quad (\text{B1d})$$

$$J_{10} = J_{14} = J_{15} = -\frac{(m\pi)^2}{2L} \quad (\text{B1e})$$

$$J_{13} = \frac{(m\pi)^4}{2L^3} \quad (\text{B1f})$$

where, for this end condition, m is defined as the number of longitudinal (or axial) half-waves. The reduction of each series of longitudinal terms in equations (5) to a single trigonometric function is due to the relations

$$\int_0^L \sin \frac{i\pi x}{L} \sin \frac{m\pi x}{L} dx = \int_0^L \cos \frac{i\pi x}{L} \cos \frac{m\pi x}{L} dx = 0 \quad (i \neq m)$$

By use of equations (B1) and equations (6) in equation (10), calculated frequencies were obtained for the models of table I with the same numbers of circumferential terms as those used for the free-free models. Results are given in tables VII and VIII and are compared in figures 15 and 16 with frequencies calculated by reference 10. The two sets of results are seen to be in close agreement, and the decrease in frequency with increasing eccentricity is similar to that found for the free-free shells for $m = 2$ and 3.

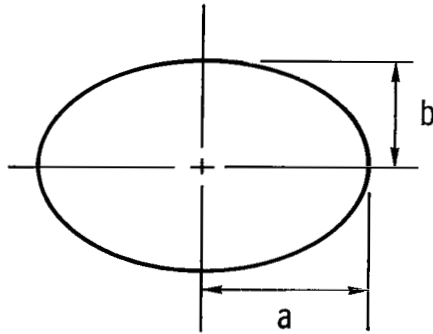
REFERENCES

1. Romano, Frank; and Kempner, Joseph: Stresses in Short Noncircular Cylindrical Shells Under Lateral Pressure. *Trans. ASME, Ser. E: J. Appl. Mech.*, vol. 29, no. 4, Dec. 1962, pp. 669-674.
2. Vafakos, William P.; Nissel, Neil; and Kempner, Joseph: Pressurized Oval Cylinders With Closely Spaced Rings. *AIAA J.*, vol. 4, no. 2, Feb. 1966, pp. 338-345.
3. Nissel, N. B.; and Vafakos, W. P.: Asymptotic Solution for Short Ring-Reinforced Oval Cylinders. *AIAA J.*, vol. 6, no. 1, Jan. 1968, pp. 133-140.
4. Mah, Gordon B. J.: Numerical Analysis of Noncircular Cylindrical Shells. *J. of Eng. Mech. Div., Amer. Soc. Civil Eng.*, vol. 93, no. EM3, June 1967, pp. 219-237.
5. Boyd, Donald E.: Analysis of Open Noncircular Cylindrical Shells. *AIAA J.*, vol. 7, no. 3, Mar. 1969, pp. 563-565.
6. Herrmann, G.; and Mirsky, I.: On Vibrations of Cylindrical Shells of Elliptic Cross-Section. *Tech. Note No. 5, CU-17-57-AF-1247-CE, Columbia Univ.*, Dec. 1957.
7. Klosner, Jerome M.; and Pohle, Frederick V.: Natural Frequencies of an Infinitely Long Noncircular Cylindrical Shell. *PIBAL Rep. No. 476 (Contract No. Nonr 839(17))*, Polytech. Inst. Brooklyn, July 1958.
8. Klosner, Jerome M.: Frequencies of an Infinitely Long Noncircular Cylindrical Shell. Pt. II - Plane Strain, Torsional and Flexural Modes. *PIBAL Rep. No. 552 (Contract No. Nonr 839(17))*, Polytech. Inst. Brooklyn, Dec. 1959.
9. Klosner, Jerome M.: Free and Forced Vibrations of a Long Noncircular Cylindrical Shell. *PIBAL Rep. No. 561 (Contract No. Nonr 839(17))*, Polytech. Inst. Brooklyn, Sept. 1960.
10. Malkina, R. L.: Vibrations of Noncircular Cylindrical Shells. *Lockheed Missiles & Space Co. Transl. (From Izv. Akad. Nauk SSSR, Mekhan. Mashinostr., No. 1, 1960, pp. 172-175)*.
11. Sal'nikov, G. M.; and Zenukov, A. G.: Determination of the Natural Oscillating Frequencies of Shells of Complex Shape With Free Edges. *NASA TT F-11,719, 1968*.
12. Hung, F. C.; Park, A. C.; Chan, C.; Andrew, L. V.; and Au, L. L. T.: Dynamics of Shell-Like Lifting Bodies. Part II. The Experimental Investigation. *AFFDL-TR-65-17, Pt. II, U.S. Air Force, June 1965. (Available from DDC as AD 620 699.)*
13. Ivanyuta, E. I.; and Finkel'shteyn, R. M.: Determination of the Free Oscillations of a Cylindrical Shell of Elliptical Cross Section. *NASA TT F-12,548, 1969*.

14. Kurt, Carl E.; and Boyd, Donald E.: Free Vibrations of Noncircular Cylindrical Shell Segments. AIAA J., vol. 9, no. 2, Feb. 1971.
15. Naumann, Eugene C.; and Flagge, Bruce: A Noncontacting Displacement Measuring Technique and Its Application to Current Vibration Testing. Preprint No. 16.18-5-66, Instrum. Soc. Amer., Oct. 1966.
16. Herr, Robert W.: A Wide-Frequency-Range Air-Jet Shaker. NACA TN 4060, 1957.
17. Mixson, John S.: Experimental Modes of Vibration of 14° Conical-Frustum Shells With Free Ends. NASA TN D-4428, 1968.
18. Warburton, G. B.: Vibration of Thin Cylindrical Shells. J. Mech. Eng. Sci., vol. 7, no. 4, Dec. 1965, pp. 399-407.
19. Sanders, J. Lyell, Jr.: An Improved First-Approximation Theory for Thin Shells. NASA TR R-24, 1959.
20. Young, Dana; and Felgar, Robert P., Jr.: Tables of Characteristic Functions Representing Normal Modes of Vibration of a Beam. Publ. No. 4913, Eng. Res. Ser. No. 44, Bur. Eng. Res., Univ. of Texas, July 1, 1949.
21. Grinsted, B.: Communications on the Flexural Vibrations of Thin Cylinders. Proc. Inst. Mech. Eng., vol. 167, no. 1, 1953, pp. 75-77.
22. Felgar, Robert P., Jr.: Formulas for Integrals Containing Characteristic Functions of a Vibrating Beam. Circ. No. 14, Bur. Eng. Res., Univ. of Texas, 1950.

TABLE I.- PROPERTIES OF CYLINDRICAL SHELLS

[$E = 10^7 \text{ lb/in}^2$ (68.95 GN/m²); $\mu = 0.3$; $\rho = 2.588 \times 10^{-4} \text{ lb-sec}^2/\text{in}^4$ (2768 kg/m³);
 $L = 24 \text{ inches}$ (61.0 cm); $h = 0.032 \text{ inch}$ (0.813 mm)]



Model	a	b	a/b	e
1	12.00 in. (30.50 cm)	12.00 in. (30.50 cm)	1.0	0
2	12.95 in. (32.90 cm)	11.01 in. (27.97 cm)	1.176	0.526
3	14.39 in. (36.55 cm)	9.35 in. (23.75 cm)	1.538	0.760
4	16.39 in. (41.63 cm)	6.56 in. (16.66 cm)	2.50	0.916

TABLE II. - EXPERIMENTAL AND ANALYTICAL FREQUENCIES
OF FREE-FREE CIRCULAR CYLINDRICAL SHELL

n	Frequency, Hz							
	m = 0		m = 1		m = 2		m = 3	
	Analysis	Experiment	Analysis	Experiment	Analysis	Experiment	Analysis	Experiment
0					^a 2733.0		^a 2594.0	
1	0		^a 2014.00		^a 2293.0		^a 2494.0	
2	5.645	5.6	7.54	7.7	1616.0		2101.0	
3	16.0	15.6	19.0	18.9	1068.0		1709.0	
4	30.6	30.0	34.2	35.7	717.8		1340.0	
5	49.5	48.9	53.4	53.0	504.8		1045.0	
6	72.6	72.0	76.7	76.4	375.6	^b 377.3	823.5	
7	100.0	99.3	104.1	103.8	299.9	299.1	663.4	
8	131.5	131.0	135.7	135.3	262.2	^c 257.4 262.1	551.4	
9	167.25	166.9 ^f 167.2	171.5	^d 170.7	253.4	^e 248.8 249.3	477.8	484.4
10	207.2	206.9	211.5	210.2	266.3	268.8	436.3	
11	251.4	250.5	255.7	253.0	294.7	290.9	421.8	422.1 425.6
12	299.7	^e 301.6	304.1	305.5	334.0	327.6	429.4	438.3
13	352.3	352.1	356.7	352.0	381.1		454.5	453.2
14	409.1	410.8	413.5	^g 412.5	434.7	436.6	493.1	493.3

^aExtensional frequency.

^bCoupled with $n = 13$.

^cCoupled with $n = 9$.

^dMaximum frequency with air shaker.

^eCoupled with $n = 10$.

^fMinimum frequency with electric shaker.

^gCoupled with $m = 3, n = 13$.

TABLE III. - EXPERIMENTAL AND ANALYTICAL INEXTENSIONAL FREQUENCIES
OF FREE-FREE ELLIPTICAL CYLINDRICAL SHELLS

(a) $\frac{a}{b} = 1.176, e = 0.526$

Frequency, Hz, at $m = 0$ from -						
p	^a Experiment		Present analysis		Reference 9	Reference 10
	Symmetric	Antisymmetric	Symmetric	Antisymmetric		
0						0
1						7.7×10^{-5}
2	5.6	5.6	5.62	5.68	5.92	5.56
3	16.1	16.2	15.89	15.89	16.3	15.4
4	30.9	30.8	30.52	30.52	31.2	31.1
5	50.1	50.1	49.41	49.41	50.3	50.45
6	74.8	74.4	72.54	72.54	73.8	71.6
7	102.4	102.4	99.87	99.87	101.5	98.9
8	134.6		131.4	134.4	133.5	133.2
9	171.5	171.7	167.2	167.2	169.8	168.1
10	212.5	212.8	207.1	207.1	210.3	204.8
11	258.8	258.4	251.3	251.3	255.2	251.1
12	312.1		299.6	299.6	304.2	302.8
13	363.8	362.3 363.0	352.2	352.2	357.5	351.9
14	423.2		409.0	409.0	415.2	405.8

Frequency, Hz, at $m = 1$ from -						
p	^a Experiment		Present analysis		Reference 10	Reference 11
	Symmetric	Antisymmetric	Symmetric	Antisymmetric		
0			^b 2576.00		(c)	0
1			^b 1886.00	^b 2148.00	(c)	0
2	7.7	7.8	7.52	7.55	6.13	6.25
3	19.1	19.1	18.94	18.94	16.2	16.9
4	34.6		34.10	34.11	32.0	33.5
5	54.3	54.3	53.28	53.28	51.5	50.7
6	79.5	78.9	76.56	76.56	72.6	73.9
7	106.8	106.9	104.0	104.0	100.0	101.4
8	138.9		135.6	135.6	134.3	133.0
9	174.8	175.4	171.4	171.4	169.2	168.9
10	215.9	216.3	211.4	211.4	205.9	209.0
11	261.7	261.8	255.6	255.6	252.2	253.3
12			304.0	304.0	303.9	301.9
13			356.6	356.6	353.0	354.7
14	430.1		413.4	413.4	406.9	411.7

^aFrequencies for $p \leq 5$ obtained with air shaker.

^bExtensional frequency.

^cNegative eigenvalue.

TABLE III.- EXPERIMENTAL AND ANALYTICAL INEXTENSIONAL FREQUENCIES
OF FREE-FREE ELLIPTICAL CYLINDRICAL SHELLS - Continued

(b) $\frac{a}{b} = 1.538, e = 0.760$

Frequency, Hz, at $m = 0$ from -						
p	Experiment		Present analysis		Reference 9	Reference 10
	Symmetric	Antisymmetric	Symmetric	Antisymmetric		
0			^a 2554.00			0
1			0	^a 4821.00		1.02×10^{-4}
2	5.1	5.7	5.47	5.89	7.28	4.90
3	15.0	14.9	15.5	15.5	18.1	16.4
4	29.2	29.3	29.9	30.0	34.1	31.8
5	^b 48.0 ^c 48.3	^b 48.0 ^c 48.4	48.8	48.8	54.7	46.9
6	71.0	71.2	71.85	71.9	80.0	74.4
7	98.1	98.0	99.2	99.2	109.9	101.2
8	129.4	129.5	130.7	130.7	144.4	127.4
9	164.9	164.9	166.4	166.4	183.5	171.1
10	^d 203.4		206.3	206.3	227.2	207.4
11	248.8	248.9	250.5	250.5	275.5	246.5
12	295.6	296.3	298.9	298.9	328.4	305.9

Frequency, Hz, at $m = 1$ from -						
p	Experiment		Present analysis		Reference 10	Reference 11
	Symmetric	Antisymmetric	Symmetric	Antisymmetric		
0			^a 2336.00		(e)	0
1			^a 1694.00	^a 2343.00	(e)	0
2	7.5	7.3	7.40	7.59	5.40	6.35
3	18.1	17.8	18.5	18.5	17.2	17.2
4	32.6	32.9	33.5	33.5	32.8	32.2
5	^b 51.0 ^c 52.0	^b 51.8 ^c 52.8	52.6	52.6	47.8	51.6
6	74.9	74.9	75.8	75.8	75.5	75.3
7	101.6	101.9	103.3	103.2	102.2	103.2
8	133.1	132.9	134.9	134.9	128.4	135.5
9	168.6	168.2	170.6	170.6	172.2	172.0
10		^f 207.9	210.6	210.6	208.4	212.9
11	253.3	253.1	254.8	254.8	247.5	258.0
12	301.7	301.4	303.3	303.3	307.0	307.5

^aExtensional frequency.

^bMaximum frequency with air shaker.

^cMinimum frequency with electric shaker.

^dCoupled with $m = 2, p = 9$.

^eNegative eigenvalue.

^fCoupled with $m = 2$.

TABLE III.- EXPERIMENTAL AND ANALYTICAL INEXTENSIONAL FREQUENCIES
OF FREE-FREE ELLIPTICAL CYLINDRICAL SHELLS - Concluded

(c) $\frac{a}{b} = 2.5, e = 0.916$

Frequency, Hz, at $m = 0$ from -						
p	Experiment		Present analysis		Reference 10	
	Symmetric	Antisymmetric	Symmetric	Antisymmetric		
0			^a 2584.00		0	
1			0	^a 5346.00	4.71×10^{-5}	
2	4.8		5.13	6.79	5.39	
3	14.0	13.7	14.4	14.4	16.6	
4	27.4	28.5	28.2	29.0	29.3	
5	^b 46.3	^b 45.8 ^c 46.9	46.7	46.5	51.5	
6	69.2	69.9	69.2	69.7	69.7	
7	96.4	96.0	96.4	96.2	103.7	
8	126.9	128.3	127.5	127.8	126.7	
9	163.1	^d 162.7	163.1	163.0	172.9	
10	202.6	203.0	202.9	203.1	200.6	
11	246.5	247.4	247.1	247.0	258.6	
12	297.1	296.8	295.4	295.5	291.8	

Frequency, Hz, at $m = 1$ from -						
p	Experiment		Present analysis		Reference 10	Reference 11
	Symmetric	Antisymmetric	Symmetric	Antisymmetric		
0			^a 3700.00		(e)	0
1			^a 1401.00	^a 2525.00	(e)	0
2	7.2	7.4	7.11	7.74	5.94	6.76
3	^b 17.2 ^c 18.0	^b 16.2	17.3	17.2	17.5	18.3
4	^b 30.9	^b 31.4	31.7	32.1	30.2	34.4
5	^b 49.0 ^c 51.4	^b 49.9 ^c 49.5	50.3	50.2	52.6	55.1
6	72.9	73.1	73.1	73.4	70.7	80.5
7	100.0	100.4	100.3	100.2	104.8	110.4
8	130.7	130.8	131.6	131.8	127.7	144.9
9	167.1	167.3	167.6	167.2	174.0	184.0
10	206.4	204.8	207.1	207.3	201.6	227.7
11	^f 256.6	^g 250.3 ^g 260.0	251.3	251.2	259.75	276.0
12	301.4	300.9	299.6	299.7	292.8	329.0

^aExtensional frequency.

^bObtained with air shaker.

^cObtained with electric shaker.

^dStrongly coupled with $m = 1, p = 8$.

^eNegative eigenvalue.

^fCoupled with $m \geq 2$.

^gCircumferential nodes (i.e., for $m = 1$) at opposite ends of shell.

TABLE IV.- EXPERIMENTAL AND ANALYTICAL FREQUENCIES OF FREE-FREE ELLIPTICAL CYLINDRICAL SHELLS

Frequency, Hz, for $\frac{a}{b} = 1.176, e = 0.526$				Frequency, Hz, for $\frac{a}{b} = 1.538, e = 0.760$				Frequency, Hz, for $\frac{a}{b} = 2.5, e = 0.916$								
Experiment	Analysis	Experiment	Analysis	Experiment	Analysis	Experiment	Analysis	Experiment	Analysis	Experiment	Analysis	Experiment	Analysis			
		362.3														
212.5	207.1	363.0	352.2		496.6	200.7	332.3	330.6		475.6	148.1		278.9	405.4		
				^a 508.2												
212.8	207.1	363.8	352.2		496.6	201.7	206.3	343.6	345.3	476.2	151.5	165.6	279.5	409.6		
215.9	211.4		356.6		500.9	203.4	206.3	344.5	345.3	476.2	158.4	165.6	260.6	279.5	409.7	
216.3	211.4		356.6		500.9	207.9	210.6		345.4	461.5			296.8	295.4	411.7	
241.4	244.1	375.9	373.8			208.4	210.6	347.9		477.7	163.2		297.1	295.5	412.3	
241.8	244.1	376.6	373.8			211.9	213.9	349.5	351.7	484.5	167.1	167.2	300.9	299.6	423.0	431.9
250.6	246.5	390.6	381.5				213.9		351.7	484.5	167.3	167.6	301.4	299.7		432.2
	246.5	391.0	381.5			218.4	214.0		356.0		202.6	202.9		327.9		476.7
258.4	251.3		400.6				214.0		356.0		203.0	203.1		327.9		476.9
258.8	251.3		400.6			248.8	250.5	362.2	366.6		204.8	207.1		328.4		478.7
261.7	255.6		401.6			248.9	250.5	367.2	366.6		206.4	207.3		328.4		479.0
261.8	255.6		401.6			253.1	254.8		383.8			217.6		340.6		
^a 279.7	274.4	423.1	409.0			253.3	254.8	380.8	383.8			217.6		340.6		
	274.4	423.2	409.0				264.3	399.4	410.2		209.1	219.2		347.8		
						259.2	264.3		401.0	410.2		219.2		347.9		
304.5	292.1	430.1	413.4			265.2	268.8	403.9	410.5		246.5	247.0		352.2		
	292.1		413.4				268.8		410.5		247.4	247.1		352.3		
312.1	299.6	445.8	434.8				268.8		410.5		250.3	251.2		356.5		
	299.6	450.9	434.8			295.6	298.9		411.9		255.1	251.3	360.6	356.5		
	304.0		444.6			296.3	298.9	418.0	411.9		256.6	265.3	363.0	398.6		
295.7	304.0		444.6			301.4	303.3		414.7			265.3		398.7		
297.9	304.4	465.0	452.8			301.7	303.3		414.7			265.4		399.4		
306.7	304.4	466.3	452.8				311.5	440.4	438.1			260.0				
						308.5			438.1							
340.3							311.5		438.1			265.4		399.4		
341.4	334.8	476.1	484.2													
343.7	334.8	^a 491.0	484.2			323.4	330.6		475.6		260.4	278.9		405.3		

^aObscure circumferential nodal pattern.

TABLE V.- CONVERGENCE CHARACTERISTICS FOR
 VARIOUS CIRCUMFERENTIAL MODAL
 APPROXIMATIONS WITH A SINGLE
 LONGITUDINAL TERM

$$\left[\frac{a}{b} = 2.5; e = 0.916; \text{symmetric} \right]$$

p	Number of circumferential terms			
	30	32	34	35
m = 0				
0				
2	5.126	5.126	5.126	5.126
4	28.23	28.23	28.23	28.23
6	69.19	69.19	69.19	69.19
8	127.5	127.5	127.5	127.5
10	203.0	202.9	202.9	202.9
12	295.5	295.4	295.3	295.3
14	407.2	405.4	404.8	404.7
m = 1				
0	a ₀	a ₀	a ₀	a ₀
2	7.106	7.106	7.106	7.106
4	31.70	31.70	31.70	31.70
6	73.07	73.07	73.07	73.07
8	131.6	131.6	131.6	131.6
10	207.1	207.1	207.1	207.1
12	299.8	299.6	299.6	299.6
14	411.4	409.6	409.1	409.0

a_u-mode.

TABLE V.- CONVERGENCE CHARACTERISTICS FOR
VARIOUS MODAL APPROXIMATIONS - Concluded

$$\left[\frac{a}{b} = 2.5; e = 0.916; \text{symmetric} \right]$$

p	Number of circumferential terms					
	30	31	32	33	34	35
m = 2						
0	3519.0	3519.0	3519.0	3519.0	3519.0	3519.0
2	908.8	908.5	908.0	906.8		911.5
	5209.0	5209.0	5209.0	5209.0	5209.0	5209.0
4	7034.0	7034.0	7034.0	7034.0	7034.0	7034.0
6						
8	167.6	167.6	167.6	167.6	167.6	167.6
	536.2	534.9				
10	221.3	221.3	221.3	221.3	221.3	221.3
	282.7	282.7	282.7	282.7	282.7	282.7
12	343.5	343.3	343.3	343.2	343.2	343.2
			533.9	533.2	532.7	532.4
14	434.8	433.7	433.0	432.7	432.5	432.4
16	581.6	577.1	574.0	571.9	570.6	569.7
					902.2	
m = 3						
0						
2	5415.0	1396.0	1396.0	1395.0	1394.0	1394.0
		5415.0	5415.0	5415.0	5415.0	5415.0
4	8521.0	8521.0	8521.0	8521.0	851.5	8521.0
					8521.0	
6	1400.0					
8	861.8	858.3	855.6	853.4		849.9
10	269.9	269.9	269.9	269.9	269.9	269.9
12	333.8	333.7	333.7	333.7	333.7	333.7
	405.6	405.4	405.2	405.1	405.1	405.1
14	485.1	483.9	483.2	482.8	482.6	482.4
	664.2	660.3	657.4	655.2	653.6	652.6
16	584.0	580.6	578.3	576.6	575.6	574.9

TABLE VI.- RIGID-BODY (ZERO FREQUENCY) MODES

m	p	Mode	e = 0	e = 0.526	e = 0.760	e = 0.916
0	0	Symmetric	-----	---	---	---
		Antisymmetric	v	v	v	v
	1	Symmetric	v or w	v	w	w
		Antisymmetric	v or w	v	v	v
1	0	Symmetric	u	u	u	u
		Antisymmetric	-----	---	---	---
	1	Symmetric	u	v	v	a _v
		Antisymmetric	u	u	u	u
Number of terms		Longitudinal	1 or 4	4	4	2
		Circumferential	1	13	16	32

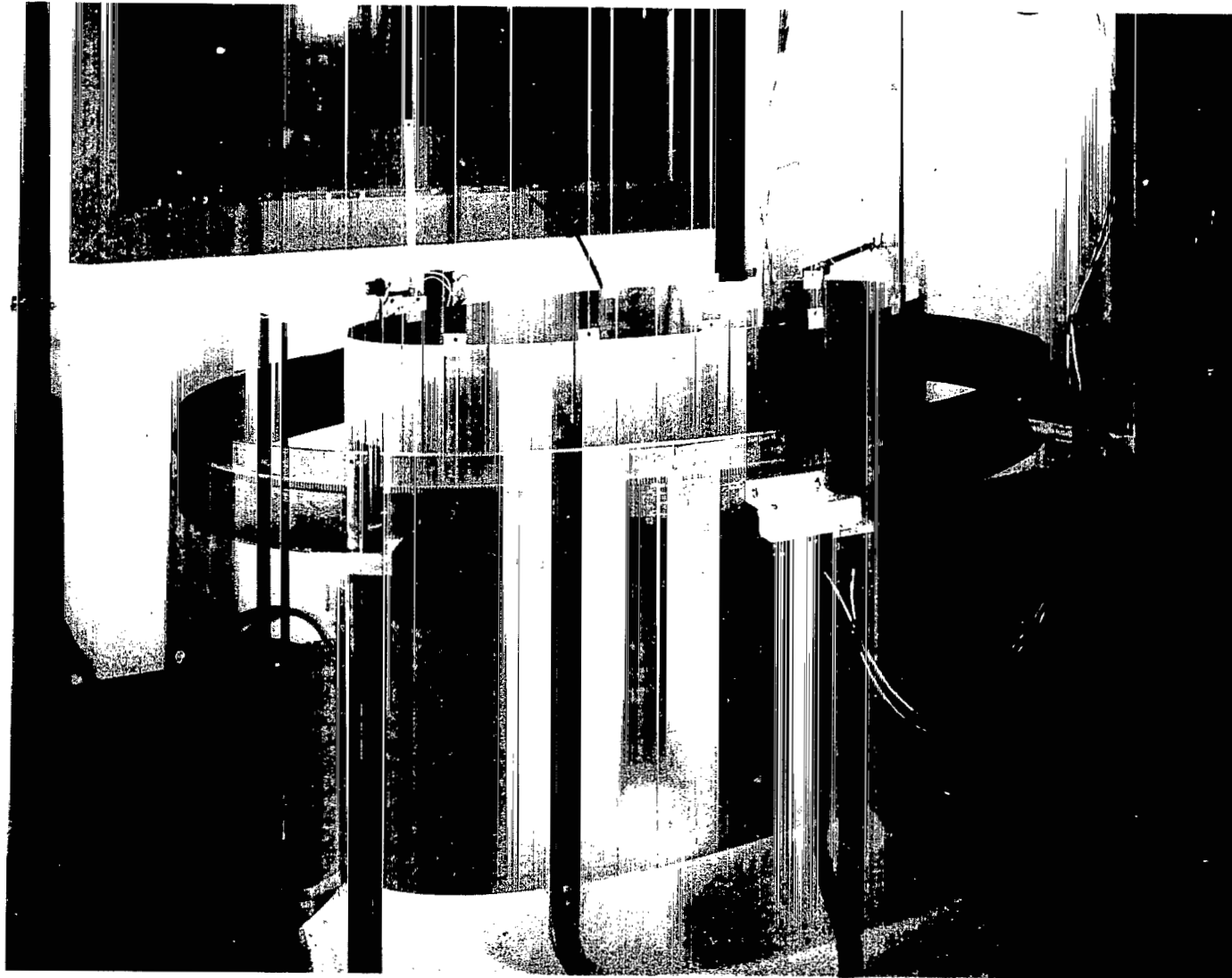
^aActual frequency, 1.01 Hz.

TABLE VII.- ANALYTICAL FREQUENCIES FOR FREELY SUPPORTED
CIRCULAR SHELL (MODEL 1)

n	Frequency, Hz	
	m = 1	m = 2
0	2537.0	2594.0
1	1565.0	2309.0
2	894.1	1782.0
3	529.8	1315.0
4	338.6	968.4
5	235.6	726.3
6	182.1	560.3
7	162.2	448.6
8	166.9	377.2
9	188.6	338.1
10	221.3	325.1
11	261.7	335.0
12	308.0	361.0
13	359.5	399.5
14	415.6	447.5

TABLE VIII.- ANALYTICAL FREQUENCIES FOR FREELY SUPPORTED
ELLIPTICAL SHELLS

p	Frequency, Hz					
	e = 0.526 (model 2)		e = 0.760 (model 3)		e = 0.916 (model 4)	
	Symmetric	Antisymmetric	Symmetric	Antisymmetric	Symmetric	Antisymmetric
m = 1						
0	2550.0		2612.0		2723.0	
1	1440.0	1686.0	1238.0	1856.0	931.1	2039.0
2	876.6	888.9	785.2	858.5	555.6	748.1
3	524.1	524.2	491.1	492.4		
4	335.5	335.5	319.4	319.4		
5	234.3	234.3		226.9		392.4
6	184.2	184.2			106.8	106.8 258.2
7	157.1	157.0	138.5	138.5	107.0 388.4	107.7 151.6
8	160.2	160.2	140.1 178.3	140.1 178.3	148.2 257.0	148.2
9	189.8	189.8	184.1 226.9	184.1	151.7 194.8	194.9
10	221.9	221.9	223.9	223.9	206.5	206.6
11	261.9	261.9	263.6	263.6	259.3	259.4
12	308.1	308.1	307.3	307.3	310.2	310.5
13	359.5	359.5	359.4	359.4	351.4	351.9
14	415.6	415.6	417.1	417.1	413.3	413.5
m = 2						
0	2726.0		3248.0		4155.0	
1	2083.0	2607.0	1876.0	3188.0	1694.0	4081.0
2	1696.0	1782.0	1419.0	1775.0	1035.0	
3	1291.0	1297.0	1145.0	1214.0	793.2	989.0
4	956.5	956.7	886.1	893.0		1675.0
5	718.8	718.8	677.0	677.4		
6	555.6	555.6	531.3	531.6		
7	446.6	446.6	441.5			
8	381.8	381.8			659.7	
9			268.3	268.3	202.4	202.4
10	310.6	310.6	268.1 328.2	268.1	202.5 258.5	202.5 258.5
11	312.4 347.5	312.4 347.5	325.4	325.4	259.2	259.2
12	359.4	359.4	382.3	328.2 382.3	323.8 398.0	323.8 398.2 700.3
13	401.5	401.5	393.4	393.4 441.5	393.2 550.4	393.4
14	448.4	448.4	454.7	454.7	466.3	467.2



L-69-3508

Figure 1.- View of free-free elliptical cylindrical shell and circumferential track.

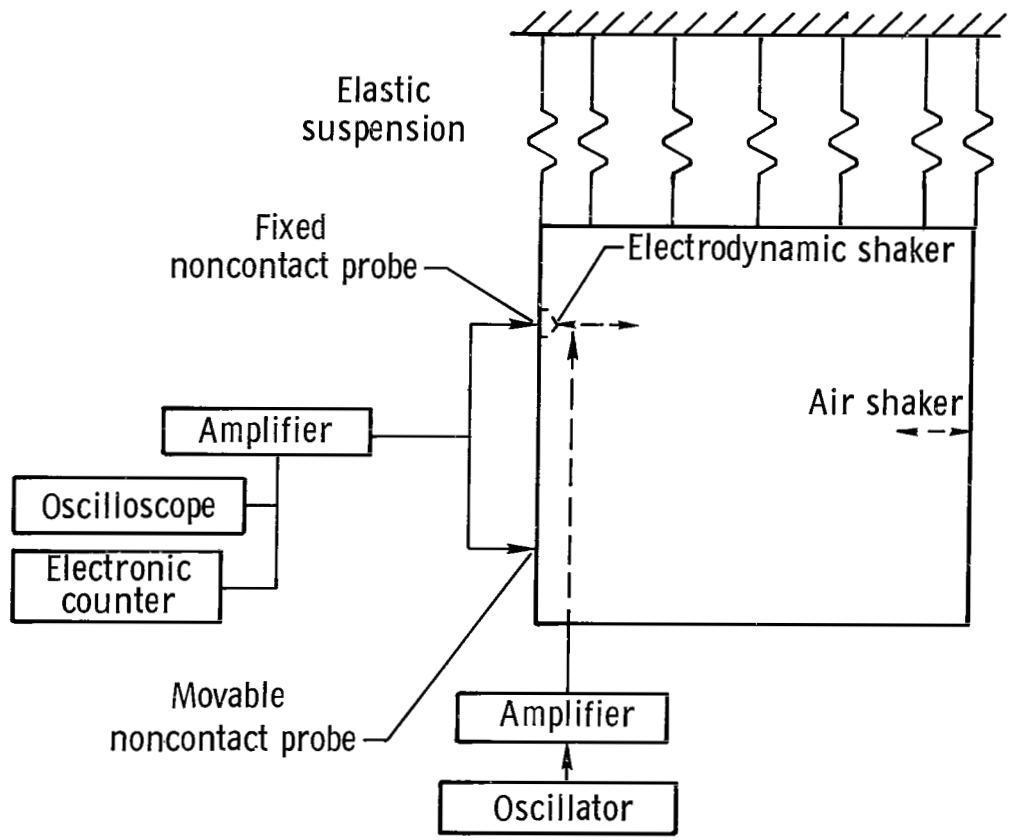
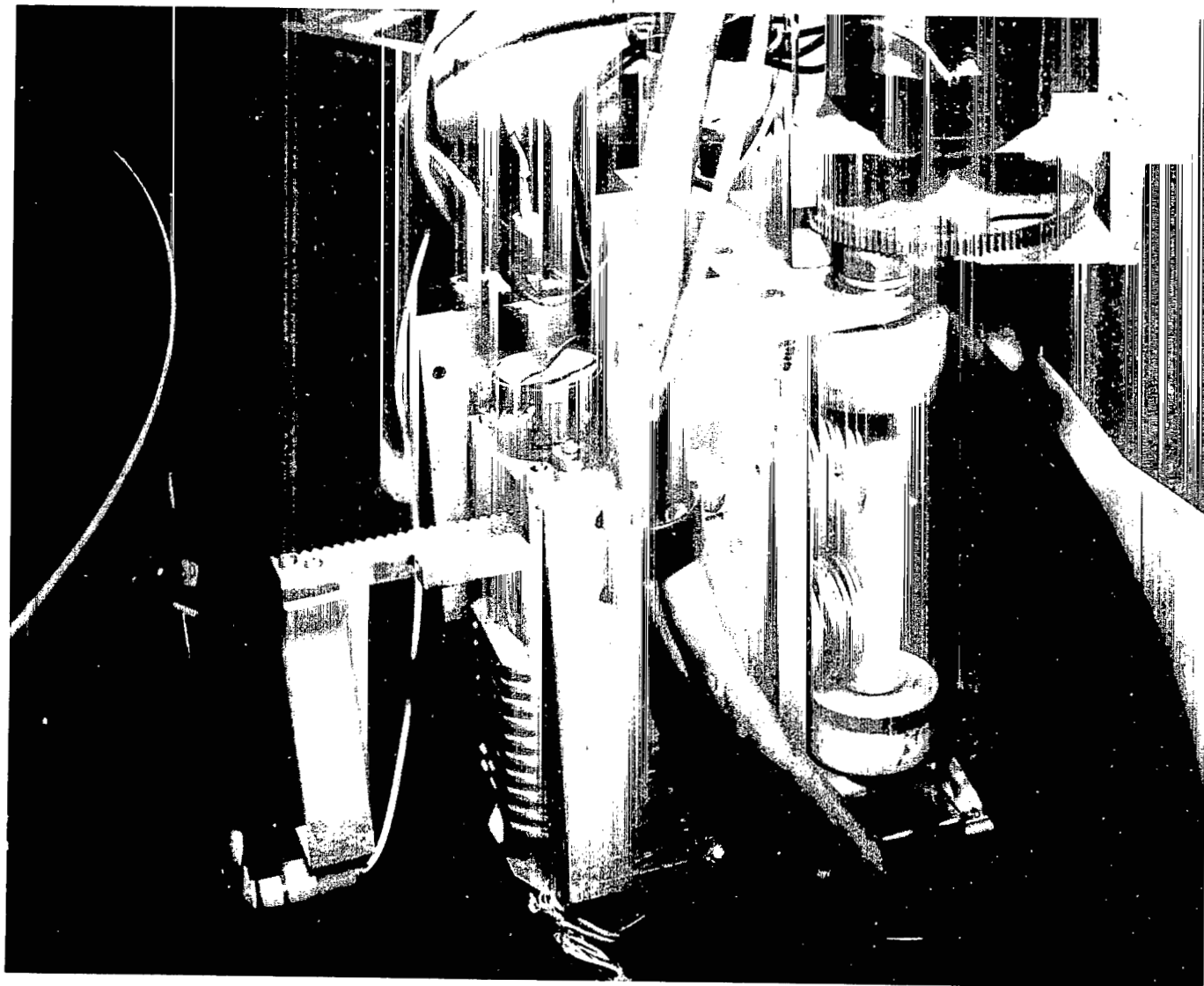
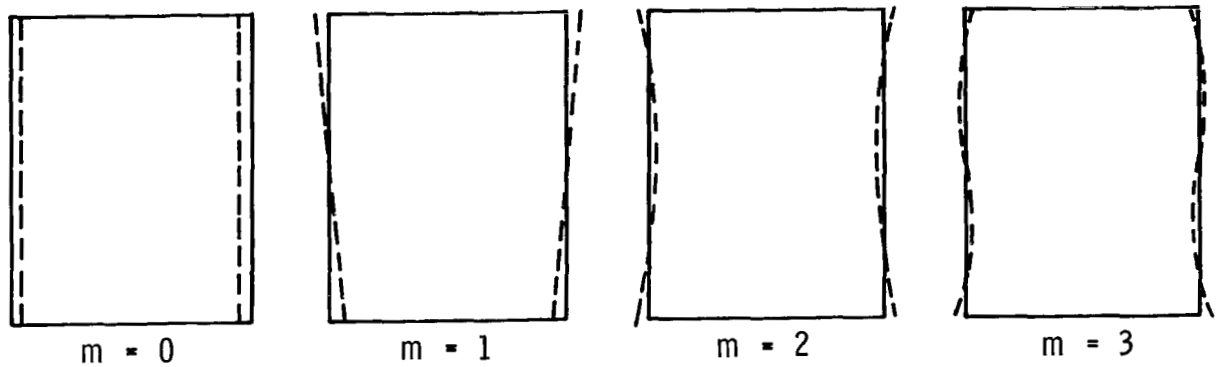


Figure 2.- Schematic of simplified test apparatus.

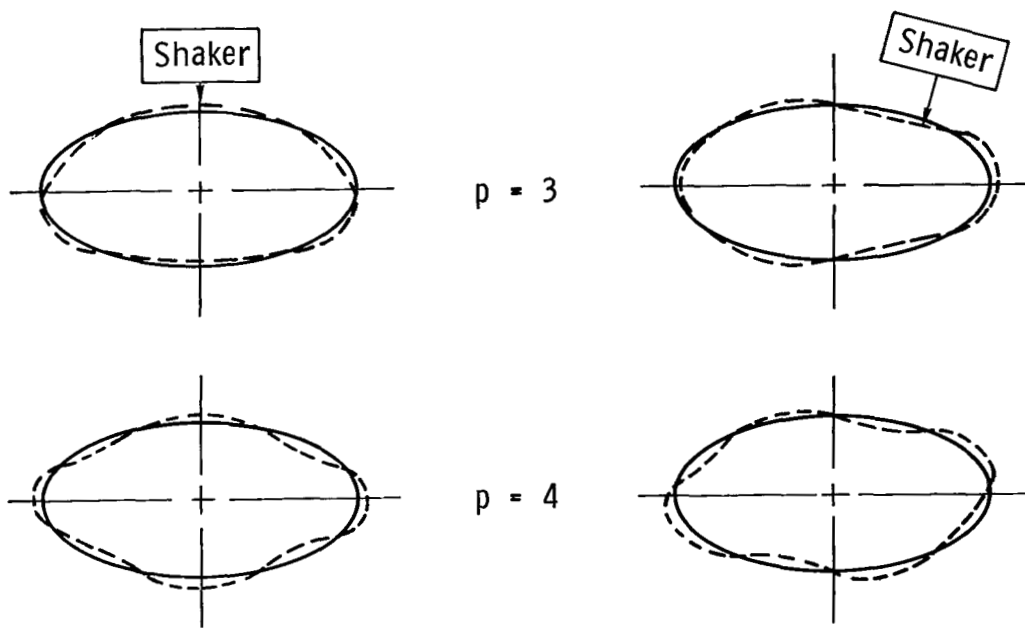


L-70-4773

Figure 3.- Closeup of movable inductance probe assembly.



Longitudinal



Symmetric

Anti-symmetric

Circumferential

Figure 4.- Mode-shape classifications for normal (or radial) displacements w of free-free elliptical cylindrical shell. For the circular shell, $p = n$ where n is the number of circumferential waves.

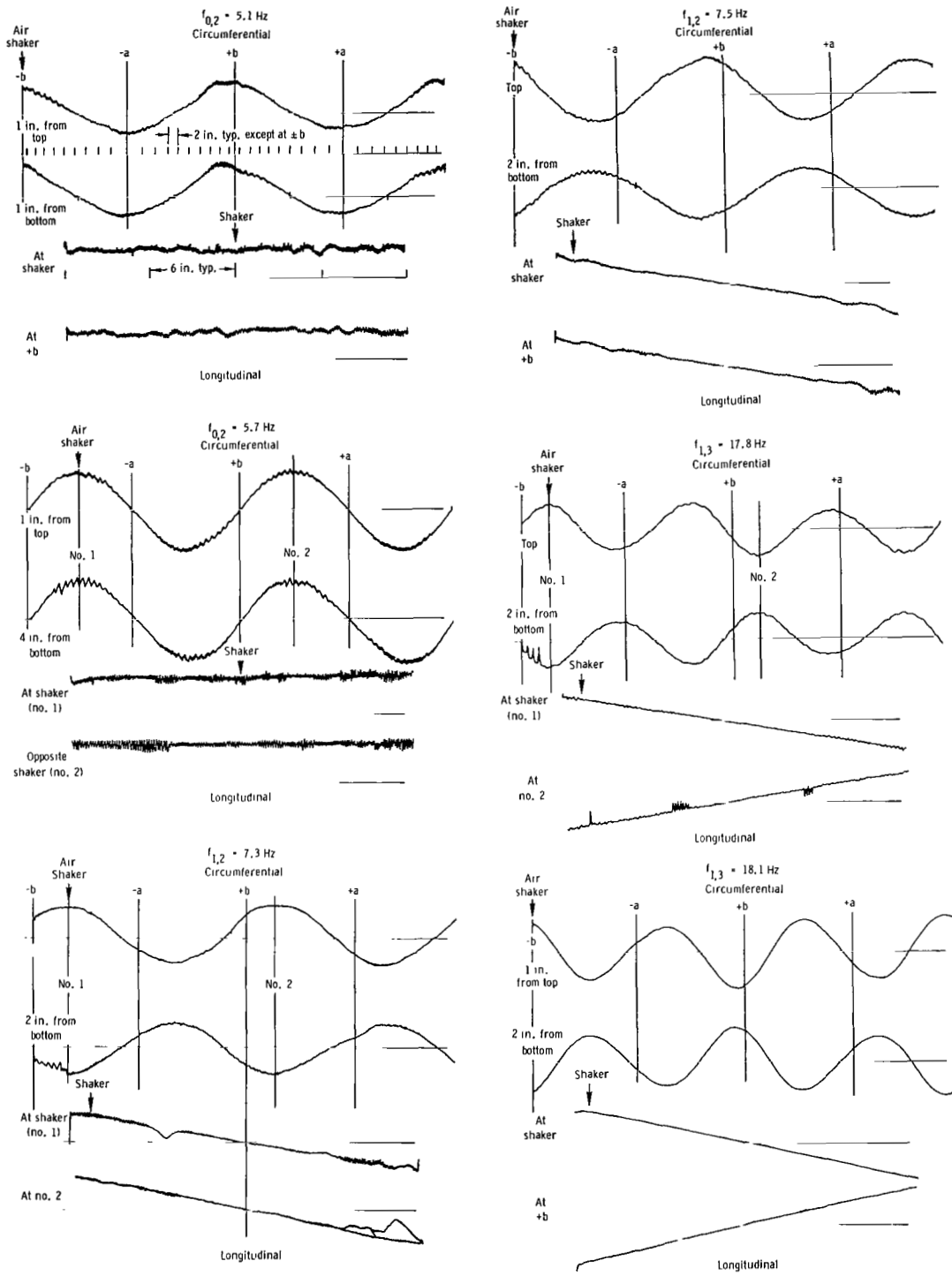


Figure 5.- Experimental mode shapes for free-free elliptical cylindrical shell.

$$\frac{a}{b} = 1.538; \quad e = 0.760. \quad (1 \text{ inch} = 2.54 \text{ cm.})$$

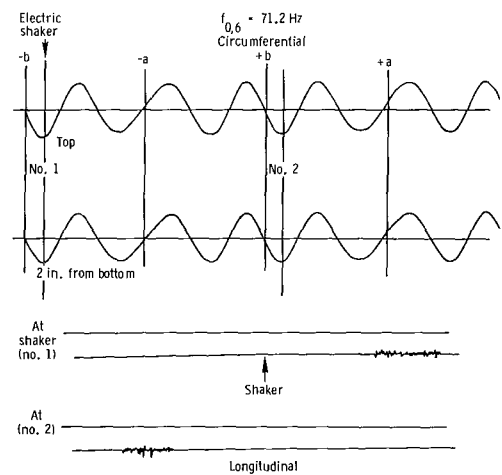
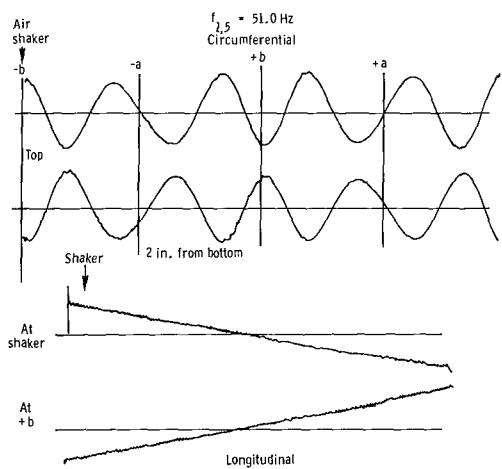
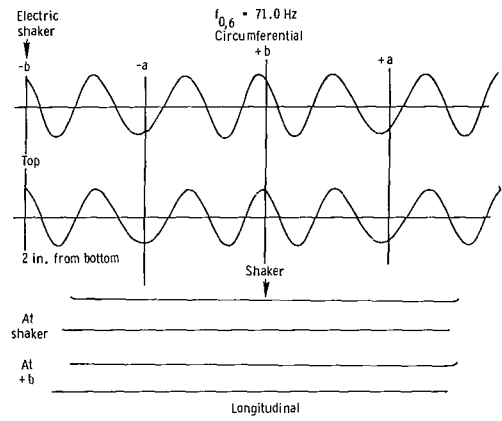
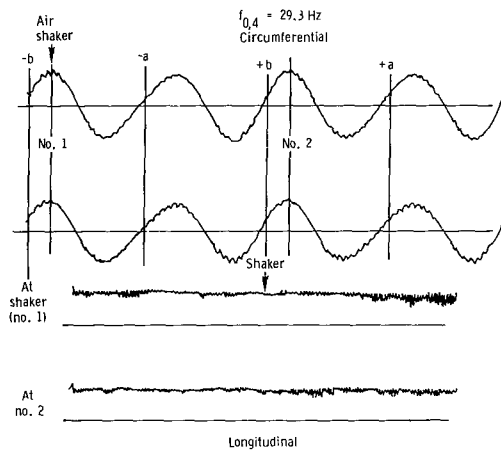
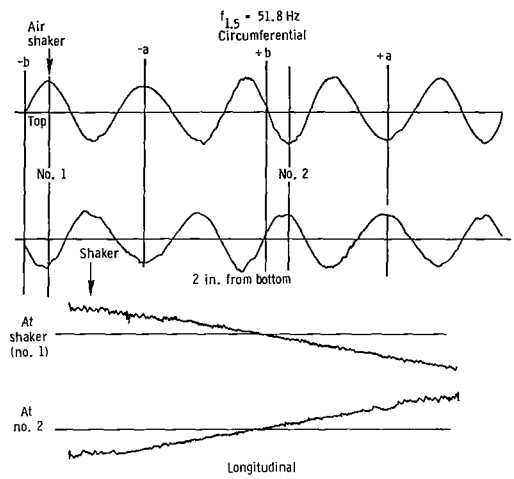
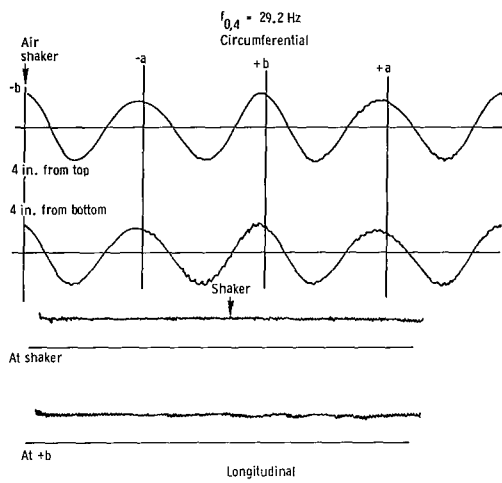


Figure 5.- Continued.

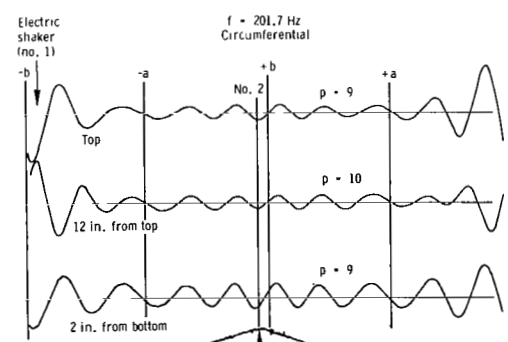
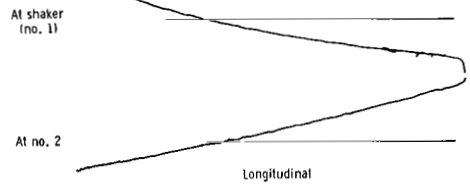
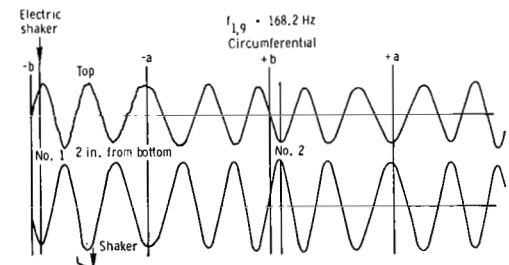
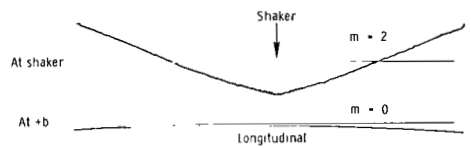
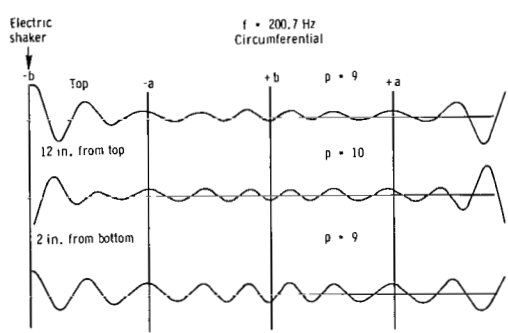
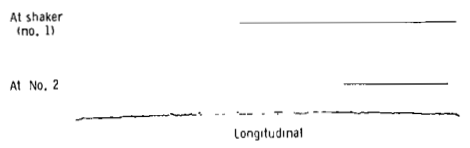
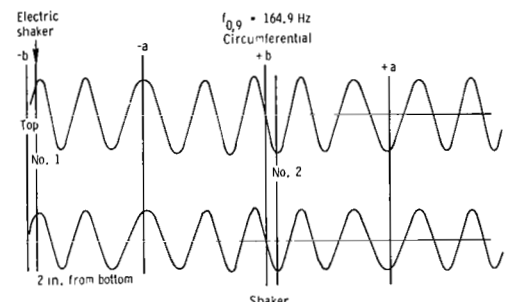
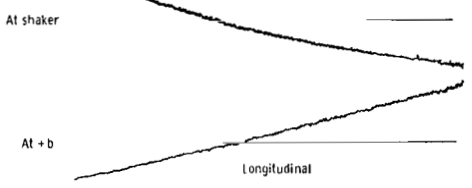
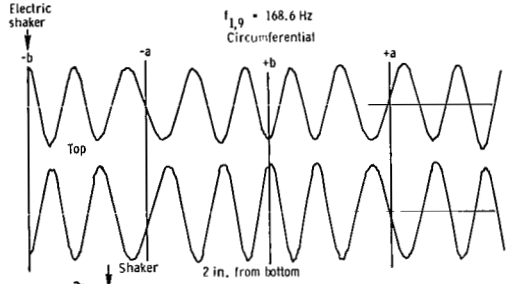
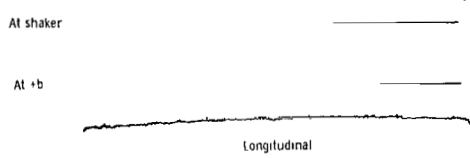
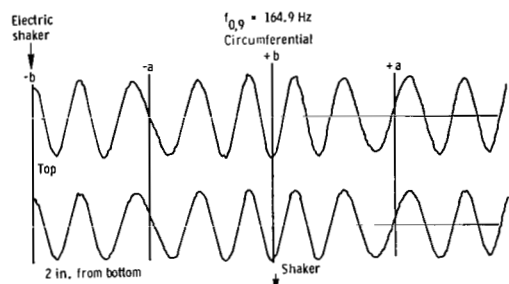


Figure 5.- Continued.

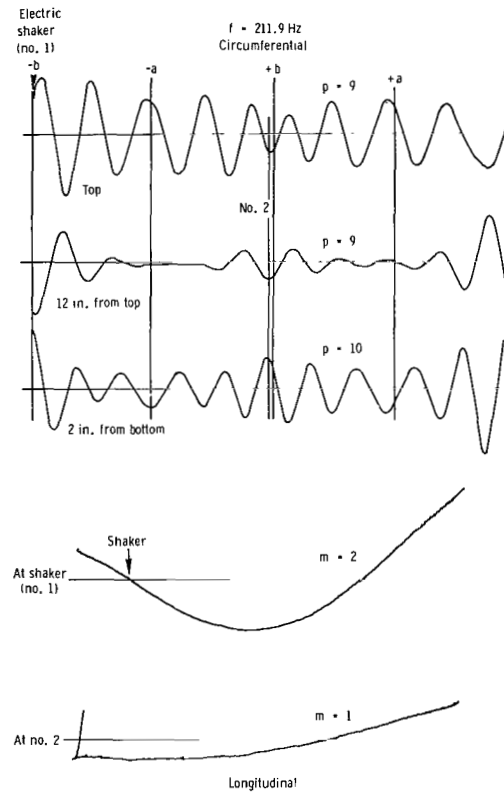
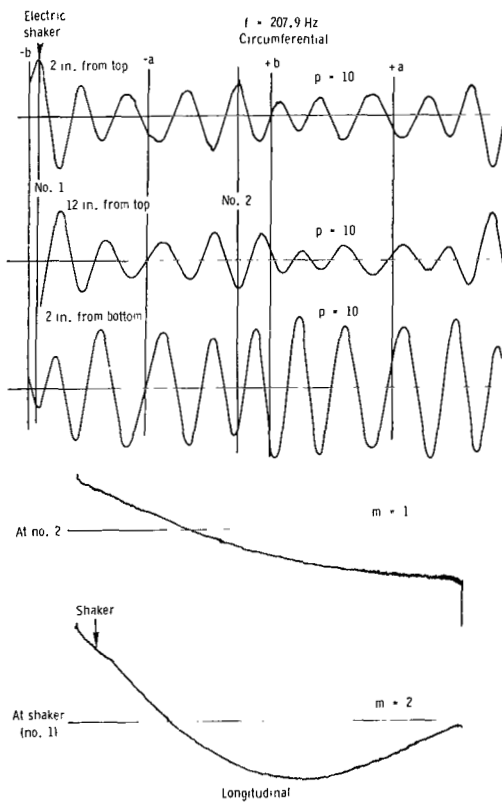
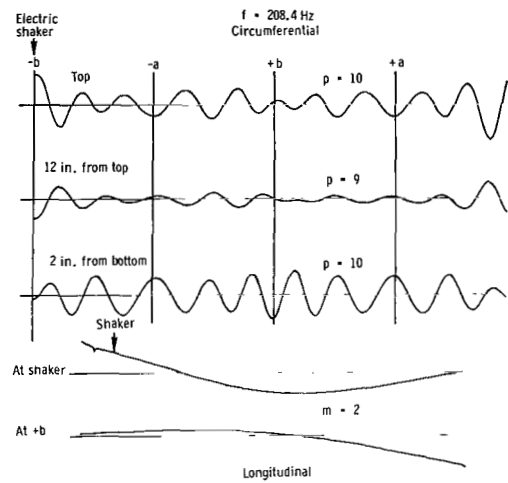
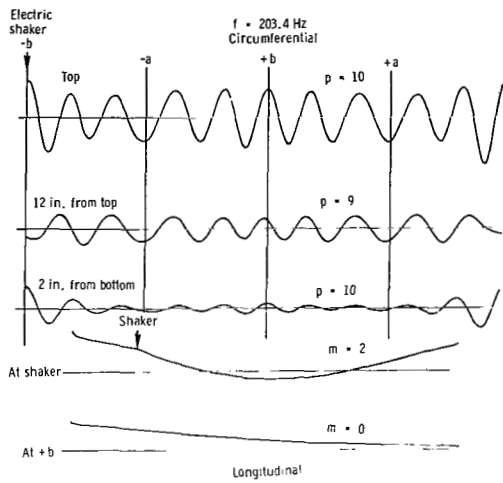


Figure 5.- Continued.

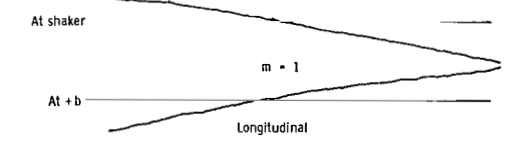
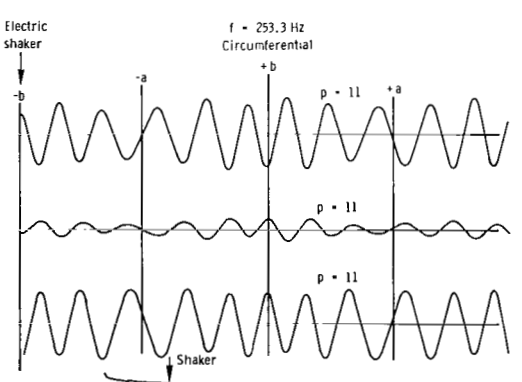
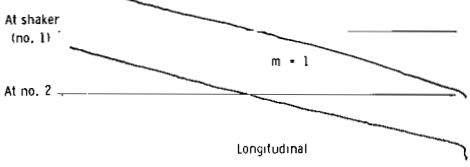
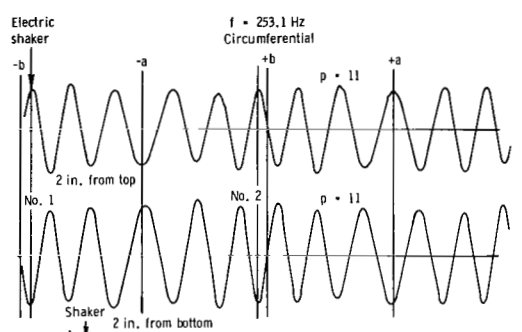
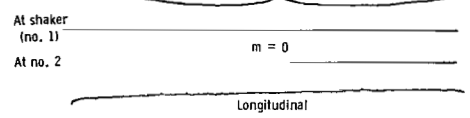
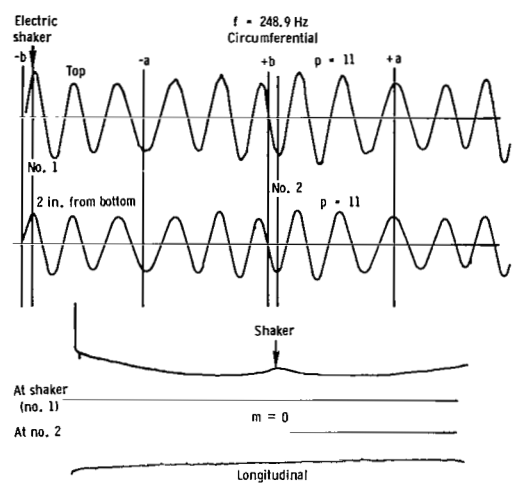
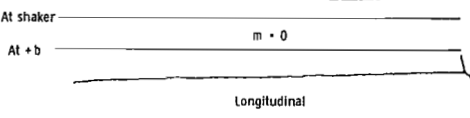
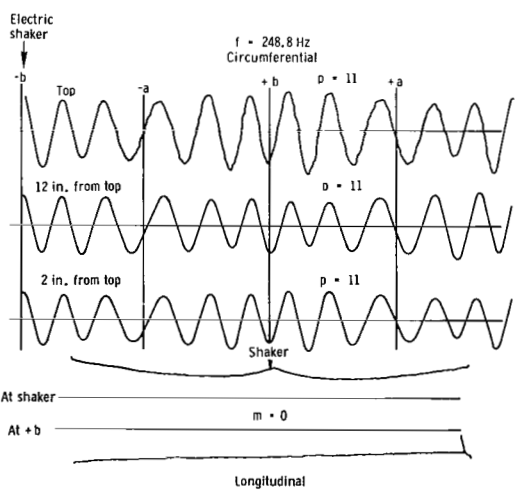
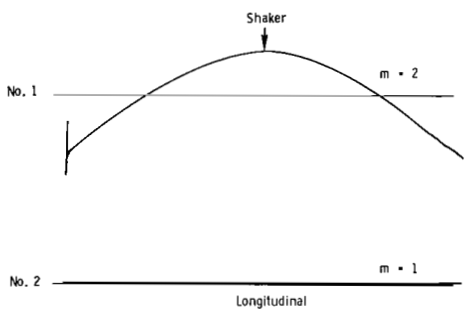
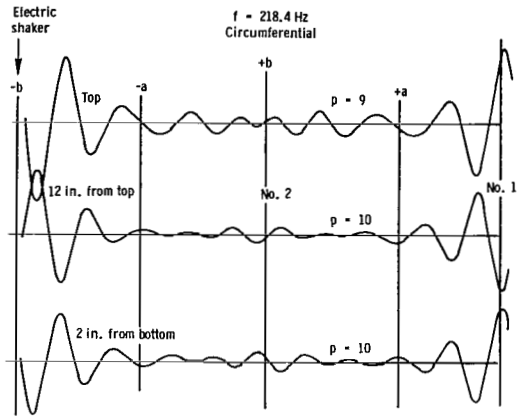


Figure 5. - Continued.

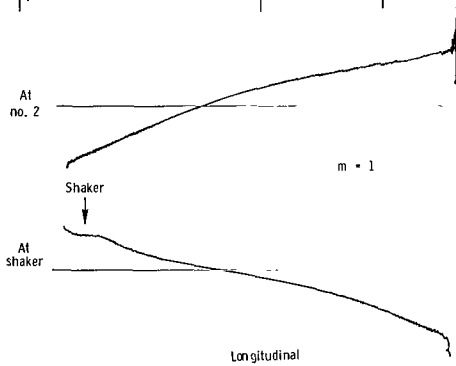
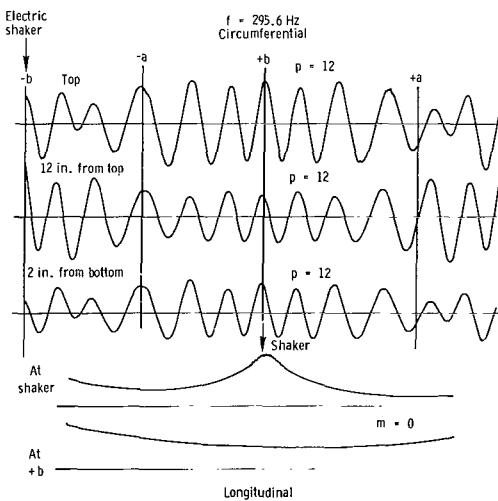
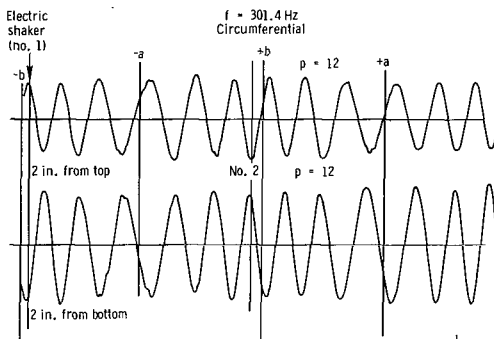
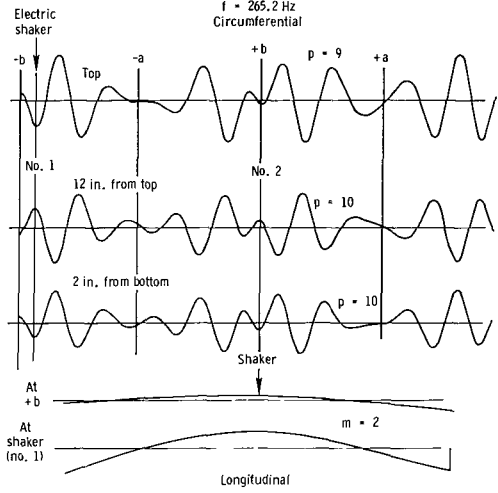
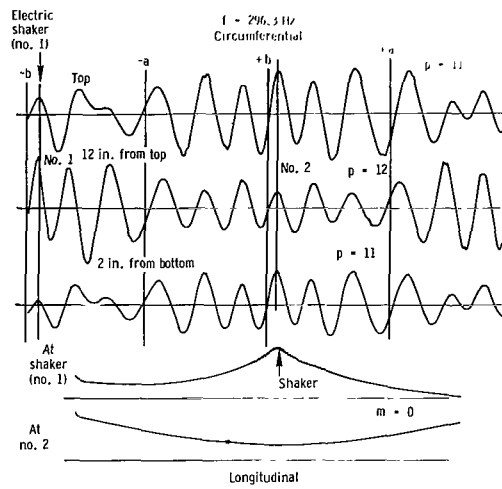
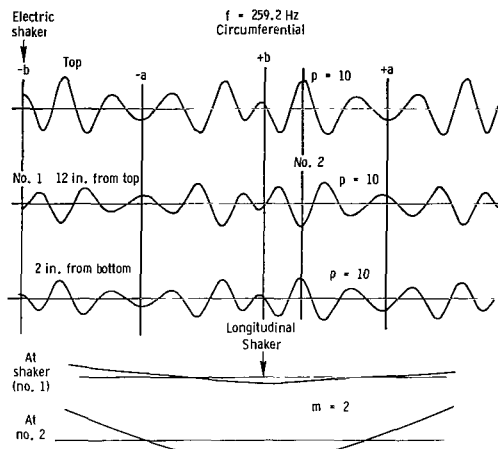


Figure 5.- Continued.

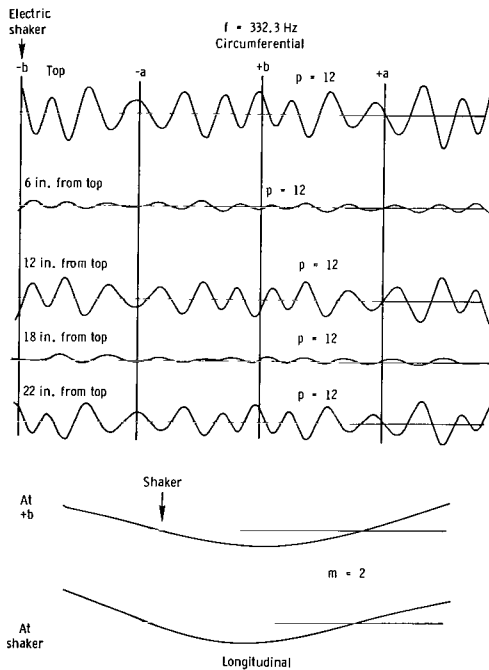
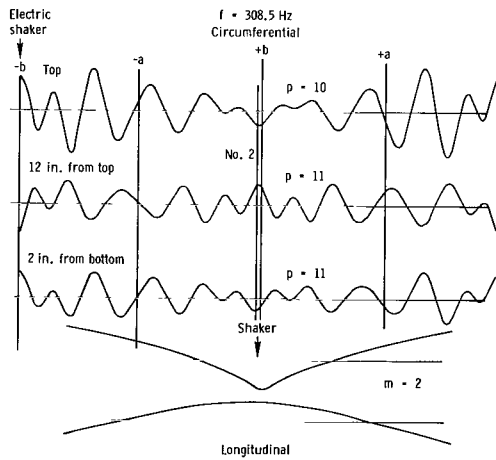
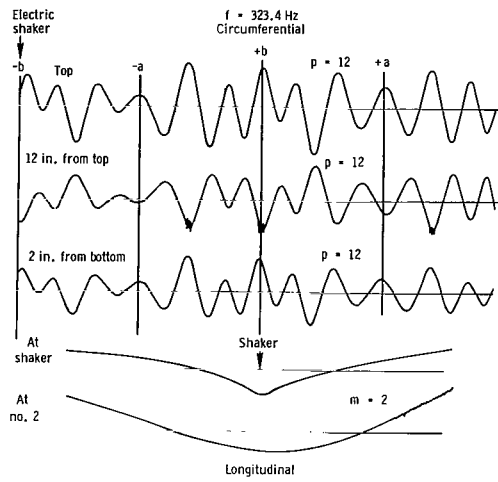
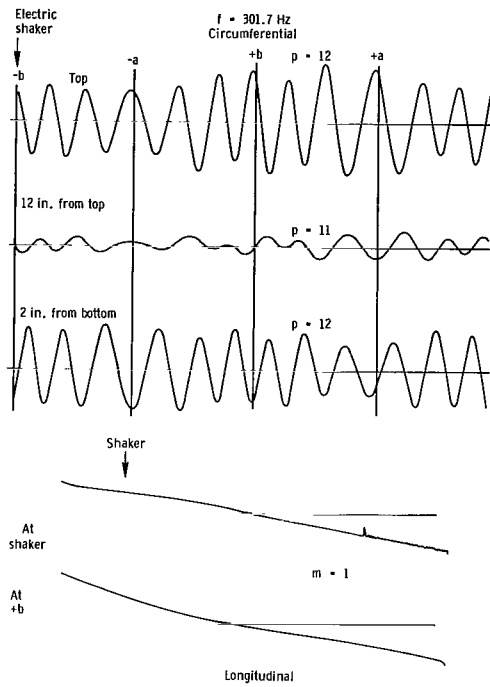


Figure 5.- Continued.

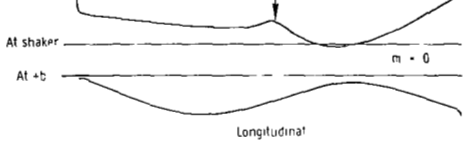
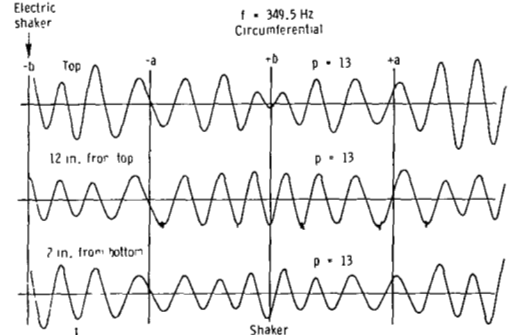
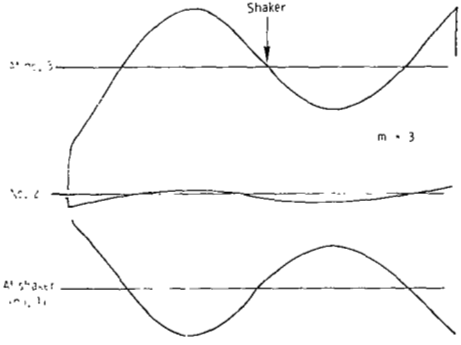
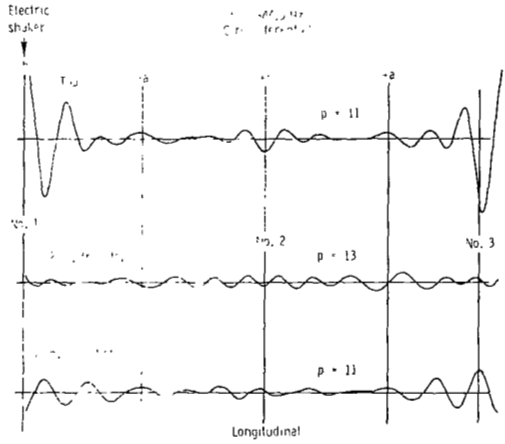
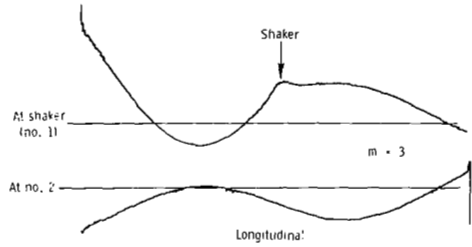
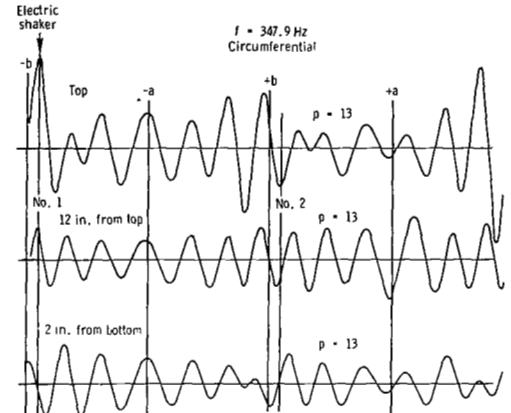
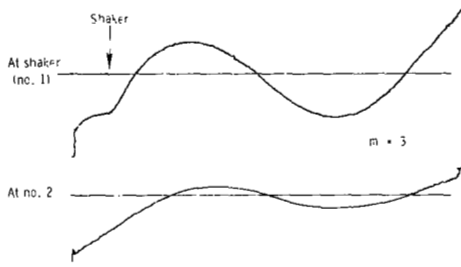
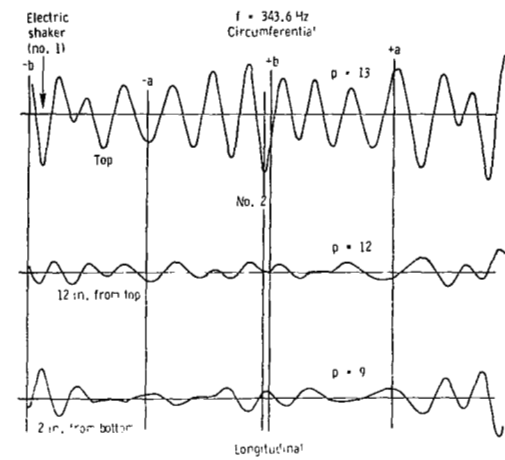


Figure 5.- Continued.

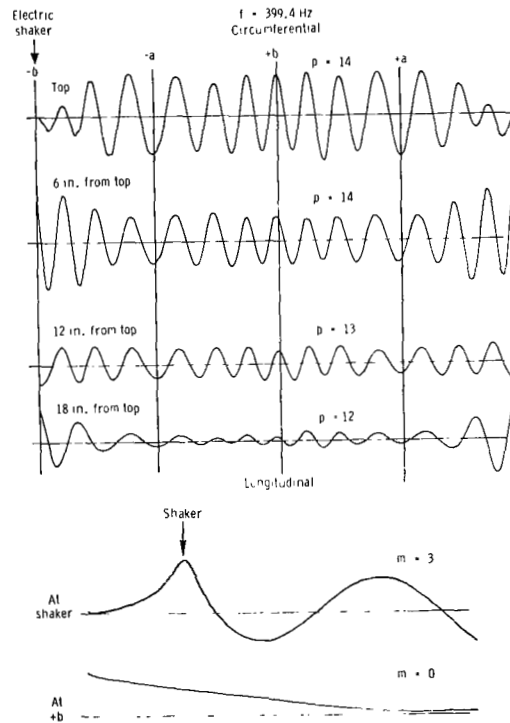
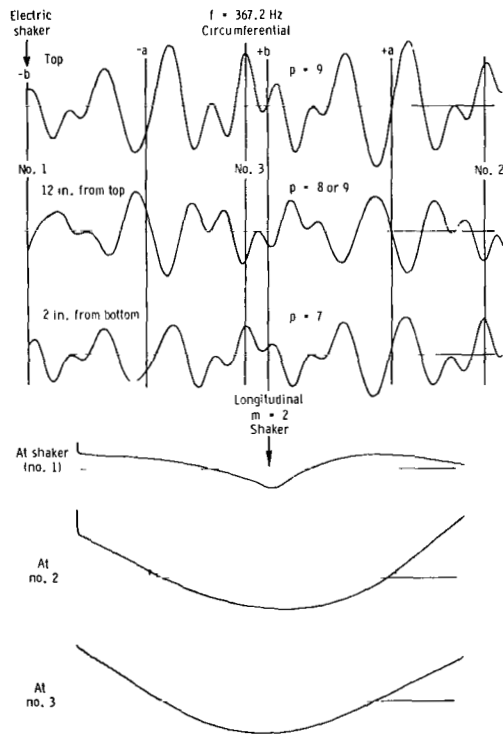
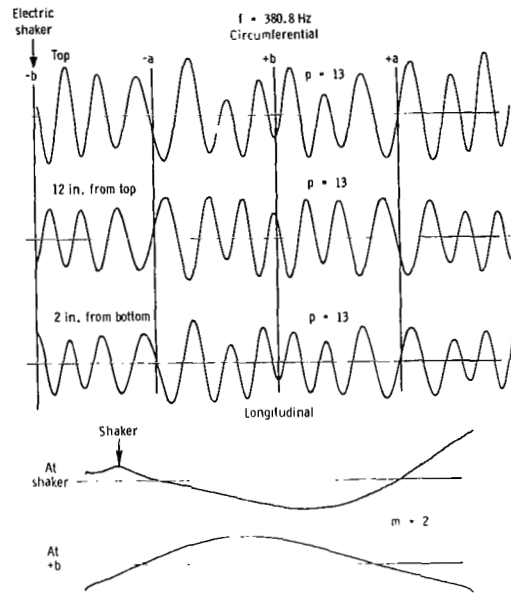
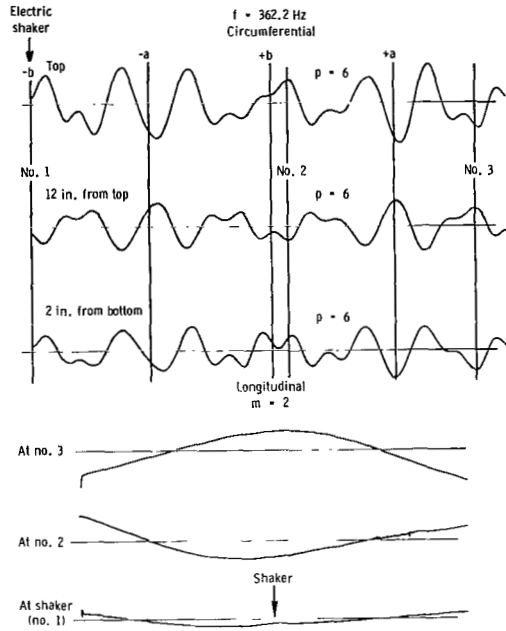


Figure 5.- Continued.

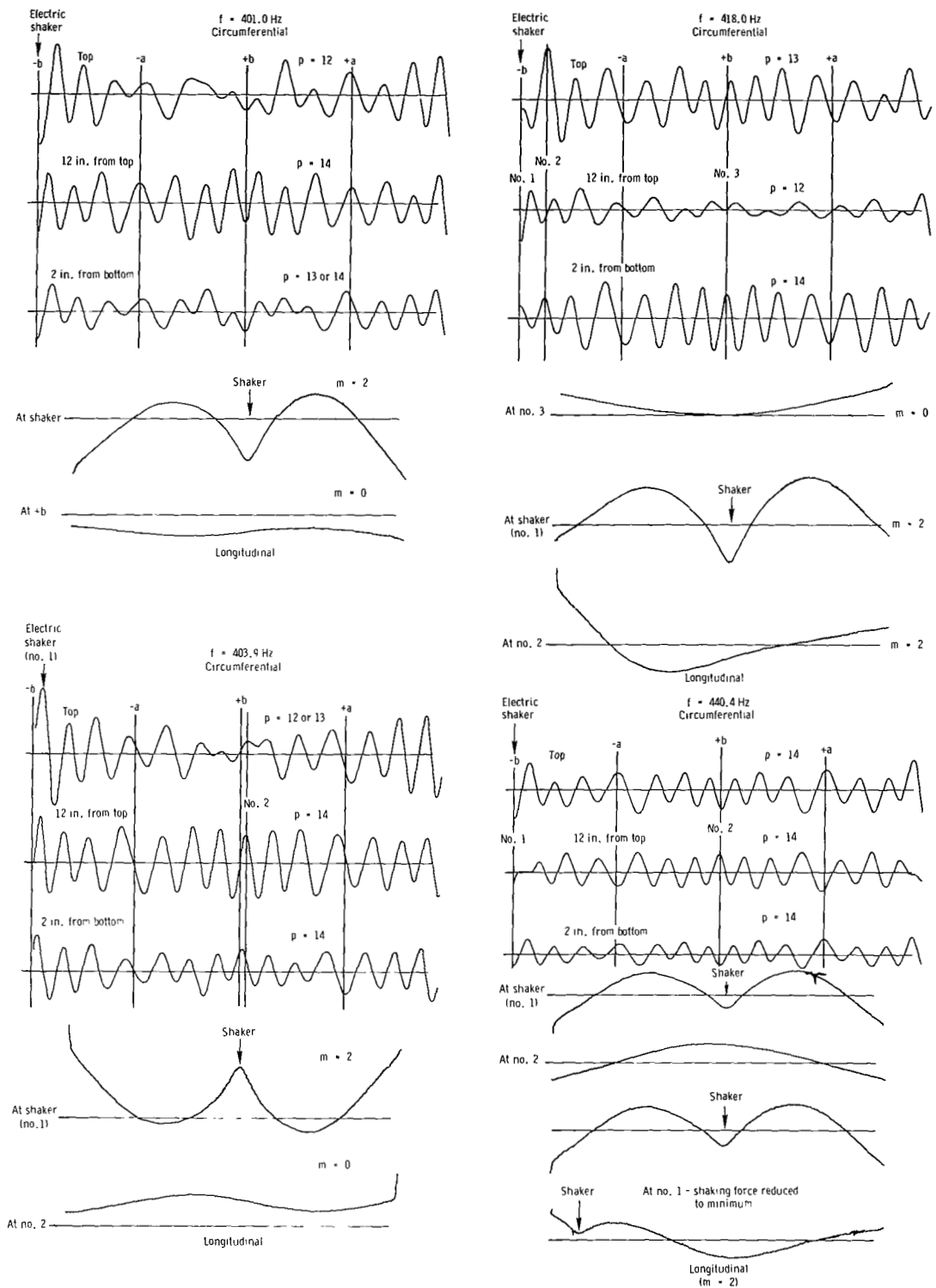


Figure 5.- Continued.

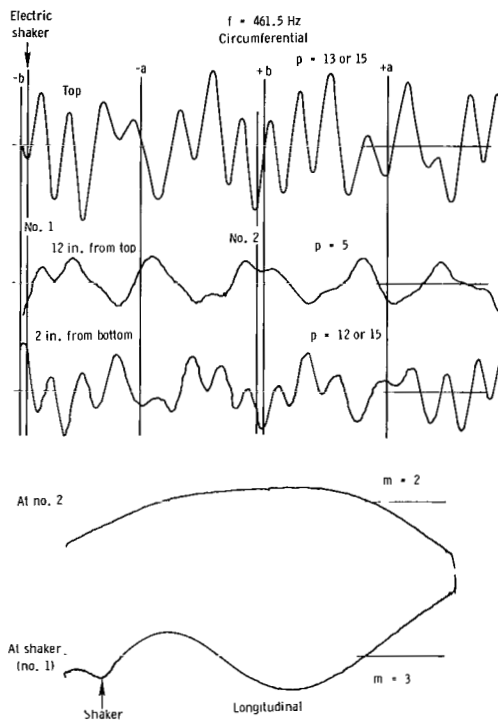


Figure 5.- Concluded.

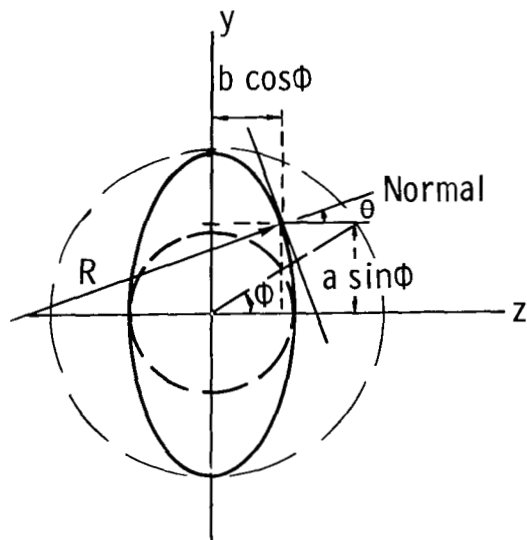
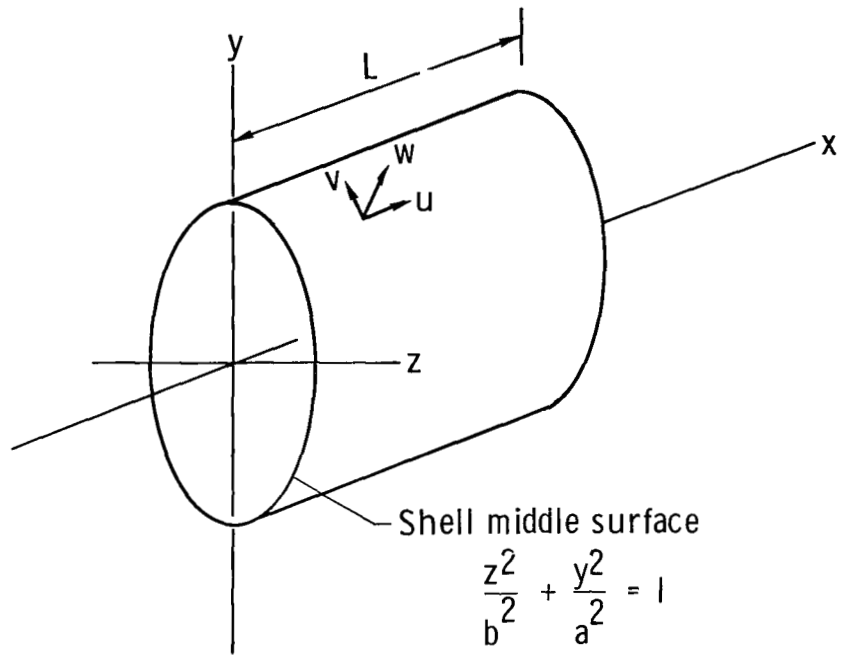


Figure 6.- Elliptical shell geometry.

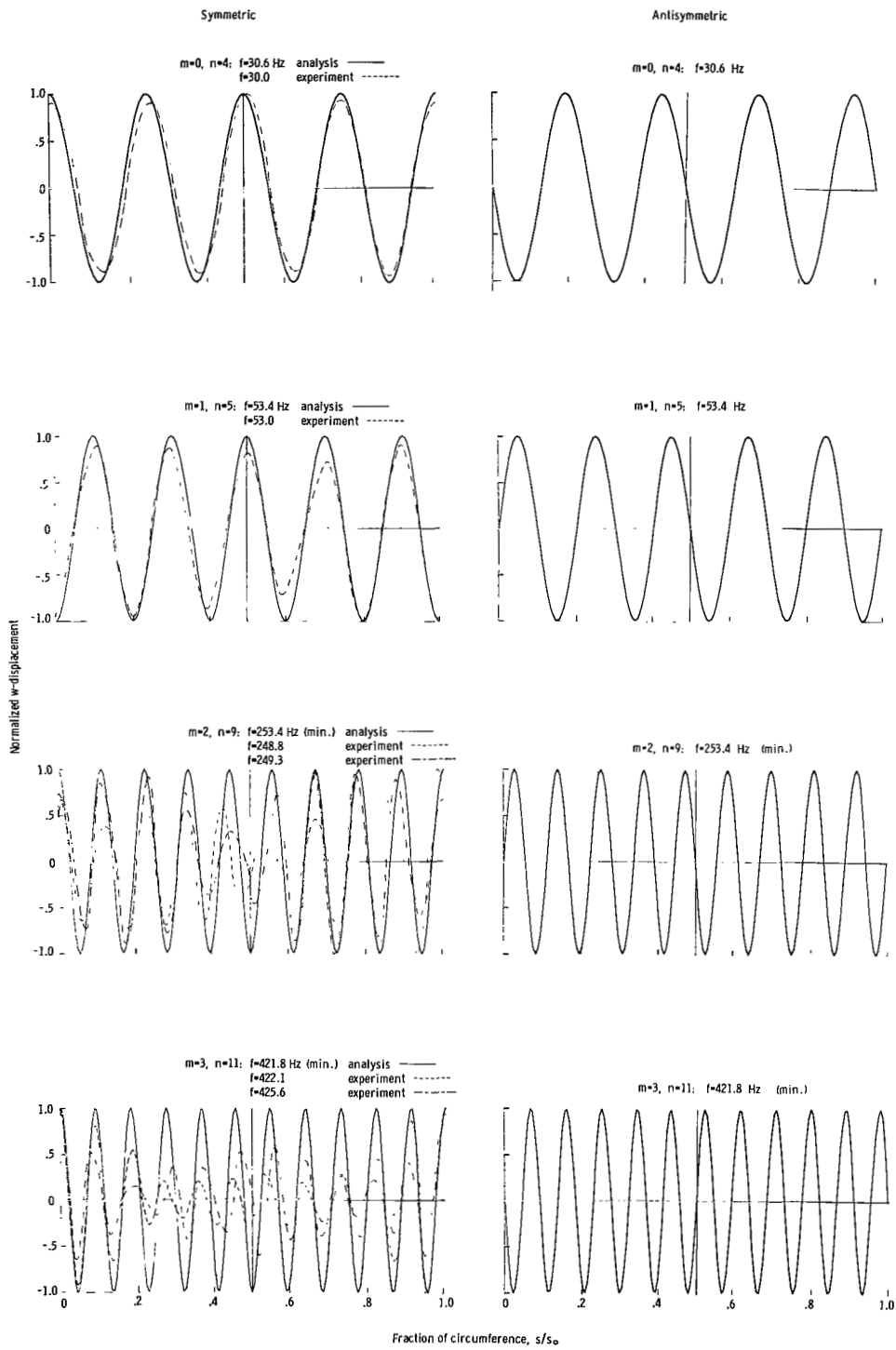
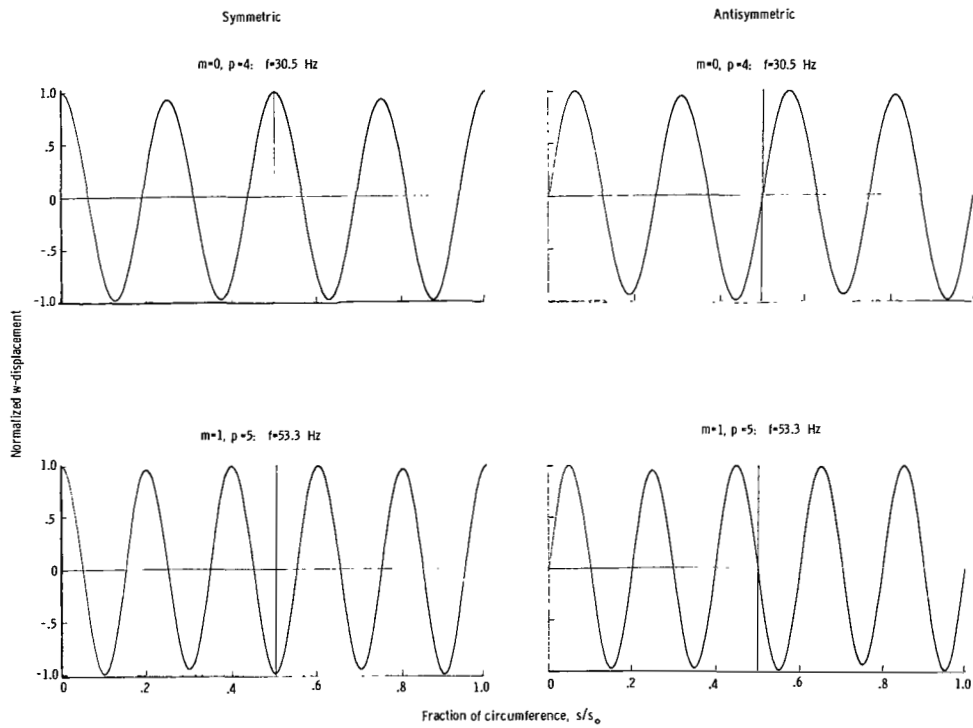
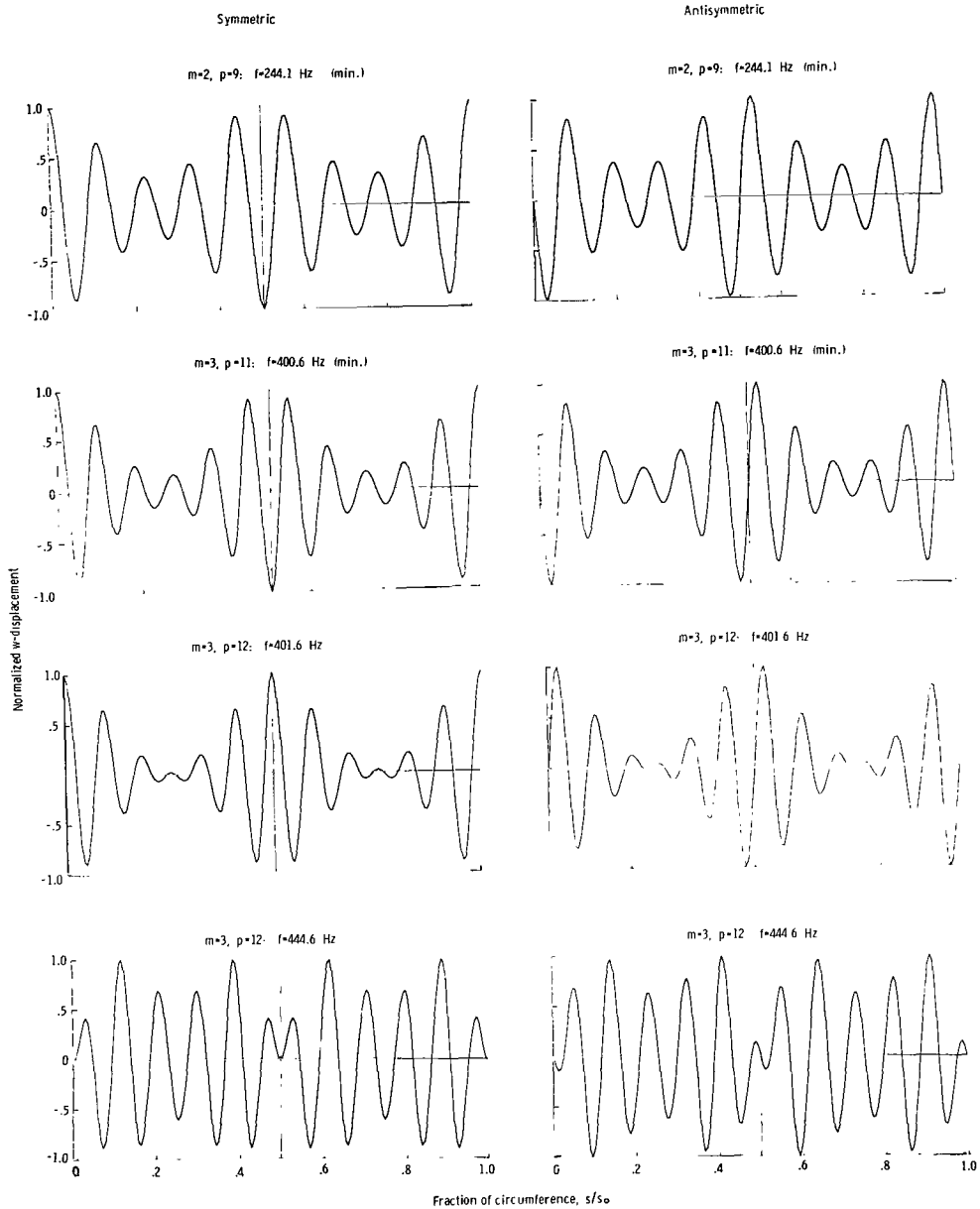


Figure 7.- Circumferential mode-shape correlation for free-free circular cylindrical shell (model 1; $e = 0$).



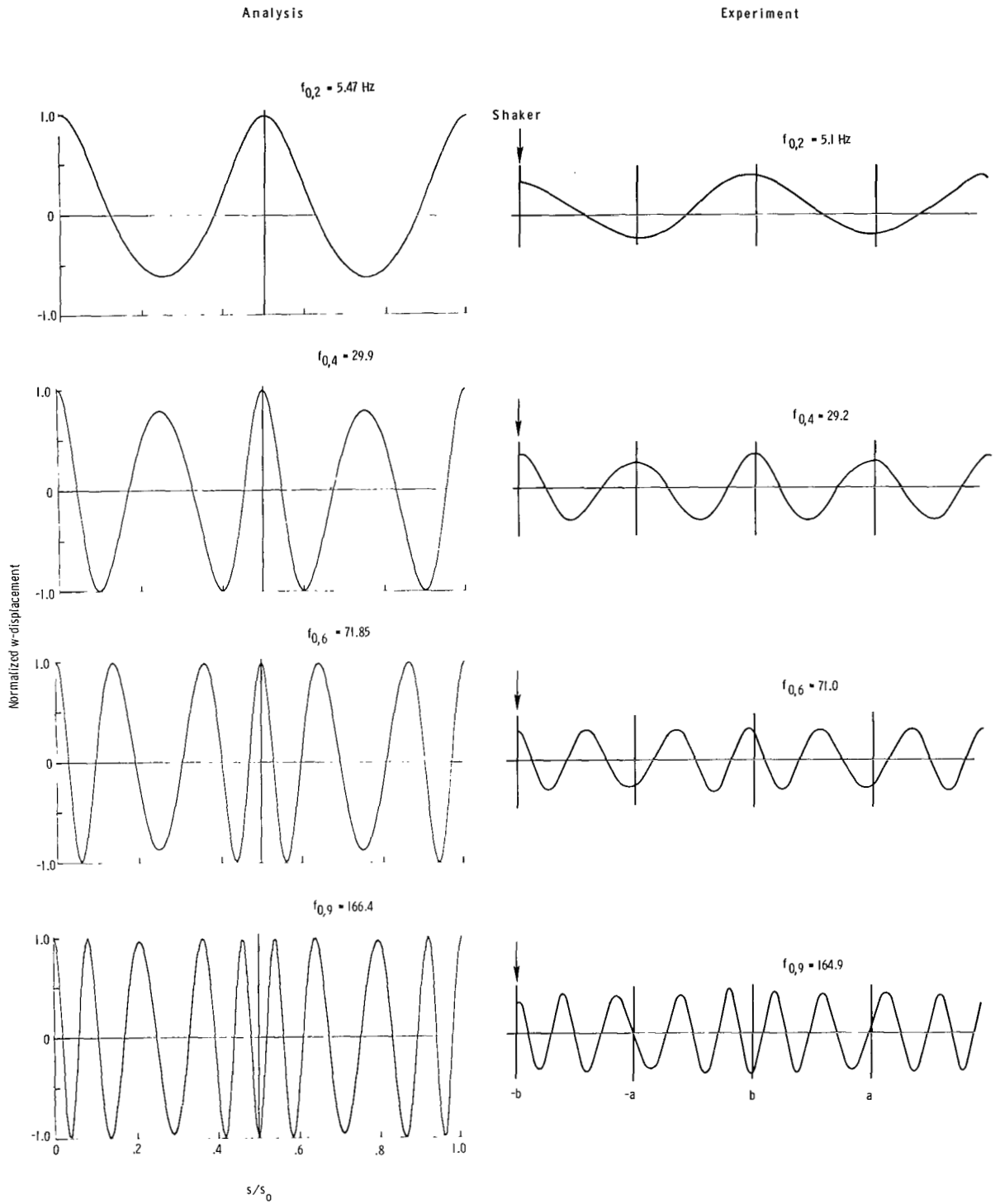
(a) Inextensional modes.

Figure 8.- Analytical circumferential mode shapes for model 2 ($e = 0.526$).



(b) Modes involving $m = 2$ and 3 .

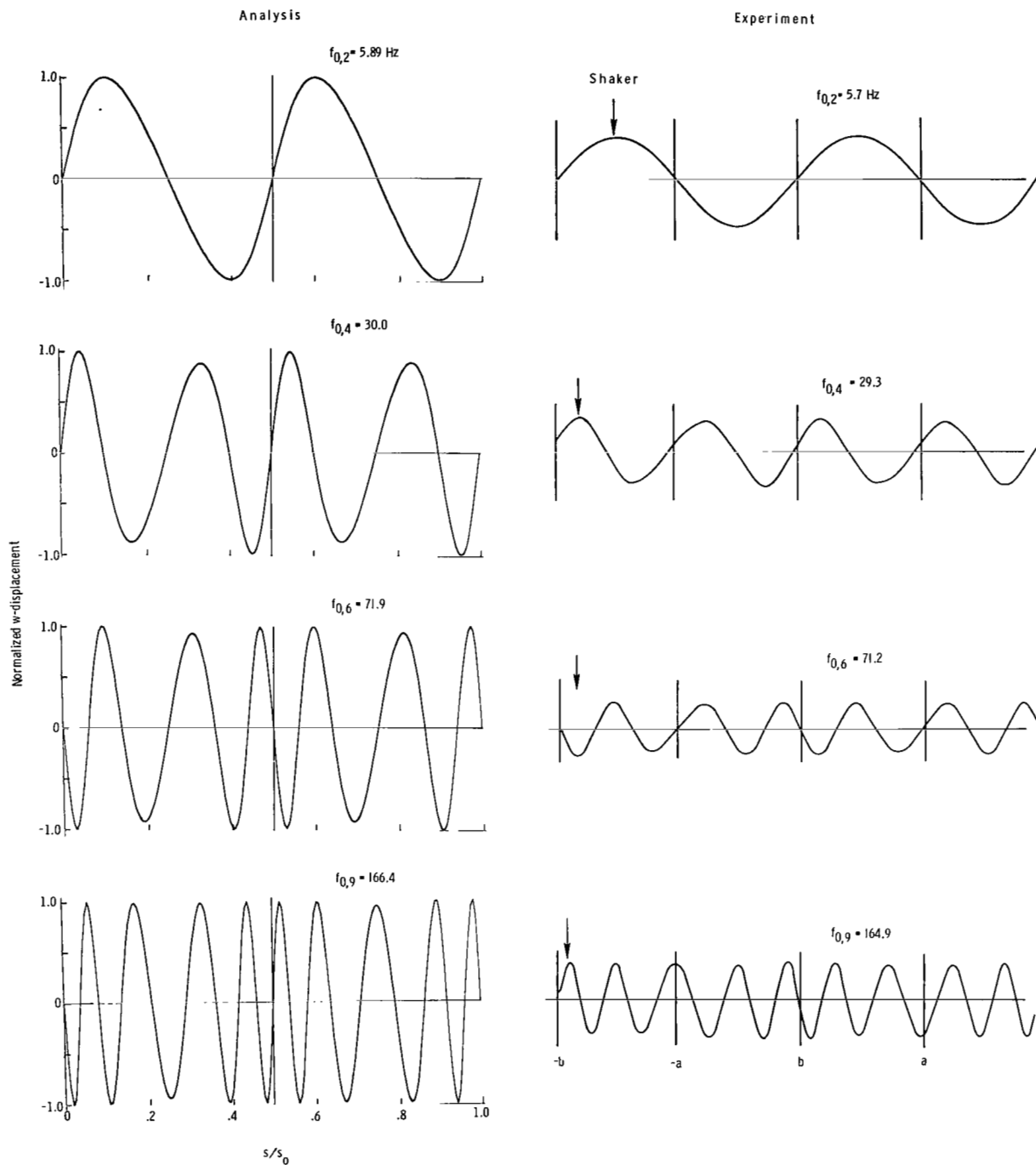
Figure 8.- Concluded.



(a) Inextensional symmetric mode. $m = 0$.

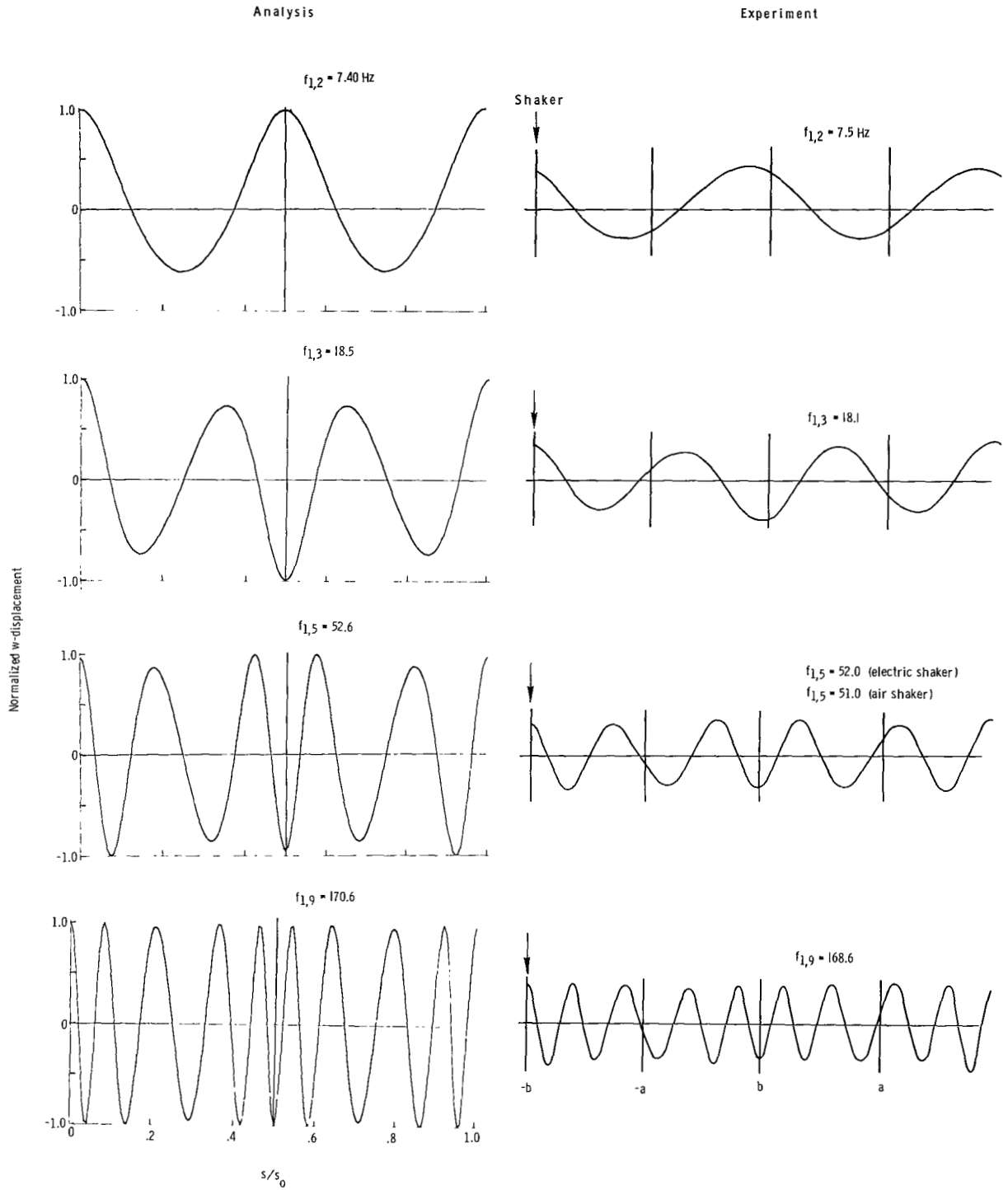
Figure 9.- Circumferential mode-shape correlation for model 3 ($e = 0.760$).

Experimental mode shapes taken from figure 5.



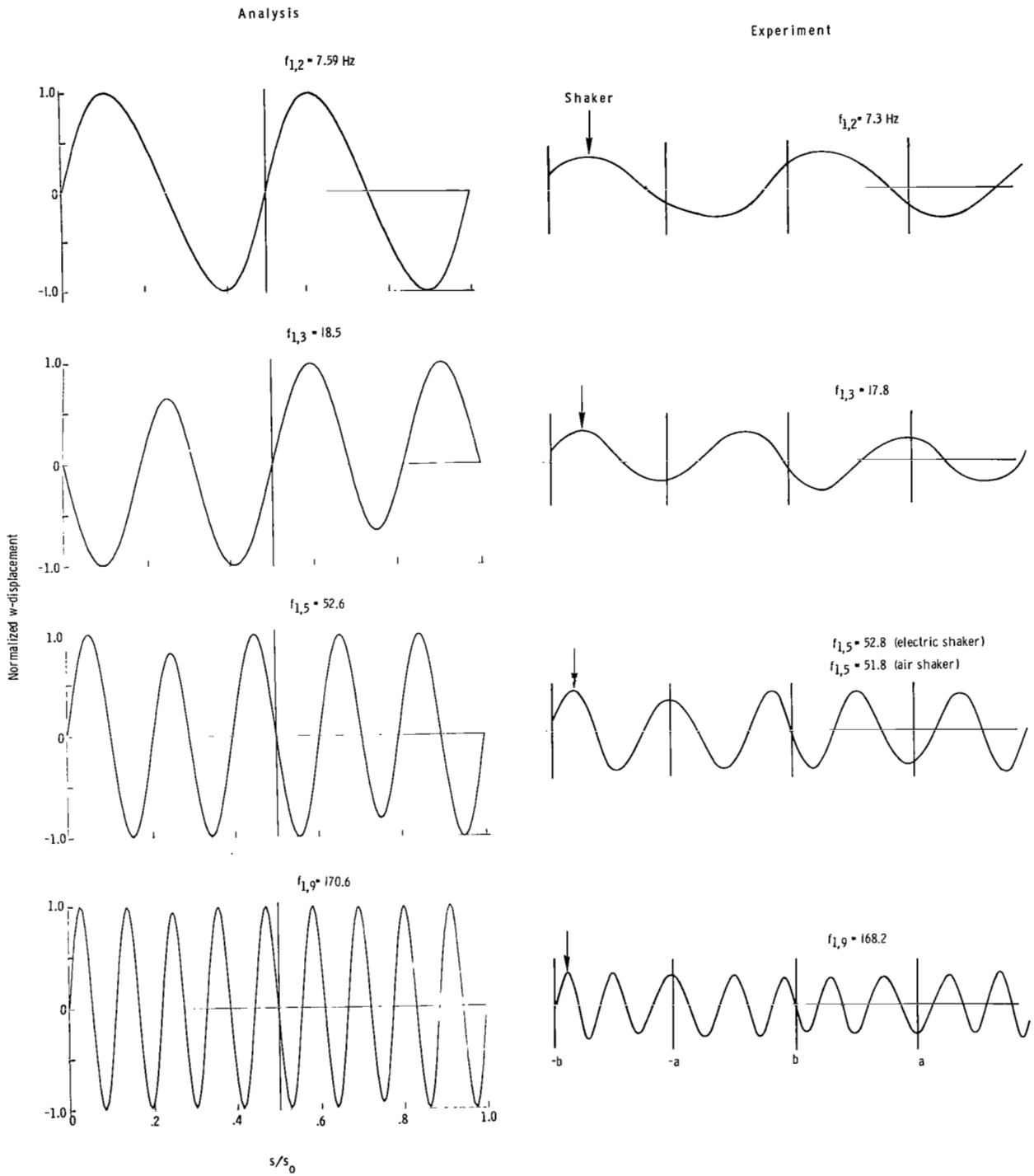
(b) Inextensional antisymmetric mode. $m = 0$.

Figure 9.- Continued.



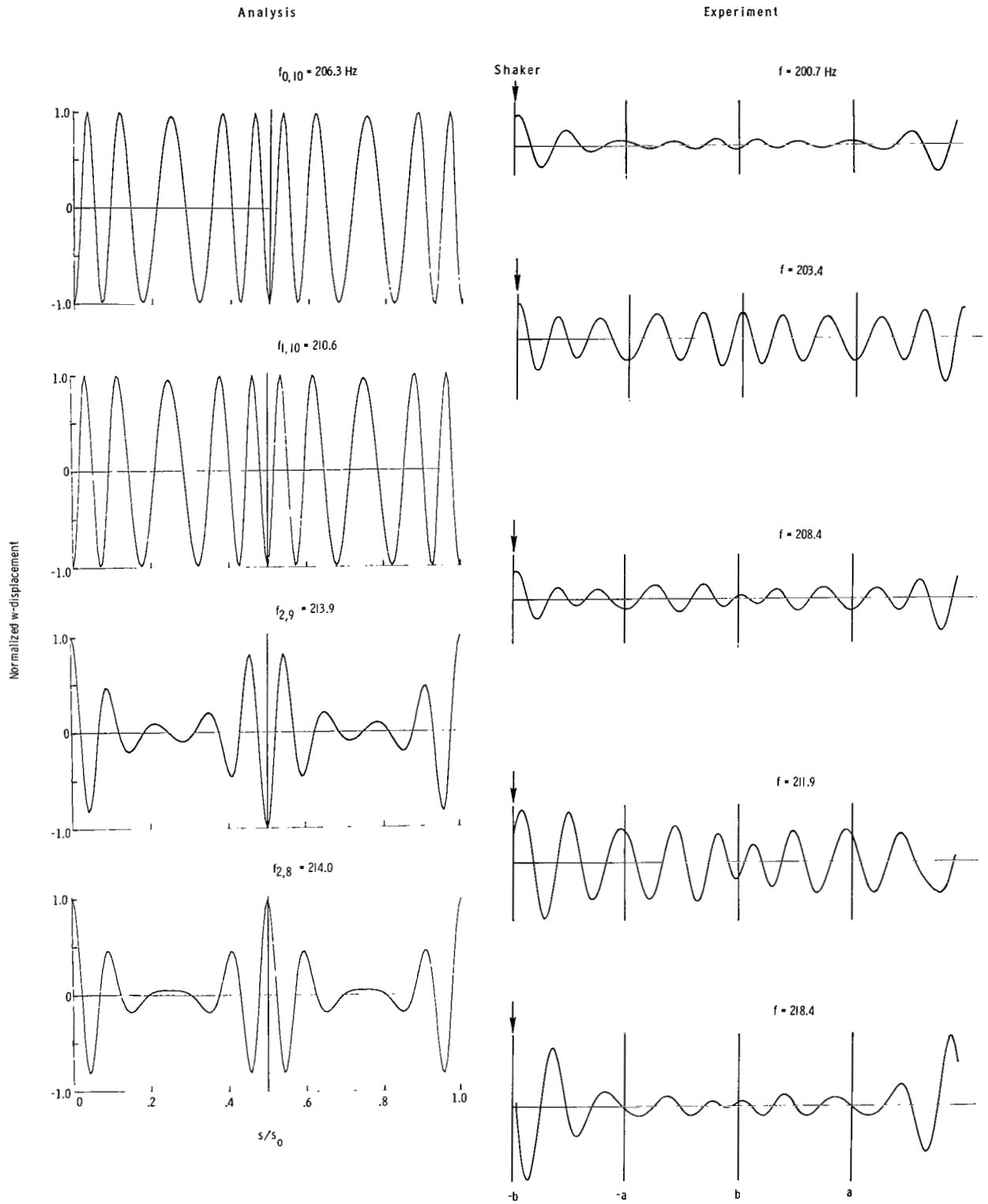
(c) Inextensional symmetric mode. $m = 1$.

Figure 9.- Continued.



(d) Inextensional antisymmetric mode. $m = 1$.

Figure 9.- Continued.

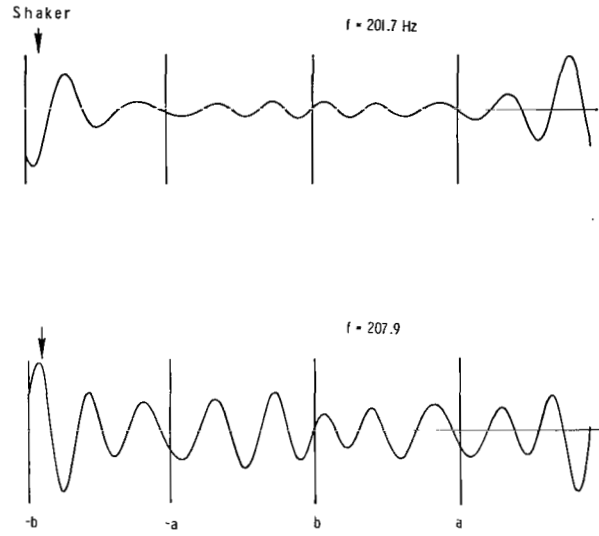
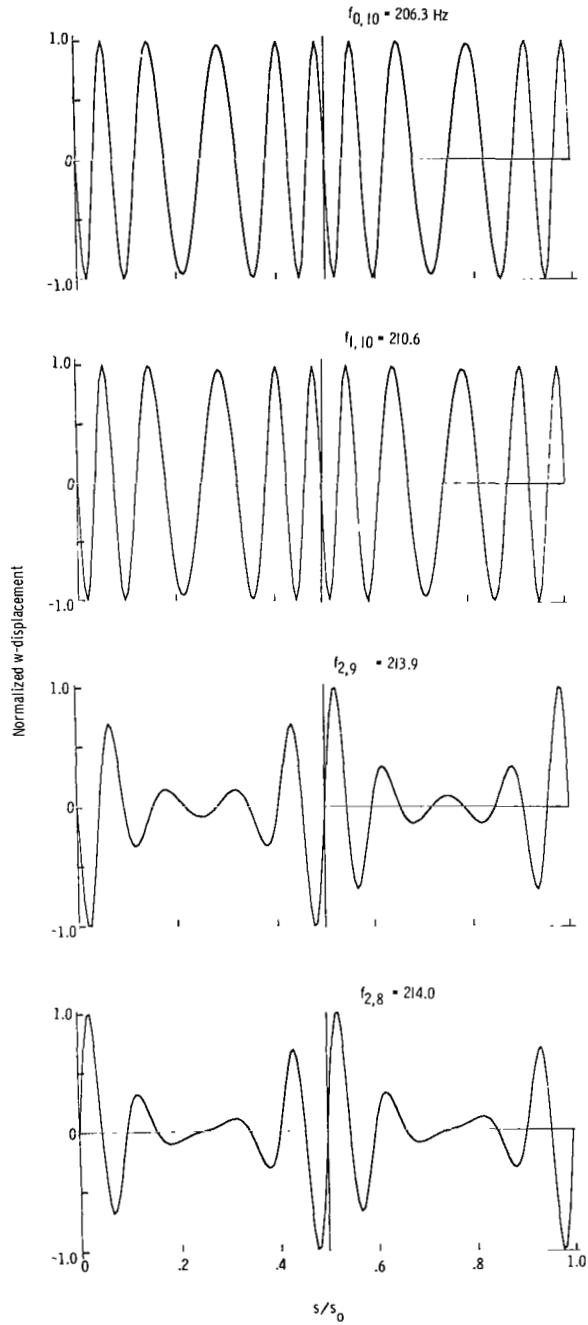


(e) Symmetric modes involving $m = 2$. Frequencies about 210 Hz.

Figure 9.- Continued.

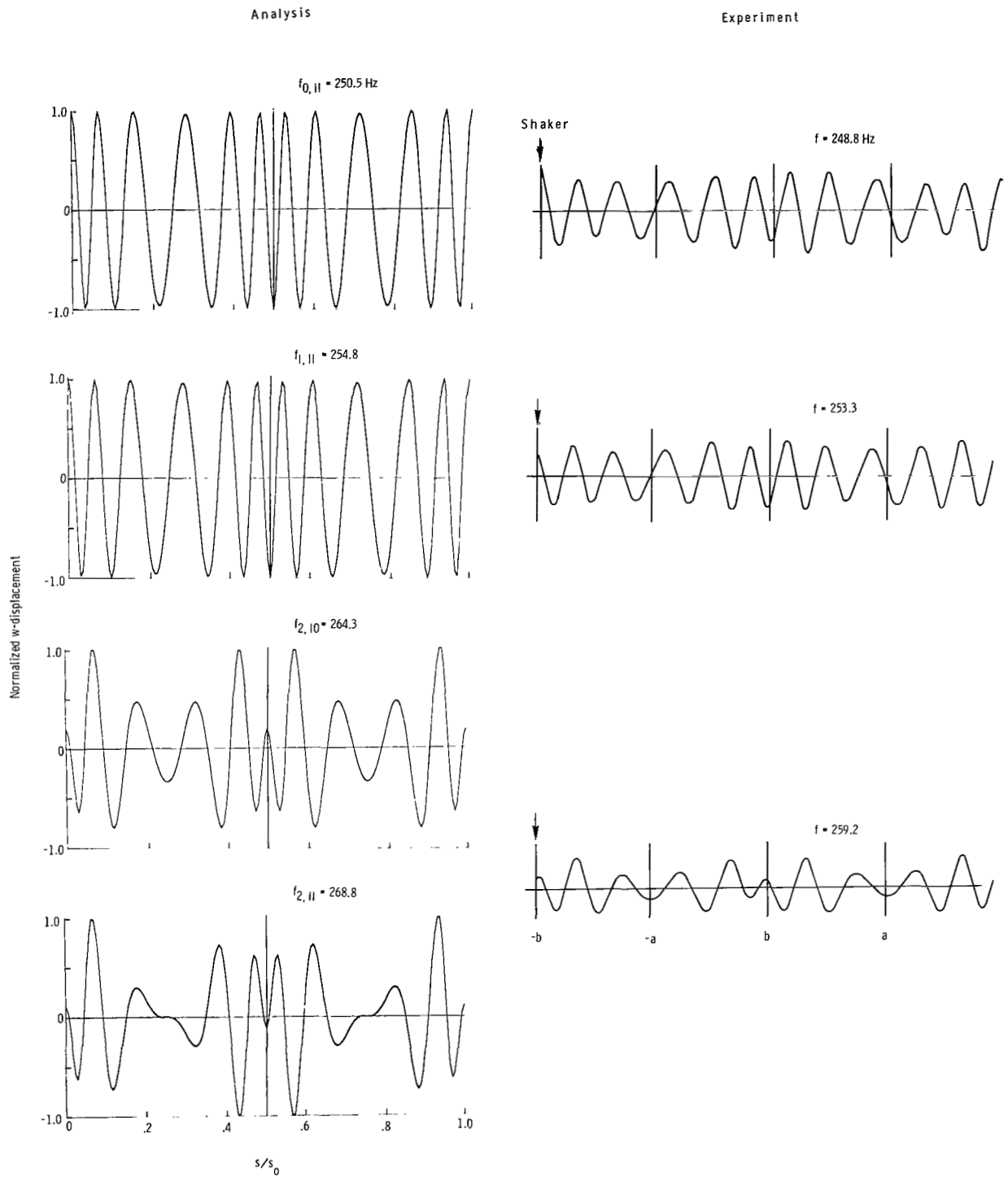
Analysis

Experiment



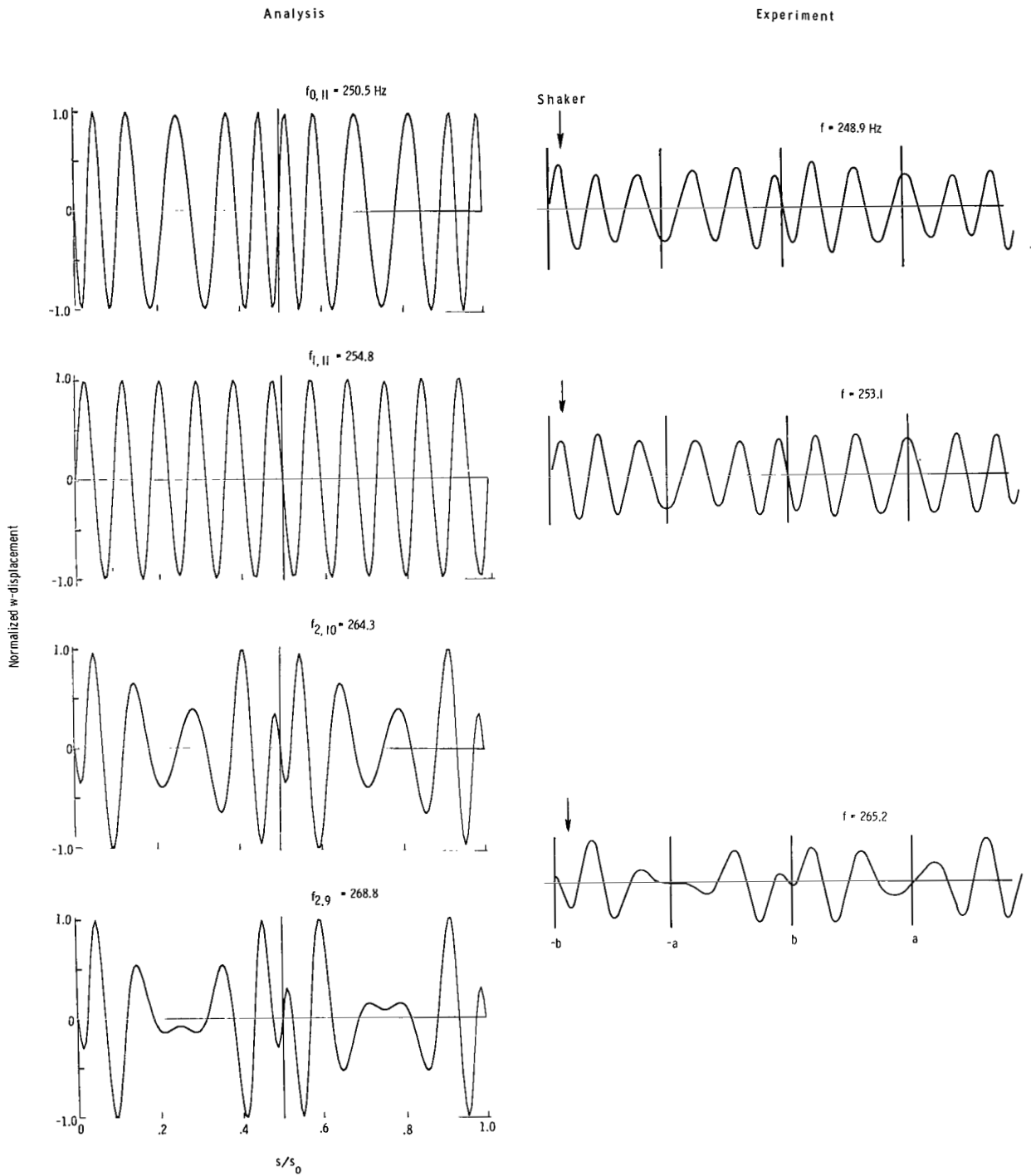
(f) Antisymmetric modes involving $m = 2$. Frequencies about 210 Hz.

Figure 9.- Continued.



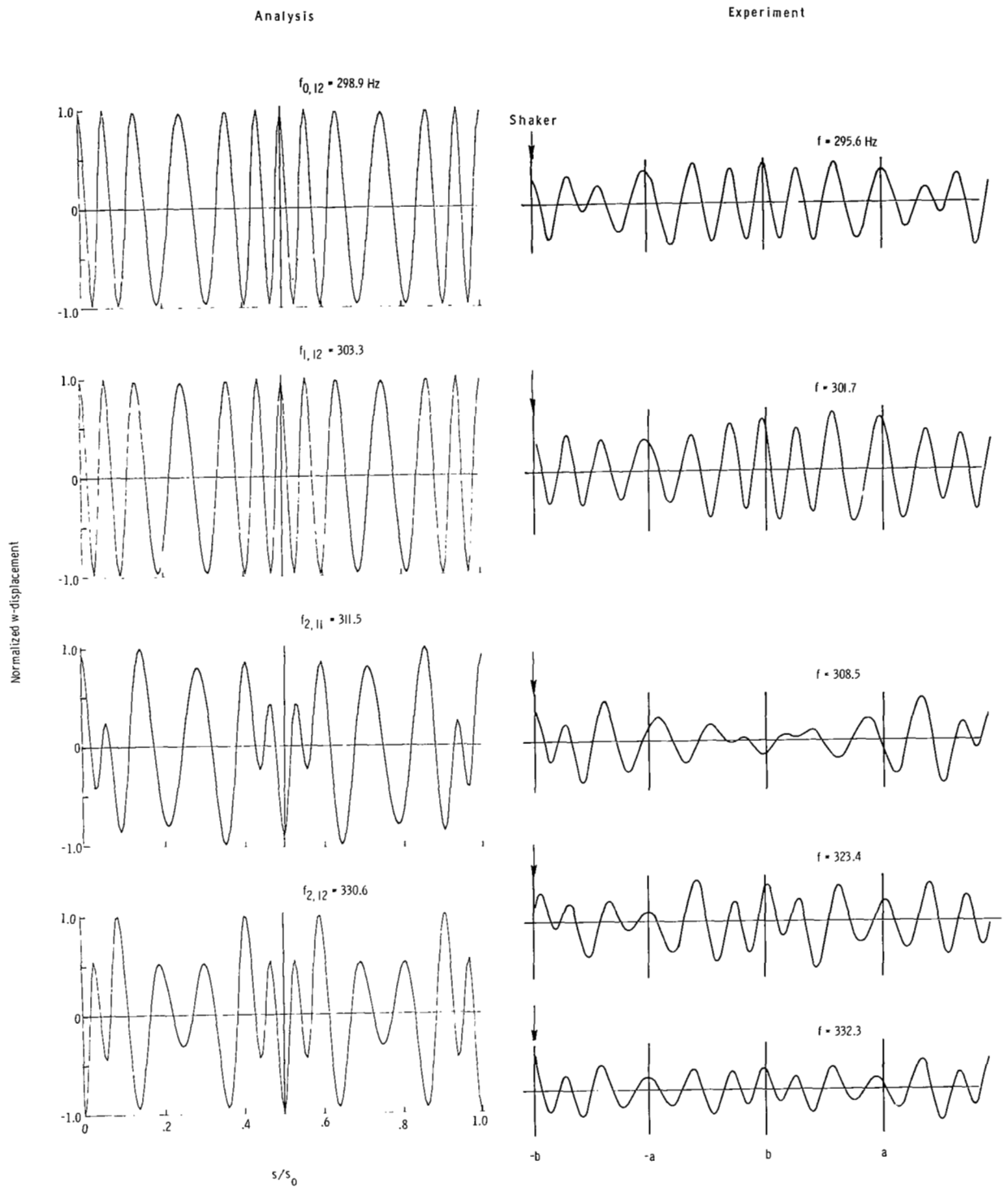
(g) Symmetric modes involving $m = 2$. Frequencies about 250 Hz.

Figure 9.- Continued.



(h) Antisymmetric modes involving $m = 2$. Frequencies about 250 Hz.

Figure 9.- Continued.

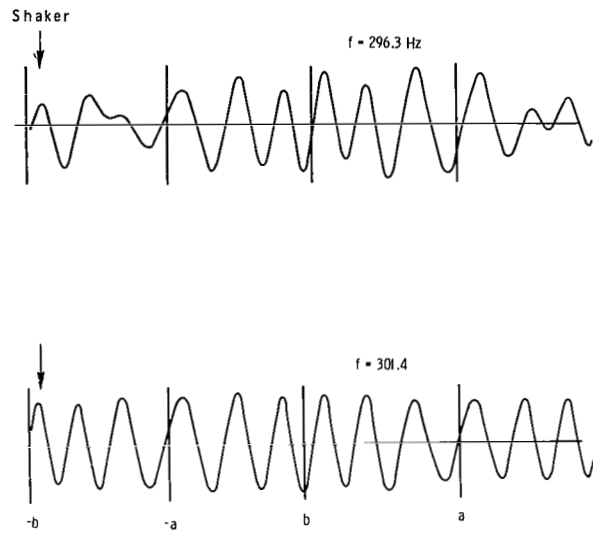
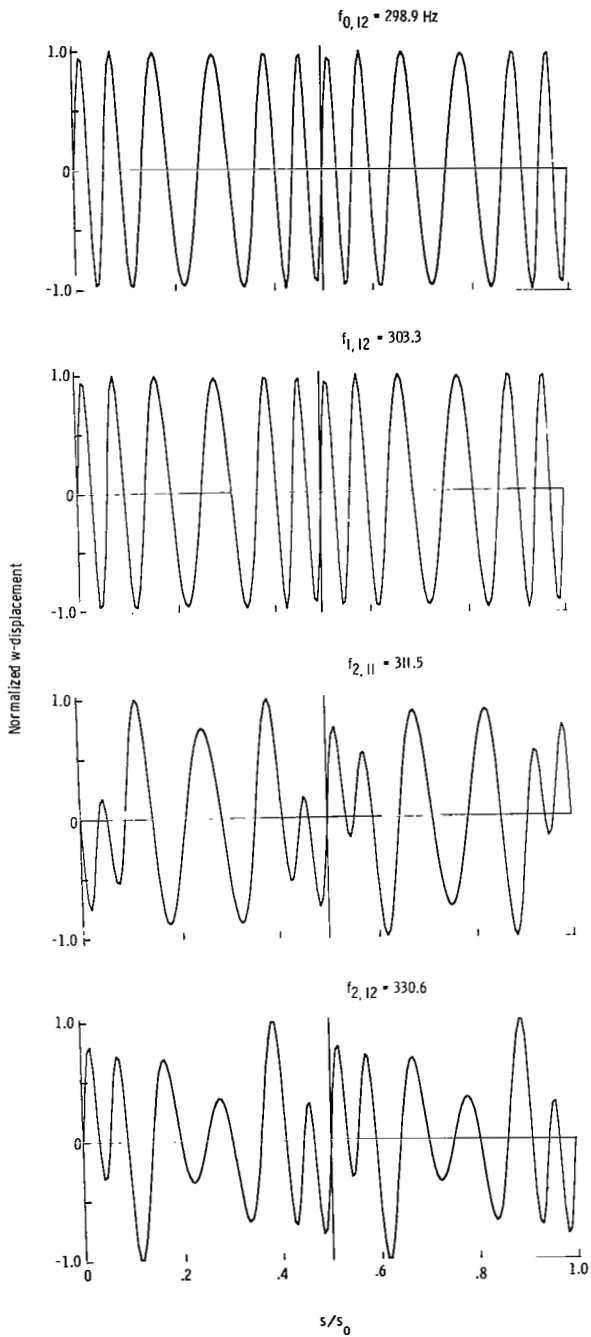


(i) Symmetric modes involving $m = 2$. Frequencies about 300 Hz.

Figure 9.- Continued.

Analysis

Experiment

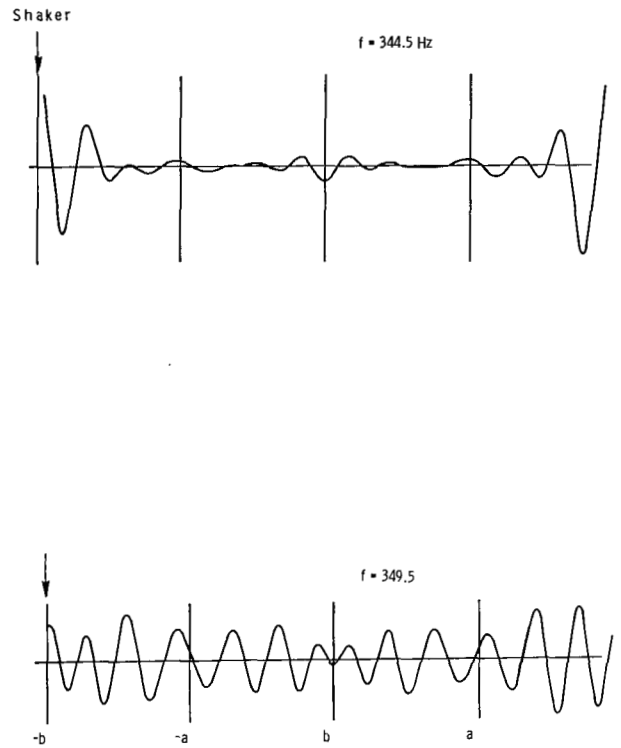
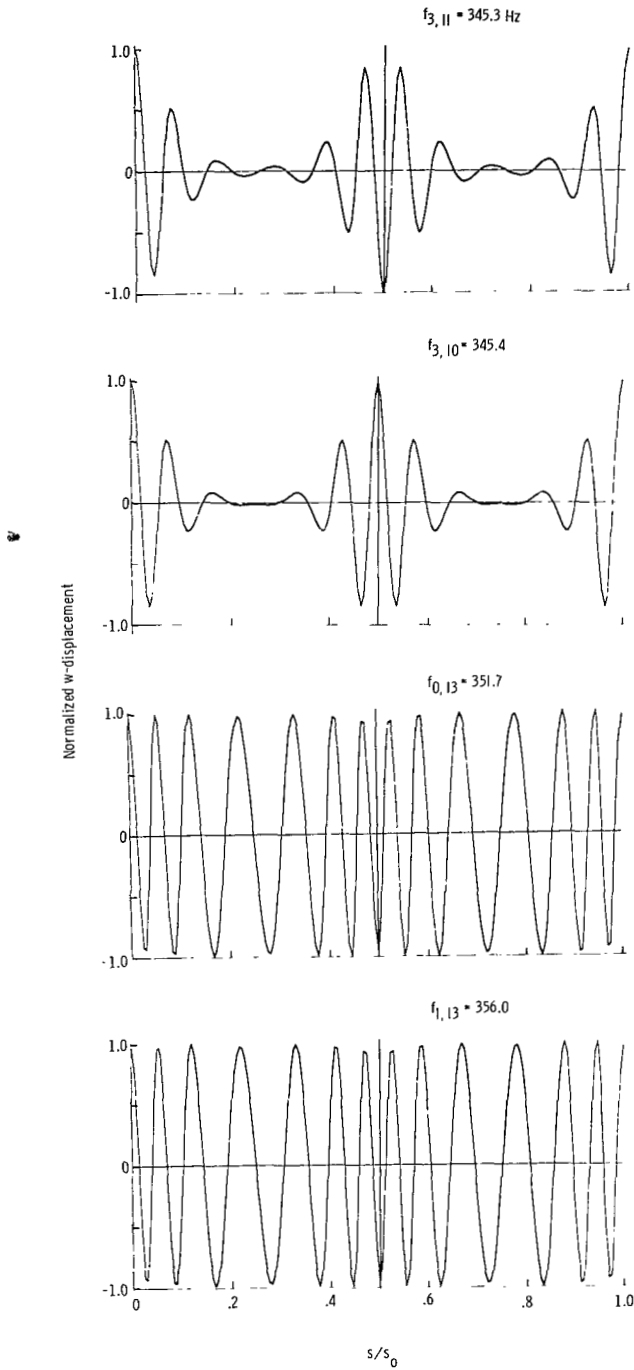


(j) Antisymmetric modes involving $m = 2$. Frequencies about 300 Hz.

Figure 9.- Continued.

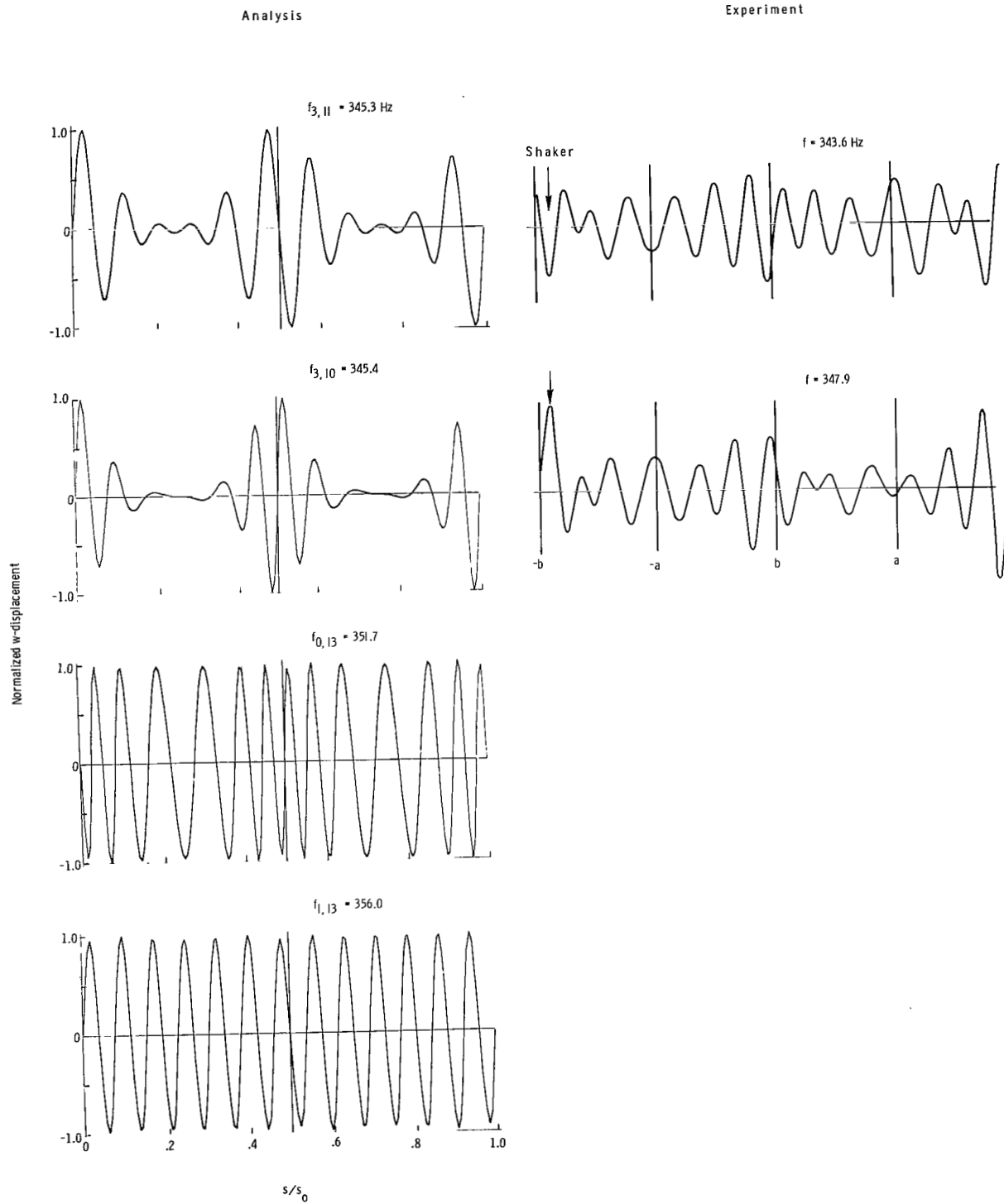
Analysis

Experiment



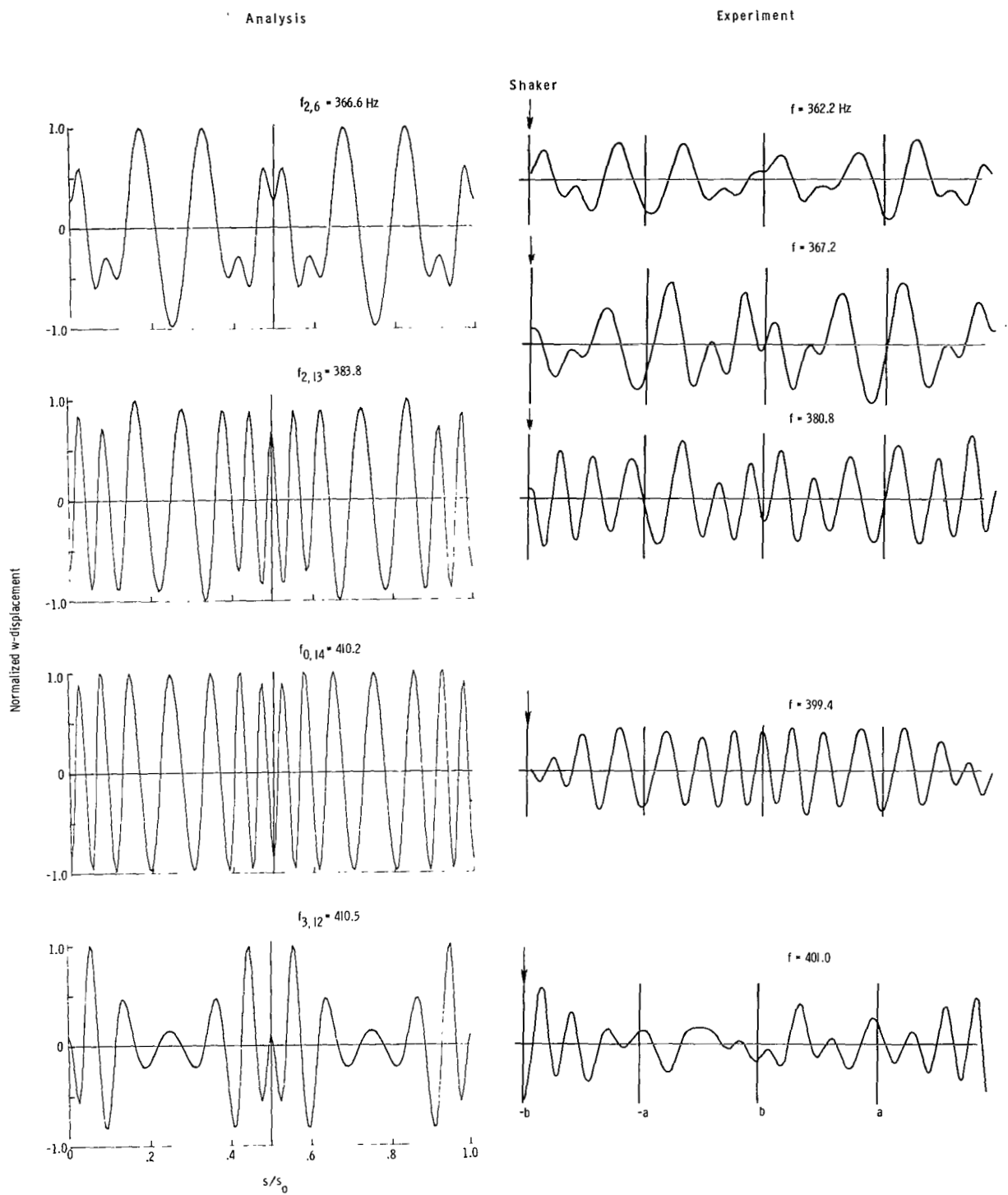
(k) Symmetric modes involving $m = 3$. Frequencies about 350 Hz.

Figure 9.- Continued.



(1) Antisymmetric modes involving $m = 3$. Frequencies about 350 Hz.

Figure 9.- Continued.

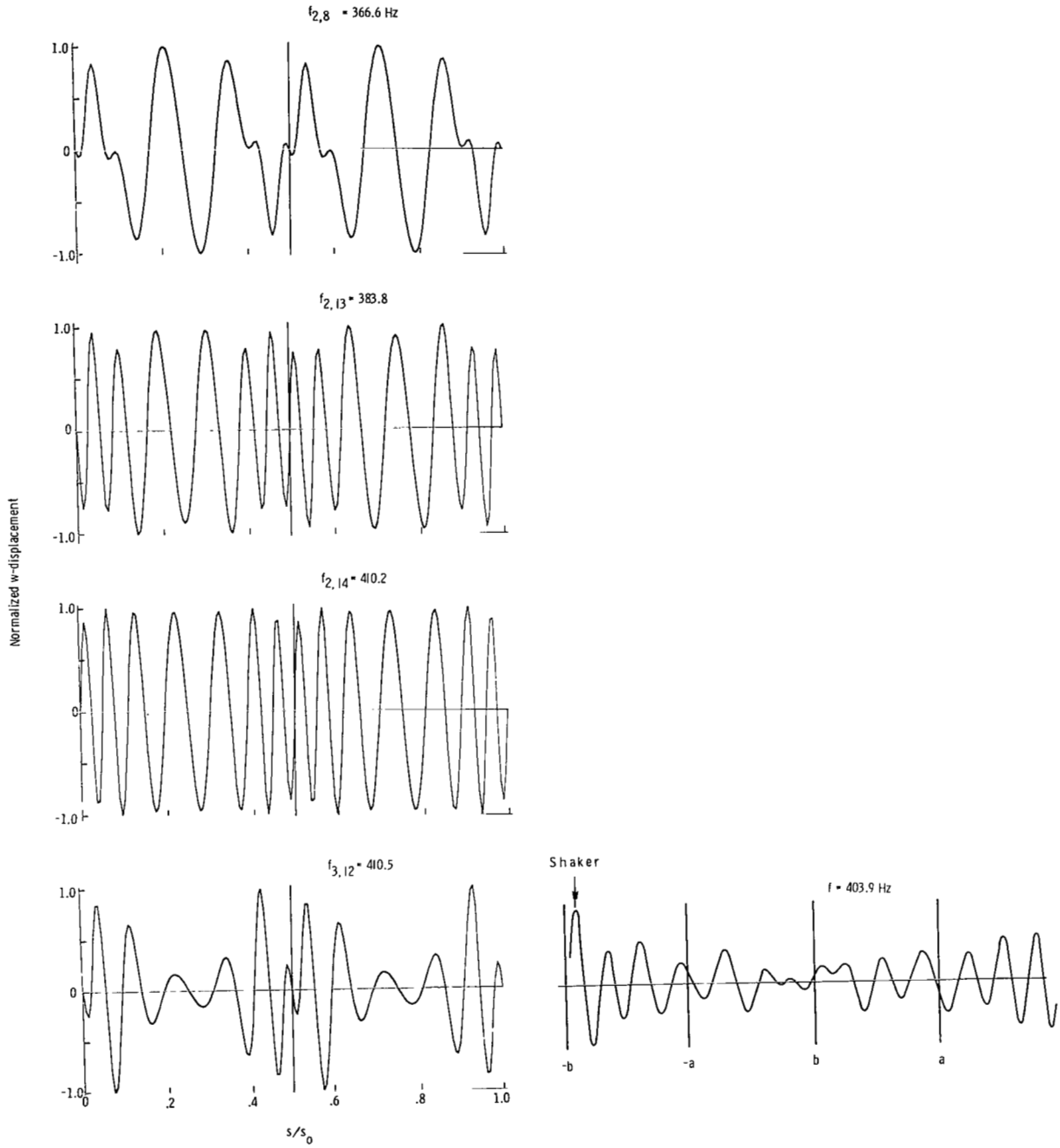


(m) Symmetric modes involving $m = 3$. Frequencies about 400 Hz.

Figure 9.- Continued.

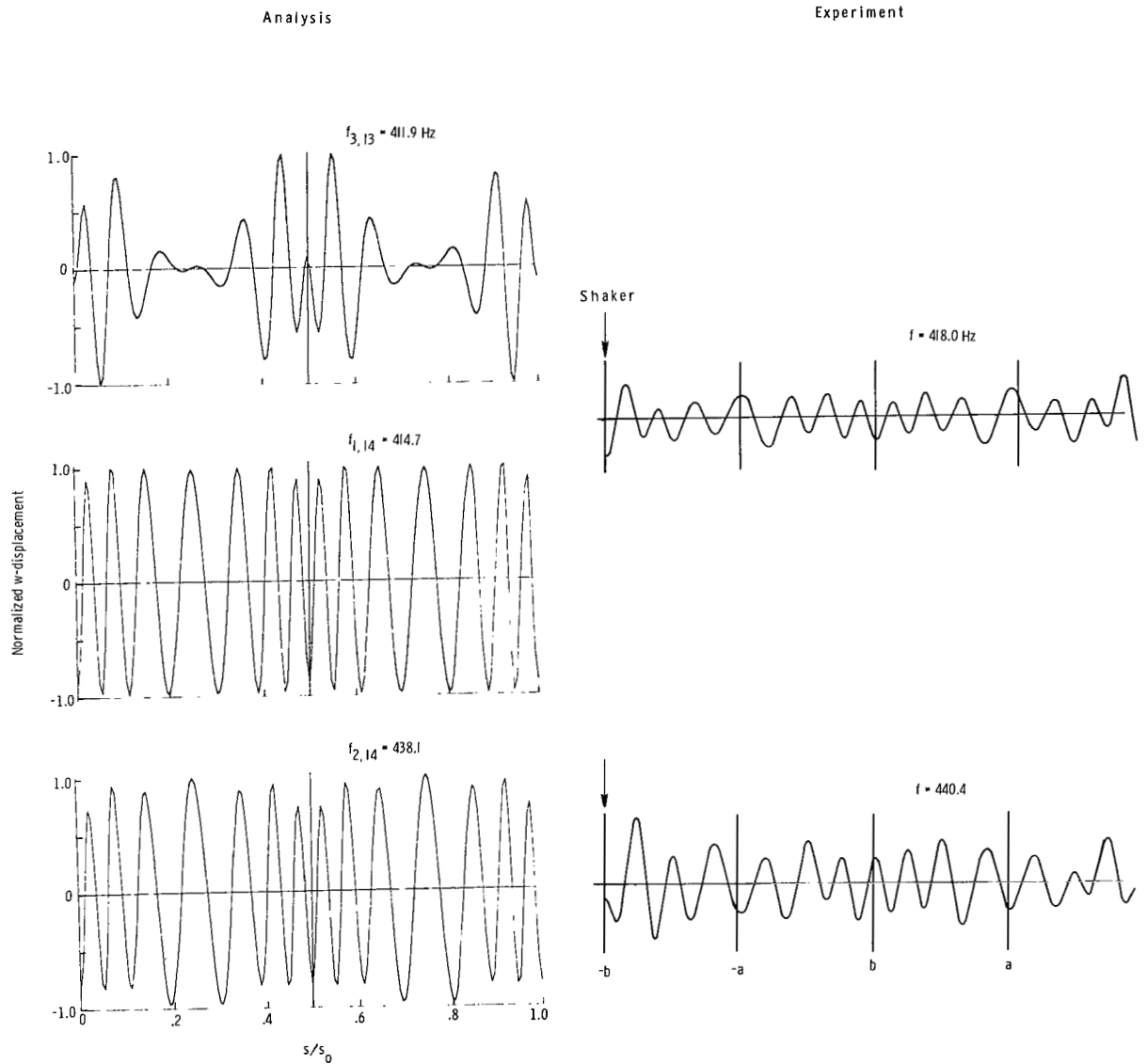
Analysis

Experiment



(n) Antisymmetric modes involving $m = 3$. Frequencies about 400 Hz.

Figure 9.- Continued.

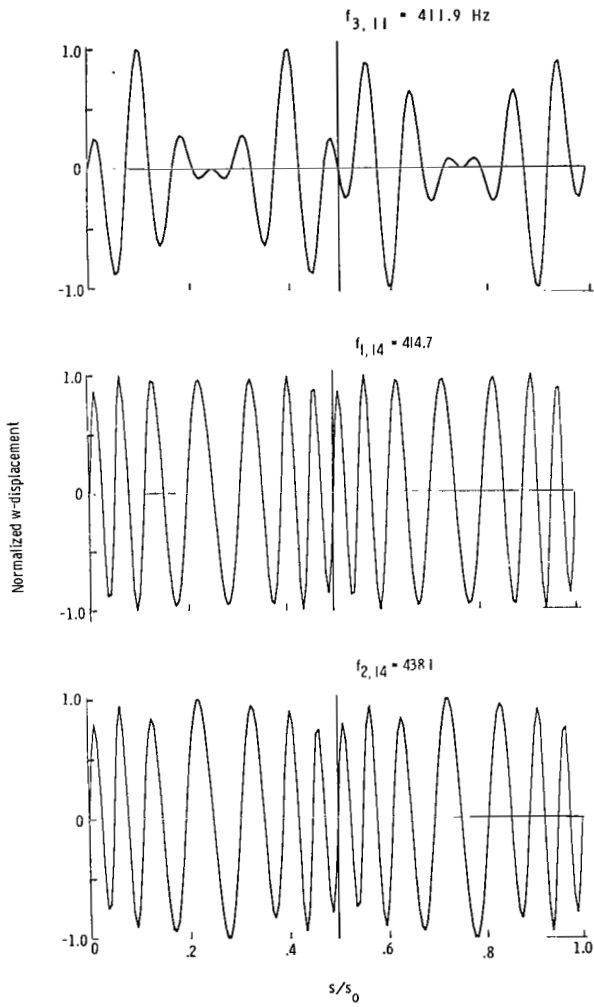


(o) Symmetric modes involving $m = 3$. Frequencies about 425 Hz.

Figure 9.- Continued.

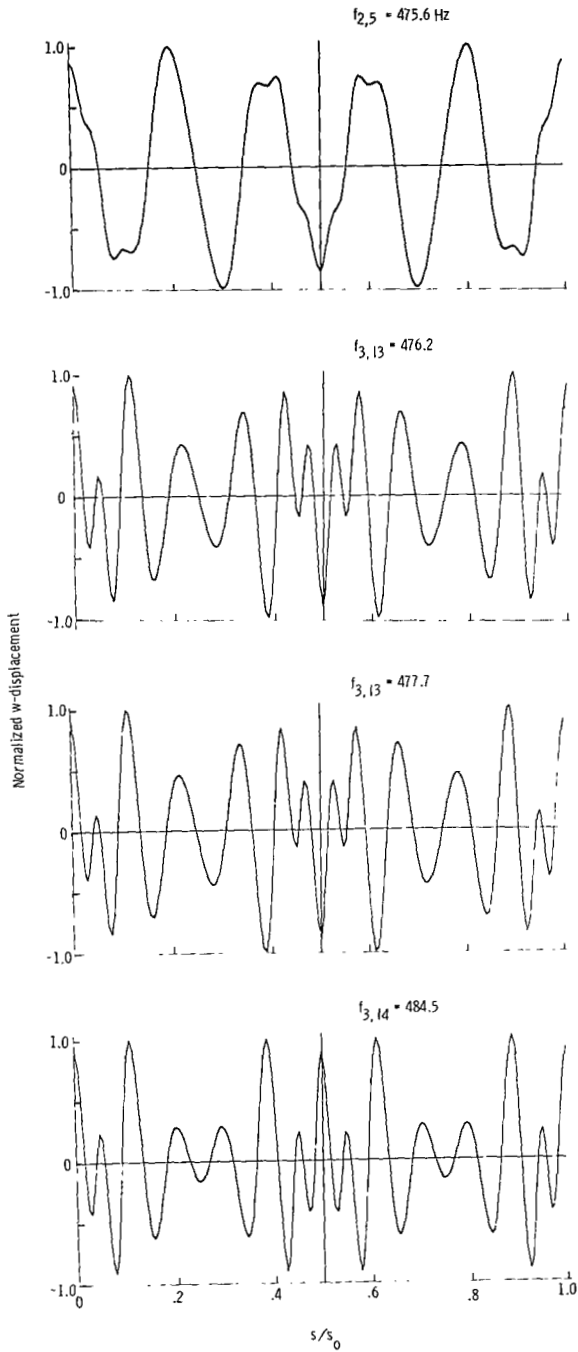
Analysis

Experiment



(p) Antisymmetric modes involving $m = 3$. Frequencies about 425 Hz.

Figure 9.- Continued.

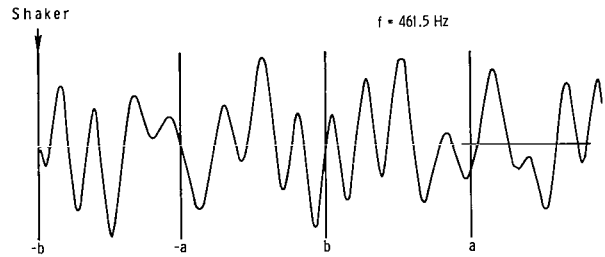
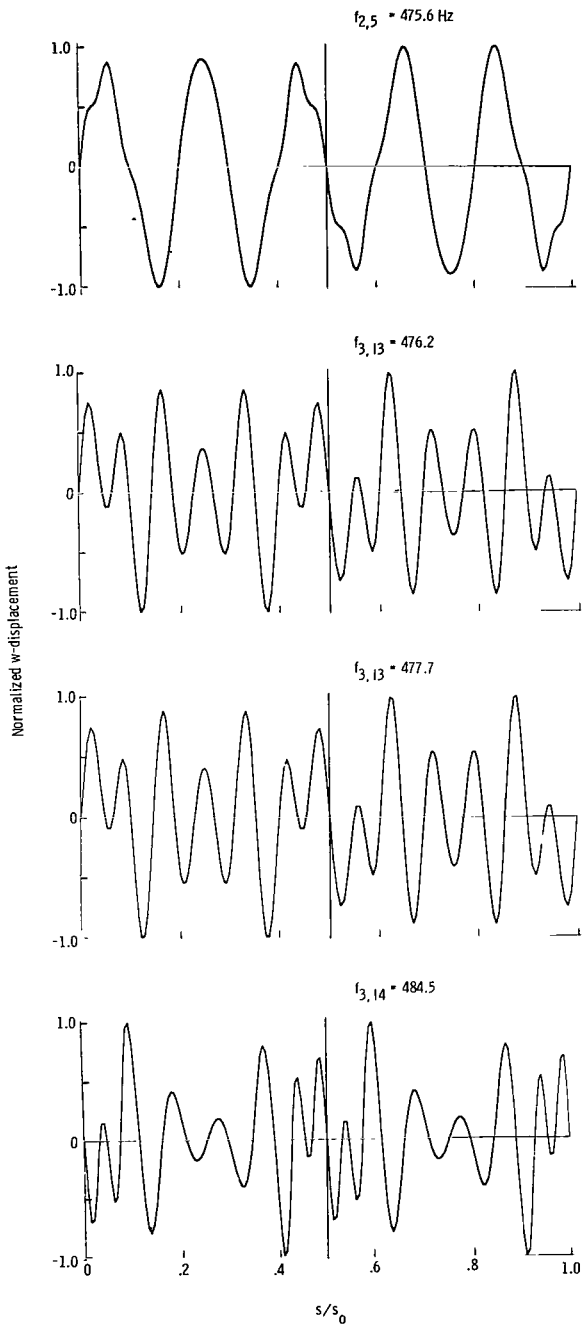


(q) Symmetric modes involving $m = 3$. Frequencies about 475 Hz.

Figure 9.- Continued.

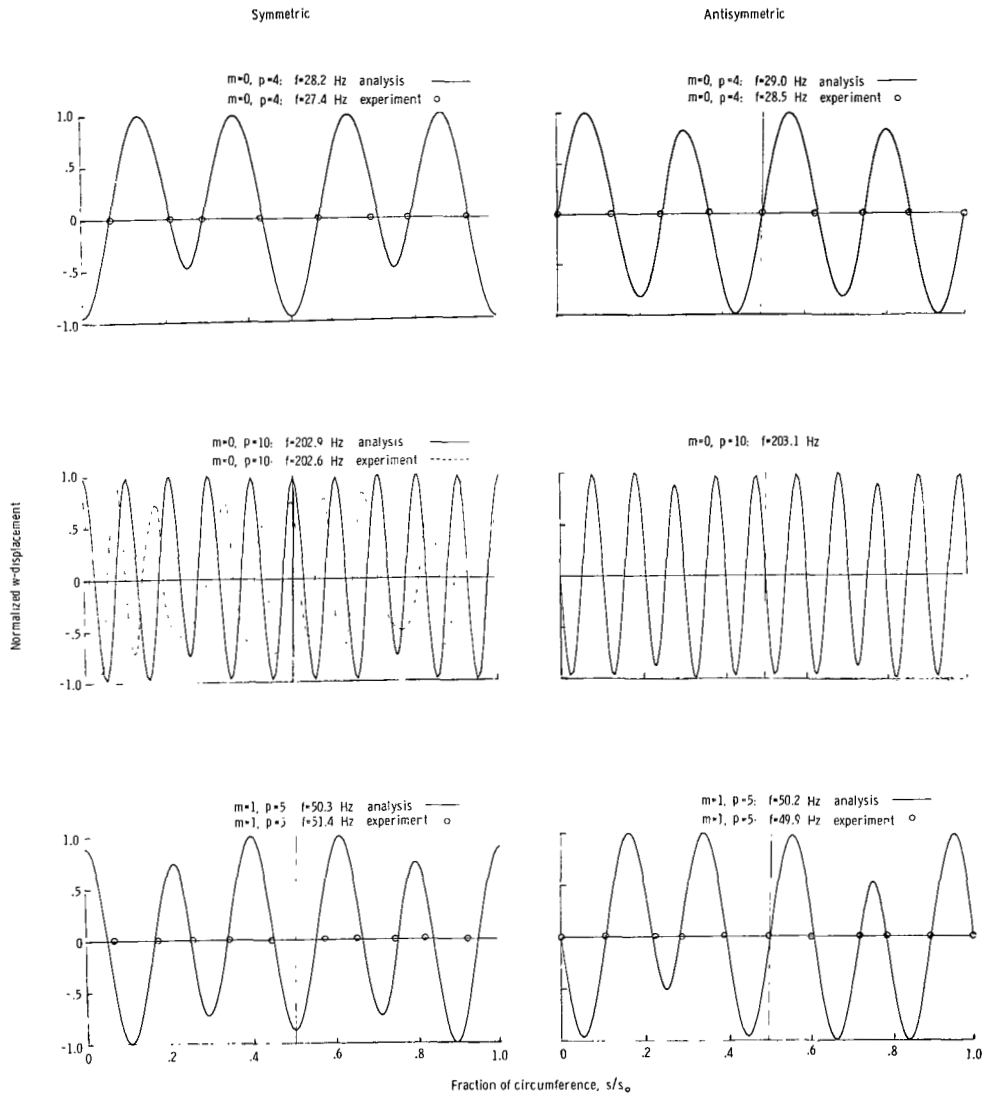
Analysis

Experiment



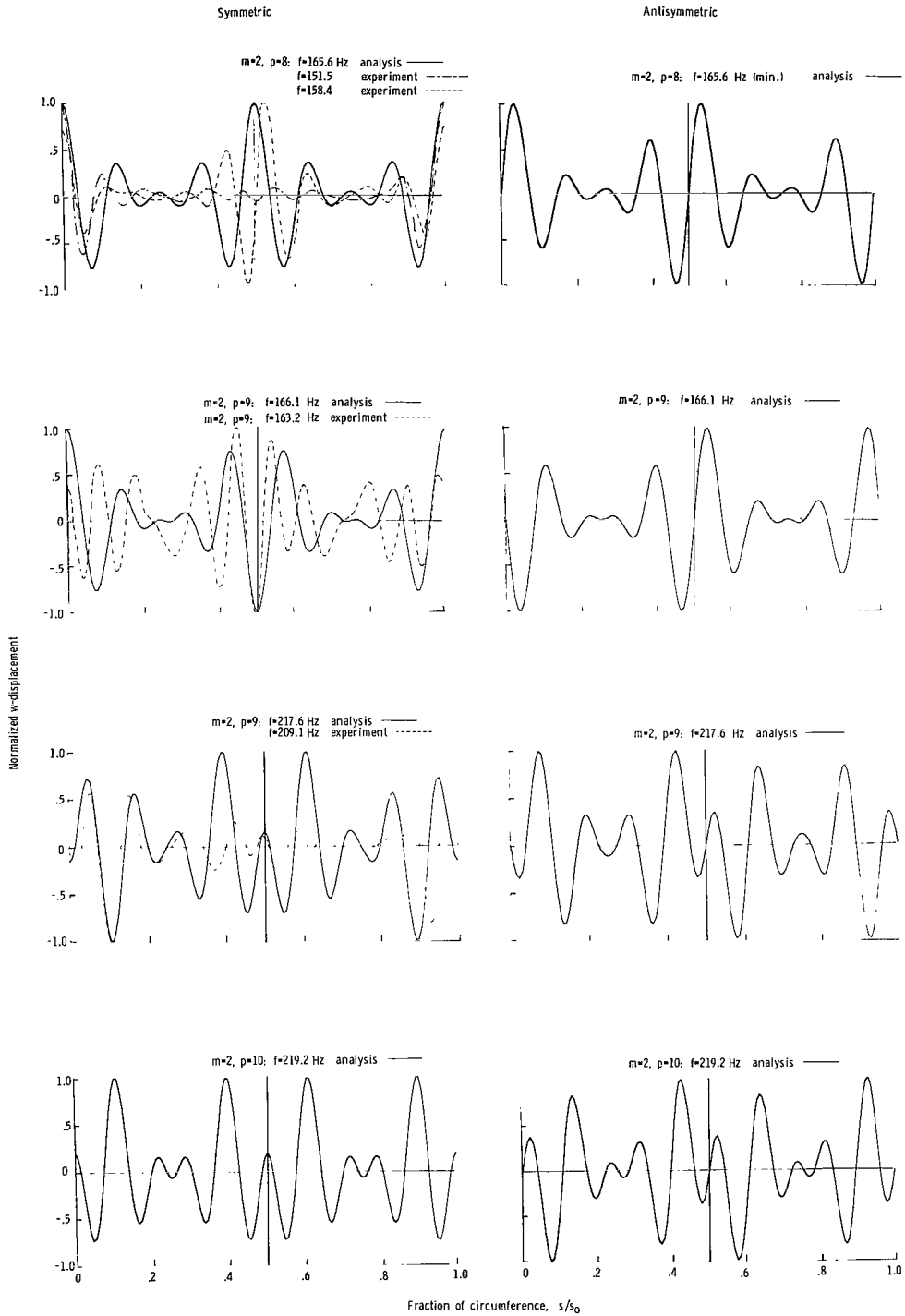
(r) Antisymmetric modes involving $m = 3$. Frequencies about 475 Hz.

Figure 9.- Concluded.



(a) Inextensional modes; $m = 0$ and 1.

Figure 10.- Circumferential mode-shape correlation for model 4 ($e = 0.916$).



(b) Modes involving $m = 2$.

Figure 10.- Concluded.

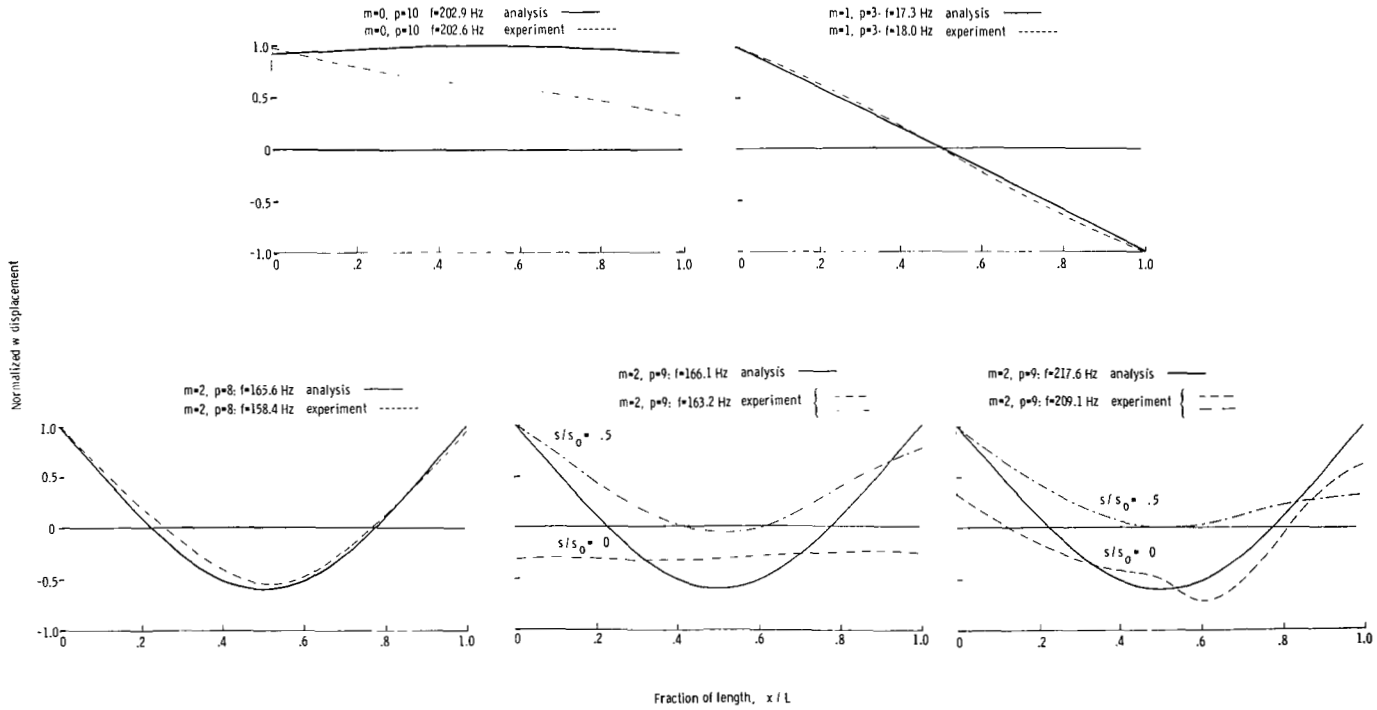


Figure 11.- Longitudinal mode-shape correlation for model 4 ($e = 0.916$).

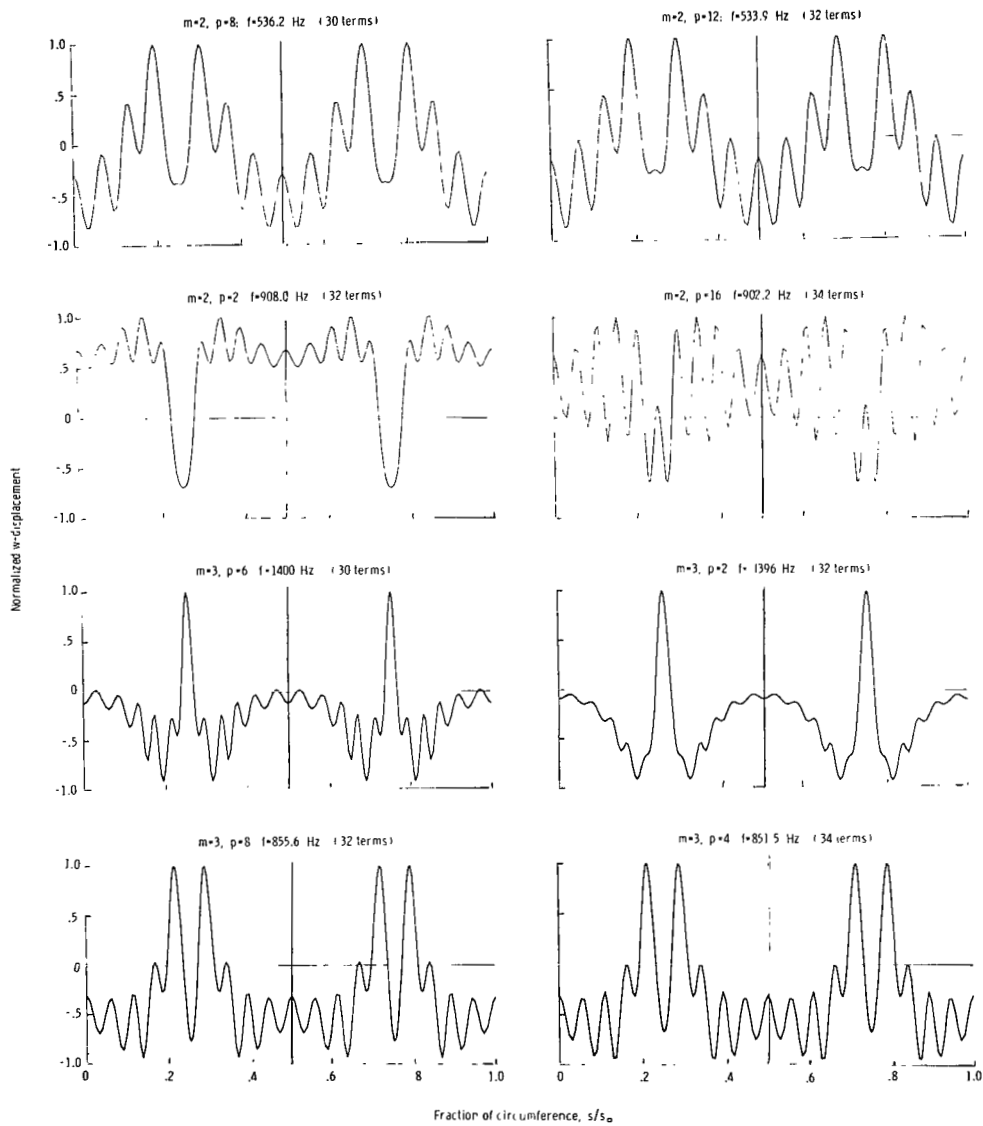


Figure 12.- Effect of various circumferential modal approximations on mode shapes of model 4 ($e = 0.916$).

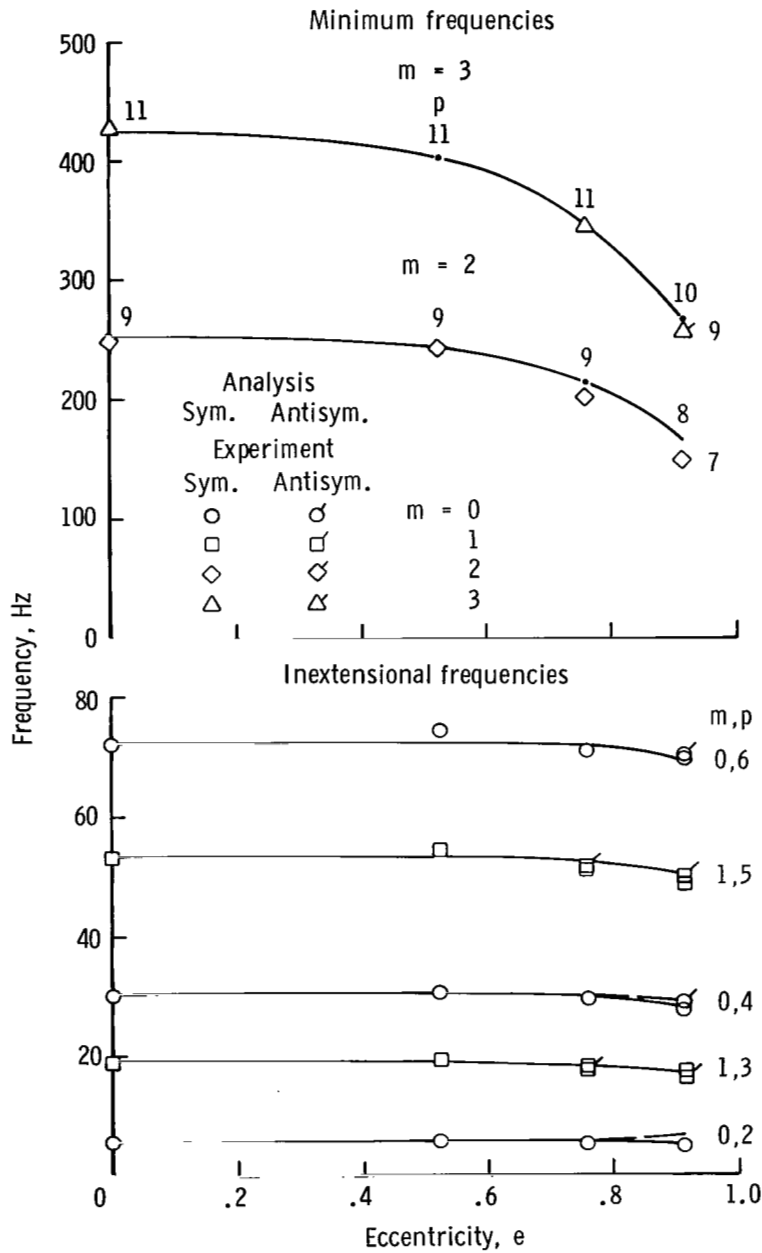


Figure 14.- Effects of eccentricity on frequencies of free-free elliptical cylindrical shell.

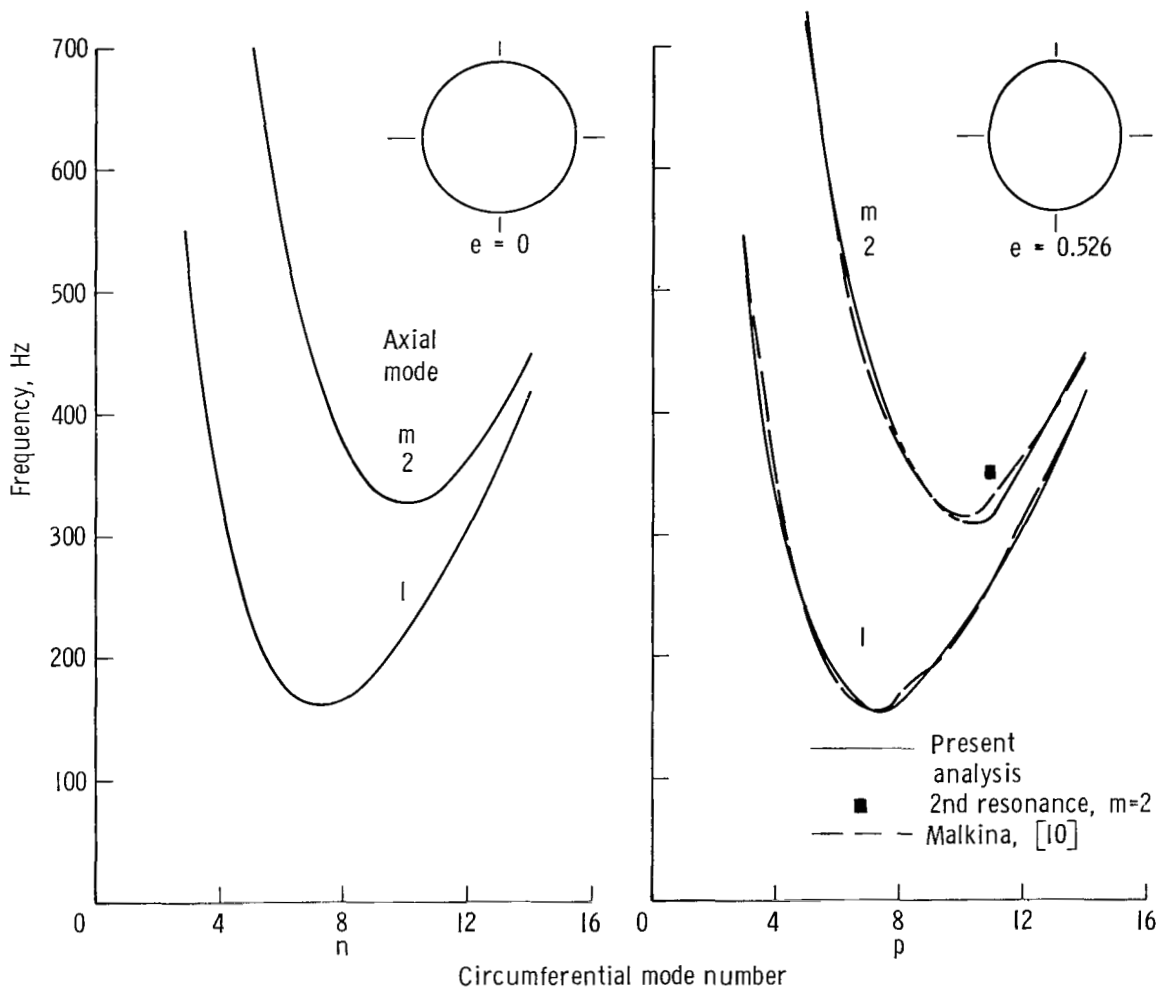


Figure 15.- Variation of frequencies with mode numbers for freely supported shells.

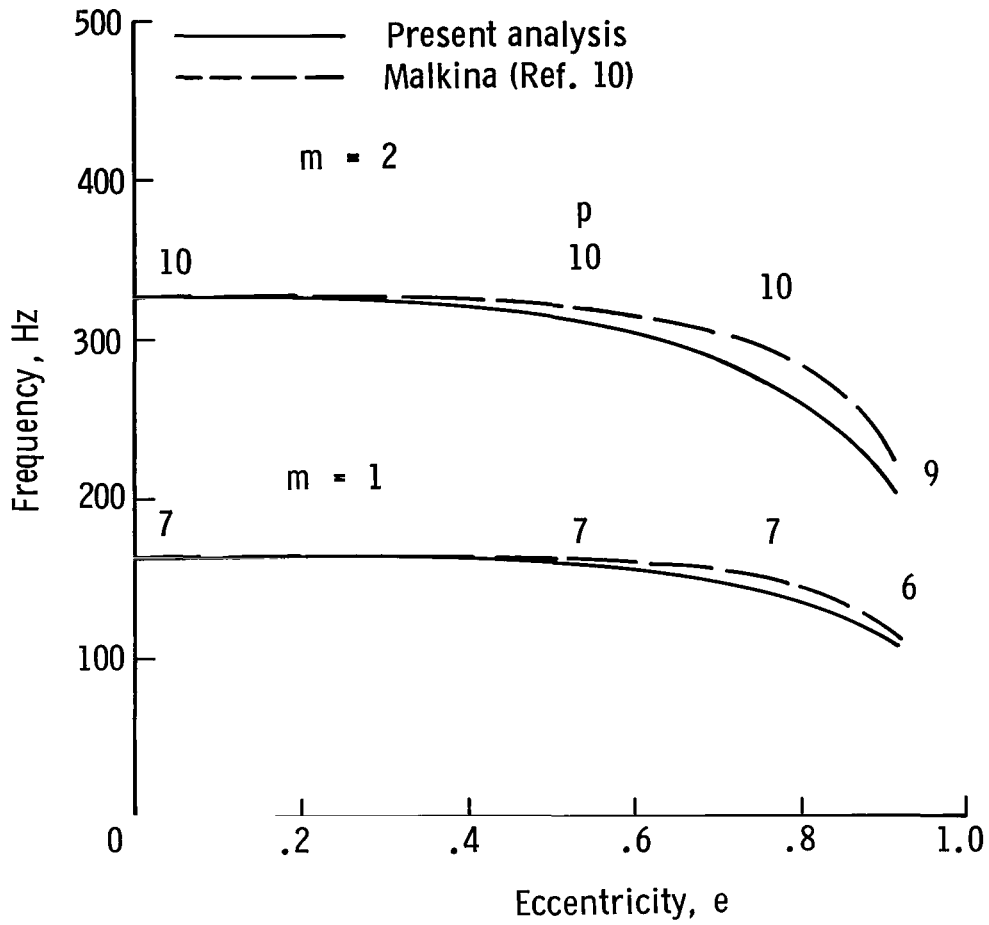


Figure 16.- Effect of eccentricity on minimum frequencies of freely supported elliptical cylindrical shells.



01U 001 57 51 3DS 71028 00903
AIR FORCE WEAPONS LABORATORY /WLOL/
KIRTLAND AFB, NEW MEXICO 87117

ATT E. LOU BOWMAN, CHIEF, TECH. LIBRARY

POSTMASTER: If Undeliverable (Section 158
Postal Manual) Do Not Return

"The aeronautical and space activities of the United States shall be conducted so as to contribute . . . to the expansion of human knowledge of phenomena in the atmosphere and space. The Administration shall provide for the widest practicable and appropriate dissemination of information concerning its activities and the results thereof."

— NATIONAL AERONAUTICS AND SPACE ACT OF 1958

NASA SCIENTIFIC AND TECHNICAL PUBLICATIONS

TECHNICAL REPORTS: Scientific and technical information considered important, complete, and a lasting contribution to existing knowledge.

TECHNICAL NOTES: Information less broad in scope but nevertheless of importance as a contribution to existing knowledge.

TECHNICAL MEMORANDUMS: Information receiving limited distribution because of preliminary data, security classification, or other reasons.

CONTRACTOR REPORTS: Scientific and technical information generated under a NASA contract or grant and considered an important contribution to existing knowledge.

TECHNICAL TRANSLATIONS: Information published in a foreign language considered to merit NASA distribution in English.

SPECIAL PUBLICATIONS: Information derived from or of value to NASA activities. Publications include conference proceedings, monographs, data compilations, handbooks, sourcebooks, and special bibliographies.

TECHNOLOGY UTILIZATION PUBLICATIONS: Information on technology used by NASA that may be of particular interest in commercial and other non-aerospace applications. Publications include Tech Briefs, Technology Utilization Reports and Technology Surveys.

Details on the availability of these publications may be obtained from:

SCIENTIFIC AND TECHNICAL INFORMATION OFFICE

NATIONAL AERONAUTICS AND SPACE ADMINISTRATION

Washington, D.C. 20546